

**RUNNING HEAD:** Low homozygosity in Spanish sheep

**Low genome-wide homozygosity in eleven Spanish ovine breeds**

M.G. Luigi<sup>1</sup>, T.F. Cardoso<sup>1,2</sup>, A. Martínez<sup>3</sup>, A. Pons<sup>4</sup>, L.A. Bermejo<sup>5</sup>, J. Jordana<sup>6</sup>, J.V. Delgado<sup>3</sup>, S. Adán<sup>7</sup>, E. Ugarte<sup>8</sup>, J. J. Arranz<sup>9</sup>, J. Casellas<sup>6</sup> and M. Amills<sup>1,6\*</sup>

<sup>1</sup>Department of Animal Genetics, Centre for Research in Agricultural Genomics (CRAG), CSIC-IRTA-UAB-UB, Campus Universitat Autònoma de Barcelona, Bellaterra 08193, Spain; <sup>2</sup>CAPES Foundation, Ministry of Education of Brazil, Brasília D. F., 70.040-020, Brazil; <sup>3</sup>Departamento de Genética, Universidad de Córdoba, Córdoba 14071, Spain; <sup>4</sup>Unitat de Races Autòctones, Servei de Millora Agrària i Pesquera (SEMILLA), Son Ferriol 07198, Spain; <sup>5</sup>Departamento de Ingeniería, Producción y Economía Agrarias, Universidad de La Laguna, 38071 La Laguna, Tenerife, Spain; <sup>6</sup>Departament de Ciència Animal i dels Aliments, Facultat de Veterinària, Universitat Autònoma de Barcelona, Bellaterra 08193, Spain; <sup>7</sup>Federación de Razas Autóctonas de Galicia (BOAGA), Pazo de Fontefiz, 32152 Coles. Ourense, Spain; <sup>8</sup>Neiker-Tecnalia, Campus Agroalimentario de Arkaute, apdo 46 E-01080 Vitoria-Gazteiz (Araba), Spain; <sup>9</sup>Departamento de Producción Animal, Universidad de León, León 24071, Spain.

Corresponding author: Marcel Amills. Department of Animal Genetics, Centre for Research in Agricultural Genomics (CRAG), CSIC-IRTA-UAB-UB, Campus Universitat Autònoma de Barcelona, Bellaterra 08193, Spain. Tel. 34 93 5636600. E-mail: marcel.amills@uab.cat.

## Abstract

The population of Spanish sheep has decreased from 24 to 15 million heads in the last 75 years due to multiple social and economic factors. Such demographic reduction might have caused an increase in homozygosity and inbreeding, thus limiting the viability of local breeds with excellent adaptation to harsh ecosystems. The main goal of our study was to investigate the homozygosity patterns of 11 Spanish ovine breeds and to elucidate the relationship of these Spanish breeds with reference populations from Europe, Africa and the Near East. By using Ovine SNP50 BeadChip data retrieved from previous publications, we have found that the majority of studied Spanish ovine breeds have a close genetic relatedness with other European populations; the one exception is the Canaria de Pelo breed that is similar to North African breeds. Our analysis has also demonstrated that, with few exceptions, the genomes of Spanish sheep harbor fewer than 50 runs of homozygosity (ROH) with a total length of less than 350 Mb. Moreover, the frequencies of very long ROH ( $> 30$  Mb) are very low, and the inbreeding  $F_{ROH}$  coefficients are generally small ( $F_{ROH} < 0.10$ ), ranging from 0.008 (Rasa Aragonesa) to 0.086 (Canaria de Pelo). The low levels of homozygosity observed in the 11 Spanish sheep under analysis might be due to their extensive management and the high number of small to medium farms.

**Keywords:** ROH, homozygosity, sheep, demographic history, inbreeding.

## Introduction

The abundance of single nucleotide polymorphisms (SNPs) throughout the genome and the availability of high density SNP arrays has enabled estimates of the impact of evolutionary forces that tend to increase genome-wide homozygosity in domestic populations (Wang et al., 2014; Peripolli et al., 2017; Ceballos et al., 2018). A common approach to achieve this goal of estimating evolutionary impact consists of identifying continuous homozygous segments *i.e.* runs of homozygosity (ROH) and estimating their frequencies, genomic coverage and size distribution (Peripolli et al., 2017; Ceballos et al., 2018). The identification and study of ROH has been used to make inferences about the population history and demography of sheep breeds (Purfield et al., 2017; Mastrangelo et al., 2018). Moreover, Purfield et al. (2017) analyzed six commercial ovine breeds and found that long (>15 Mb) and very long (>20 Mb) ROH were quite uncommon and that the average proportion of the autosomal genome covered by ROH ( $F_{ROH}$ ) was generally lower than 10%. Similar patterns were observed in Italian sheep breeds (Mastrangelo et al. 2018), with  $F_{ROH}$  coefficients between 1.6% (Comisana) and 9.9% (Valle del Belice) and low frequencies of very long ROH (> 25 Mb).

Many local Spanish breeds have suffered strong population reductions due to competition with more productive breeds and the gradual abandonment of rural activities. In Spain, 44 autochthonous sheep breeds have been officially recognized, and 34 of them are under special protection because they have a low or moderate population size (<https://www.mapa.gob.es/es/ganaderia/temas/zootecnia/razas-ganaderas/razas/catalogo/>). In a previous study, Manunza et al. (2016) characterized the diversity of eleven ovine Spanish breeds and detected several putative selective sweeps on ovine

chromosomes 3, 6 and 13. Here, we aimed to analyze the patterns of homozygosity of these eleven sheep breeds to make inferences about their demographic history. Specifically, we were interested in investigating whether breeds under special protection show increased levels of homozygosity and inbreeding because of their limited population size. To achieve this goal, we used data previously published by Manunza et al. (2016) as well as data from the International Sheep Genomics Consortium (<http://www.sheephapmap.org/>).

## Materials and methods

### *Animal material and genotyping data*

We did not generate novel genotypic data in the current experiment. In contrast, we used previously published Illumina Ovine SNP50 BeadChip data from 141 sheep corresponding to the Segureña (N = 12), Xisqueta (N = 24), Ripollesa (N = 24), Gallega (N = 25), Canaria de Pelo (N = 27), and Roja Mallorquina (N = 29) breeds (Manunza et al., 2016). Genotypic data from 279 sheep belonging to the Ojalada (N = 24), Castellana (N = 23), Rasa Aragonesa (N = 22), Churra (N = 120) and Latxa (N = 90) breeds provided by the International Sheep Genomics Consortium (<http://www.sheephapmap.org/>) were also included. These 11 Spanish sheep breeds are used for the production of meat, milk and wool (**Supplementary Table 1**).

The population structure analysis (principal component analysis and Admixture) comprised the 11 Spanish breeds mentioned before as well as 28 ovine populations from the following regions: (1) **Europe**: Italy (Altamurana, N = 24; Comisana, N = 24), Switzerland (Swiss White Alpine, N = 24), Greece (Chios, N = 23), Cyprus (Cyprus fat tail, N = 30), France (Milk Lacaune, N = 103; Meat Lacaune, N = 78, Rambouillet, N =

102) and Germany (Merino Landschaf, N = 24; East Friesian, N = 48); (2) **Africa:**  
Egypt (Barki, N = 13), a pool of Algerian breeds (Barbarine, N = 5; Berber, N = 6;  
D'men, N = 5; Hamra, N = 6; Ouled-Djellal, N = 6, Rembi, N = 6; Sidaoun, N = 6 and  
Tazegzawt, N = 6), Kenya (Red Maasai, N = 45) and Ethiopia (Menz, N = 34); (3) **Near**  
**East:** Iran (Afshari, N = 37; Moghani, N = 34; Nordus, N = 20; Qezel, N = 35) and  
Turkey (Karakas, N = 18; Sakiz, N = 22); and (4) **Oceania:** Australia (Australian  
Merino, N = 50). Data from the European, Near Eastern, Australian and African breeds  
(with the exception of the Algerian breeds) were available in the web of the  
International Sheep Genomics Consortium (<http://www.sheephapmap.org>), while data  
from Algerian sheep (Gaouar et al., 2017), were retrieved from the Dryad repository  
(<https://datadryad.org/resource/doi:10.5061/dryad.h0h8d>). All individuals (N = 1,254)  
had been genotyped with the Ovine SNP50 BeadChip (Illumina).

#### *Quality control of the genotypic data*

The PLINK v. 1.90 software (Chang et al., 2015) was employed to filter SNPs  
and individuals. We removed SNPs mapping to sex chromosomes as well as those  
displaying minor allele frequencies equal to or lower than 1% and genotype call rates  
lower than 95%. We also eliminated markers showing strong departures from the  
Hardy-Weinberg equilibrium ( $P\text{-value} < 1.10^{-6}$ ) because there is evidence that a  
significant fraction of SNPs showing such departures correspond to genotyping errors  
attributable to the existence of structural variation (Chen et al., 2017). Individuals with  
more than 10% invalid SNP genotypes were also excluded from further analyses.

## *Genetic diversity and population structure analyses*

Expected and observed heterozygosities per breed were calculated with PLINK v. 1.90 (Chang et al., 2015). The Arlequin software v. 3.1 (Excoffier et al., 2007) was used to estimate pairwise  $F_{ST}$  coefficients between all pairs of breeds. We used PLINK v. 1.90 to perform a weighted principal component analysis (wPCA) which corrects for unbalanced population sizes (Burgos-Paz et al., 2014). The correction for sample size consisted of adding multiple copies of the individuals from each population until their contribution to the samples was approximately equivalent, and then a standard principal component analysis was carried out (Burgos-Paz et al. 2014). A clustering analysis with Admixture v. 1.3.0 (Alexander et al., 2009) was also carried out by considering K-values from 2 to 37. The most likely K-value was the one with the lowest cross-validation error (Alexander & Lange, 2011). The SNeP v. 1.1 software (Barbato et al., 2015) was used to estimate the magnitude of the effective population size ( $N_e$ ) of the Spanish breeds in the last 225 generations by considering a generational interval of 4 years. The reason for choosing this scale of time is that the concept of breed is relatively recent *i.e.* the first recognized ovine breed was Merino (Ciani et al., 2015), which was developed in the late Middle Ages (11<sup>th</sup>-14<sup>th</sup> centuries).

## *Detection of runs of homozygosity*

The software PLINK v. 1.90 (Chang et al., 2015) was employed to detect ROH in eleven Spanish sheep breeds. The scanning window encompassed 50 SNPs, and the maximum number of heterozygous SNPs per window was set to one. The maximum number of missing SNPs per window was set to two, and the minimum scanning window hit rate was set to 5%. The minimum length of ROH was fixed to 1000 Kb to

minimize the detection of spurious ROH. The minimum number of SNPs that constituted a ROH ( $l$ ) was calculated with the method proposed by Lencz et al. (2007):

$$l = \frac{\log_e \frac{\alpha}{n_s \times n_i}}{\log_e (1 - het)}$$

where  $n_s$  is the number of SNPs per individual,  $n_i$  is the number of individuals,  $\alpha$  is the percentage of false positive ROH (set to 0.05) and  $het$  is the mean SNP heterozygosity across all SNPs. The density of SNPs was set to one SNP for each 100 Kb, and a maximum distance of 250 Kb was allowed between two consecutive SNPs. We considered four ROH categories that were defined according to ROH length: 1-5 Mb, 5-15 Mb, 15-30 Mb and >30 Mb. For each category, the mean sum of ROH per breed was calculated by adding all ROH detected in a given individual. These individual totals were averaged within breeds. Following McQuillan et al. (2008), the inbreeding coefficient based on ROH ( $F_{ROH}$ ) was estimated as the total length of ROH ( $L_{ROH}$ ) divided by the length of the genome covered by SNPs ( $L_{auto}$ ):

$$F_{ROH} = \frac{\sum L_{ROH}}{L_{auto}}$$

Summary statistics for the total ROH found in Spanish sheep breeds were estimated, and Pearson correlations between current population size and average ROH length or mean number of ROH per breed were computed with R (R Core Team, 2018).

#### *Identification of ROH hotspots*

Regions of the genome most commonly associated with ROH (ROH hotspots) were identified by counting the occurrences of each SNP within a given ROH, and the identification of ROH hotspots was performed across breeds. Regions containing the

top 1% of SNPs most commonly associated with ROH were classified as ROH hotspots (Purfield et al., 2017; Mastrangelo et al., 2018). The BioMart tool from the Ensembl database (Kinsella et al., 2011) was used to identify genes mapping to ROH hotspots based on the annotations of the ovine Oar\_v3.1 reference genome (Archibald et al., 2010). Functional annotation of the genes was performed with the DAVID bioinformatics resources 6.8 database (Huang et al. 2009<sup>a,b</sup>) and the UniProt database (Chen et al., 2017). An enrichment score of 1.3 was set as the threshold for establishing cluster significance (Huang et al., 2007).

## Results

### *Population structure and effective population size*

After filtering the data, 41,491 SNPs and 1,204 sheep were selected to perform the population structure analyses. The expected ( $H_e$ ) and observed ( $H_o$ ) heterozygosities reached similar values in all breeds (**Supplementary Table 2**). The  $H_e$  values ranged from 0.31 (Sakiz) to 0.38 (Rasa Aragonesa), whereas  $H_o$  oscillated between 0.30 (East Friesian) and 0.39 (Rasa Aragonesa). The broad majority of  $F_{ST}$  values were low ( $F_{ST} = 0.00-0.05$ ) or moderate ( $F_{ST} = 0.05-0.15$ ) indicating the absence of a strong population structure (**Figure 1A, Supplementary Table 2**). This observation was also valid for the comparison between Spanish and North African breeds, which showed a moderate genetic differentiation (the average  $F_{ST}$  between Spanish and North African breeds was 0.047). Two of the breeds showing the highest levels of genetic differentiation were East Friesian and Canaria de Pelo, with averaged  $F_{ST}$  values of 0.156 and 0.107 (when compared to other breeds), respectively.



The population structure of the eleven Spanish ovine breeds analyzed in the current work was previously reported by Manunza et al. (2016). We repeated this analysis in our study by adding data from sheep from North Africa (Egypt and Algeria), Europe (Italy, Switzerland, France, Germany, Greece and Cyprus), the Near East (Iran and Turkey) and Oceania (Australia). The wPCAs shown in **Figure 2** (all populations) and **Supplementary Figure 1** (only European populations) indicated that breeds generally clustered according to their geographic origin. Indeed, the majority of Spanish breeds grouped with the European breeds. Of note, Roja Mallorquina and Canaria de Pelo sheep were separated from the main European cluster (**Figure 2**), and the distance between Canaria de Pelo and North African breeds was smaller than that between Canaria de Pelo and the main European cluster. We also observed that the Latxa breed showed a closer affinity to Lacaune and Merino Landschaf breeds than to other Spanish ovine populations. Two Greek breeds, Chios and Cyprus fat tail, showed a high similarity to Near Eastern breeds, a result that could be attributed to the short geographic distance between Turkey and the islands of Chios and Cyprus.

The ancestry of each animal was analyzed by using Admixture. The K-value with the lowest cross-validation error corresponded to  $K = 33$  (**Supplementary Figure 2**), showing that the most likely number of ancestral populations agrees well with the true number of populations ( $N = 33$ ). This analysis indicated that the genetic background of the eleven Spanish breeds is remarkably complex and that the two insular breeds (Roja Mallorquina and Canaria de Pelo) show a marked genetic distinctiveness when compared to their Spanish peninsular counterparts (**Figure 1B**, **Supplementary Figures 3 and 4**). In all Spanish ovine breeds, the effective population size ( $N_e$ ) decreased over time (**Figure 3**). The largest historical  $N_e$  corresponded to the Churra, one of the studied Spanish sheep breeds with the largest current population size.

The contemporary  $N_e$  (13 generations ago) oscillated between 59 in Segureña and 194 in Churra (**Figure 3**).

#### *Abundance and length of runs of homozygosity.*

In total, 5,540 ROH of varying lengths were detected in the 11 Spanish sheep breeds. The average number of ROH per individual was 16.05, and the average number of ROH per breed ranged from 2.45 in Rasa Aragonesa to 32.66 in Canaria de Pelo (**Table 1**). The longest ROH measured 55.89 Mb, the shortest one 1.98 Mb, and the average ROH length was 6.104 Mb. The majority of sheep had less than 50 ROH, and the total ROH length was below 350 Mb, showing low levels of homozygosity. Only a few individuals from the Gallega, Churra and Canaria de Pelo breeds showed higher numbers of ROH as well as longer fractions of their genomes covered by ROH (**Figure 4, Supplementary Figure 5**).

The length of ROH analysis showed that the majority (4,569 ROH) were shorter than 10 Mb, while only 971 were longer than 10 Mb. A total of 2,809 ROH were shorter than 5 Mb, 2,335 had a length between 5 and 15 Mb, 368 measured between 15-30 Mb and only 28 were longer than 30 Mb (**Figure 5**). When we calculated the correlations between the current population size of the 11 Spanish sheep breeds and the average length of ROH and the mean number of ROH per individual, we obtained values of -0.557 ( $P$ -value = 0.07) and -0.475 ( $P$ -value = 0.13), respectively. The inbreeding  $F_{ROH}$  coefficients, which indicate the proportion of the autosomal genome covered by ROH, were generally low to moderate ( $F_{ROH} < 0.10$ ) and displayed some level of variation across breeds (**Table 1** and **Figure 6**) *i.e.* from 0.008 (Rasa Aragonesa) to 0.086 (Canaria de Pelo).

## *Detection of ROH hotspots*

By counting the incidence of SNPs in ROH, several genomic regions were identified as potential ROH hotspots. The maximum frequency of SNPs in ROH was 11.65%. Twenty one regions on chromosomes 3, 6, 8, 10, 16, 19 and 25 were detected as containing putative ROH hotspots (**Supplementary Tables 3 and 4, Figure 7**), and they harbored 120 genes (**Supplementary Table 4**). Classification of genes located within ROH hotspots with DAVID analysis revealed seven significant clusters related to cell growth, immune response, cell junction and gamete and sexual cell growth and differentiation (**Supplementary Table 5**). As shown in **Supplementary Table 6**, we also compared the locations of the ROH hotspots found in our study with those identified by other authors. Such comparative analysis revealed that the positional concordance of ROH hotspots across different studies is considerably low.

## **Discussion**

In a previous study, Manunza et al. (2016) reported the population structure of eleven Spanish ovine breeds and performed a genome scan that demonstrated the existence of several selective sweeps. The current work is based on the same data set, but here we characterized the amount and patterns of homozygosity of these eleven breeds. Moreover, we investigated the relationships between these Spanish ovine breeds and other sheep populations from Europe, Asia and Africa. The sample size of the majority of the Spanish ovine breeds analyzed in the current work was in the range of 20-30 individuals. However, limited sample size was compensated for by the analysis of many markers (Willing et al., 2012; Nazareno et al., 2017). As a whole, we observed that the population structure of the 11 Spanish sheep breeds is not strong and ancestries

are complex (**Figures 1A, 1B and 2, Supplementary Figures 3 and 4**). These results agree well with data reported by others (Kijas et al., 2012) showing high levels of admixture in a worldwide sample of sheep breeds. The wPCAs shown in **Figure 2** and **Supplementary Figure 1** also demonstrate that the majority of Spanish breeds cluster with the European breeds. One of the exceptions to this general trend was Canaria de Pelo, which showed a closer relation to African breeds (**Figure 2**). This result might indicate that Canaria de Pelo has an African ancestry, as most hair sheep do (Muigai & Hanotte, 2013). Indeed, there is broad archaeological and linguistic evidence that the first settlers of the Canary Islands had an African origin (Maca-Meyer et al., 2004). Moreover, a worldwide analysis of the genetic diversity of goat populations showed that Canarian goat breeds have an African origin (Colli et al., 2018). We also observed a certain degree of separation between Roja Mallorquina and Comisana sheep, two insular breeds from Mallorca and Sicily, respectively, and the main European cluster (**Figure 2**). This suggests a process of genetic differentiation that could be the consequence of founder effects combined with geographic isolation.

We also detected a decline in the effective sizes of all Spanish populations under study (**Figure 3**), a feature that could have adverse effects on their production performance (Ragab et al., 2015). Such trend has also been evidenced in six commercial ovine breeds (Belclare, Beltex, Charollais, Suffolk, Texel and Vendeen) by Purfield et al. (2017), who showed a decrease in  $N_e$  followed by a period of stabilization in the last 50 generations. Chitneedi et al. (2017) also observed a reduction in the  $N_e$  of the Churra breed, but they warned that the accuracy of such estimates depends on the density of the chip. In Spain, historical accounts indicate that there were approximately 17.6 million sheep in 1799, and this number increased to 22.5 million in 1865 and almost to 24 million in 1940 (Estévez, 1990). However, in the last seven decades, the population of

Spanish sheep decreased to 15 million heads (<https://www.oviespana.com/informacion-de-ovino/estadisticas-de-ovino/censo-de-ovino-en-espana-2015>) due to the progressive abandonment of rural activities and increases in the price of feeding and diesel oil that negatively impacts the profitability of sheep farms.

We wanted to determine whether this decline of effective size involved an increase in inbreeding and homozygosity levels. Our results indicate that, with few exceptions, the number ( $< 50$ ) and the total length of ROH ( $< 350$  Mb) are remarkably low in Spanish sheep (**Figure 4 and Supplementary Figure 5**). Only a few Gallega, Canaria de Pelo and Churra sheep showed a relatively moderate to high ROH genomic coverage, but the significance of such finding is quite circumstantial. Similar results were obtained by Purfield et al. (2017) and Mastrangelo et al. (2018). We have also observed that very long ROH ( $> 30$  Mb) are quite rare in Spanish ovine breeds (**Figure 5**), highlighting the absence of recent inbreeding. The same pattern was observed by Al-Mamun et al. (2015) and Mastrangelo et al. (2018) in Australian and Italian sheep, respectively. The correlation coefficients between current population size and the average length ( $r = -0.557$ ,  $P$ -value = 0.07) and mean number of identified ROH ( $r = -0.475$ ,  $P$ -value = 0.13) were moderate and negative, but they did not reach statistical significance. However, this inverse relationship between population size and homozygosity is consistent with previous studies indicating that demography has a prominent role in shaping homozygosity patterns (Bosse et al., 2012).

In the eleven Spanish breeds,  $F_{ROH}$  values were below 0.10, confirming the existence of low levels of inbreeding (**Table 1 and Figure 6**). Similar  $F_{ROH}$  values were found in 21 Italian sheep breeds by Mastrangelo et al. (2018) as well as in the Churra breed by Chitneedi et al. (2017). In general, the population sizes of the Spanish ovine breeds (MAPA, <https://www.mapa.gob.es/es/ganaderia/temas/zootecnia/razas->

ganaderas/razas/ catalogo/) analyzed by us are in the range of a few thousands (Canaria de Pelo, Gallega and Roja Mallorquina), tens of thousands (Castellana, Latxa, Ojalada, Ripollesa and Xisqueta) and hundreds of thousands (Churra, Rasa Aragonesa and Segureña). According to the Spanish Ministry of Agriculture, Fisheries and Food (MAPA, <https://www.mapa.gob.es/es/ganaderia/temas/zootecnia/razas-ganaderas/razas/>), the number of farms raising these ovine breeds ranges from 15 (Ojalada) to 476 (Rasa Aragonesa), with an average of 132 farms per breed (**Supplementary Table 1**). This broad distribution of sheep in multiple farms combined with an extensive management and limited use of artificial insemination in the last decades has probably contributed to minimizing inbreeding.

The maximum frequency of SNPs in ROH was approximately 8-11% (**Supplementary Table 3 and 4, Figure 7**). Similarly, in the study of Mastrangelo et al. (2018), the incidence of SNPs in ROH also fluctuated around 10%, with the notable exception of a region on Oar6 which reached 15%. In contrast, Purfield et al. (2017) detected SNPs with incidences of 20% and, only in one case (Oar2, 7.04 Mb) it was near 40%. In humans (Pemberton et al., 2012) and cattle (Purfield et al., 2012), ROH hotspots with frequencies above 40% are more frequent than in sheep. Thus, the limited homozygosity of sheep makes it difficult to identify regions of the genome containing ROH at moderate to high frequencies. Moreover, the positional concordance of the putative ROH hotspots reported by us and those detected by other authors is very low (**Supplementary Table 6**), meaning that the evolutionary conservation of ovine ROH hotspots is quite limited. This lack of positional coincidence challenges the very same classification of these genomic regions as *bona fide* ROH hotspots, and it may have technical (*e.g.*, searching parameters to detect ROH) and biological causes. One of the main forces driving the generation of ROH hotspots is a low recombination rate (Bosse

et al., 2012). However, recombination rates are variable across individuals, populations and species (Smukowski & Noor, 2011), and the causative factors of such variability are largely unknown. Moreover, a recent study demonstrated that a significant proportion of ROH islands or hotspots detected in the bovine genome are artifacts due to gaps in SNP coverage as well as to structural variations such as deletions (Nandolo et al., 2018).

When we classified the functions of genes mapping to putative ROH hotspots (**Supplementary Table 4**), we obtained seven significant clusters with loci involved in immune response, behavior, cell proliferation and growth, and sexual cell growth and differentiation (**Supplementary Table 5**). Interestingly, we detected a ROH hotspot (Oar6, 38.61 – 38.63 Mb) located very close to the position of the *NCAPG-LCORL* genes (Oar6 37.27 - 37.45 Mb). This region was also reported by Manunza et al. (2016) as being under selection in Spanish sheep. Moreover, selective sweeps in the *NCAPG-LCORL* region have been reported in pigs and dogs, and this region is also associated with height in humans and horses (reviewed by Takasuga 2015). The ligand dependent nuclear receptor corepressor like (*LCORL*) gene encodes a transcription factor that activates the transcription of spermatocyte-specific genes during the meiotic stage (Kunieda et al., 2002). The non-SMC condensin I complex, subunit G (*NCAPG*) gene encodes a subunit of the condensin complex which is responsible for the condensation and stabilization of chromosomes during mitosis and meiosis (Kimura et al., 2001). The polymorphism of the *NCAPG* gene is associated with fetal and carcass growth in cattle (Lindholm-Perry et al., 2013), and both *NCAPG* and *LCORL* genotypes were found to be associated with body weight in Merino sheep (Al-Mamun et al., 2015) and with stature in cattle (Bouwman et al., 2018). Additionally, multiple QTLs for carcass, weaning and birth weight, feed intake and average daily gain have been reported to colocalize with the *NCAPG/LCORL* region in cattle. Taken together, these results

indicate that the ROH hotspot found on Oar 6 (38.61-38.63 Mb) in Spanish sheep might have been caused by artificial selection for body size acting on the *NCAPG/LCORL* genes.

The main conclusion that can be derived from our work is that autochthonous Spanish sheep breeds display low levels of homozygosity. Moreover, the low incidence of very long ROH also indicates the absence of recent inbreeding. These results are encouraging from a conservation genetics perspective, because there is evidence that ROH tend to be enriched in deleterious mutations both in humans (Szpiech et al., 2013) and cattle (Zhang et al., 2015). We also conclude that ROH hotspots in sheep are scarce and show a low positional concordance among studies, implying that they have likely been produced by evolutionary factors acting on a local scale as well as by the specific searching parameters employed in each study.

## Acknowledgments

Thanks to Jorge Hugo Calvo from the Centro de Investigación y Tecnología Agroalimentaria de Aragón for providing 50K data from several sheep breeds and critically revising the manuscript. This research was partially funded by a grant (RZ2011-00015-C03-01) from the Instituto Nacional de Investigación y Tecnología Agraria y Alimentaria (Spain). We acknowledge the support of the Spanish Ministerio de Economía y Competitividad for the *Centro de Excelencia Severo Ochoa 2016–2019* award SEV-2015-0533 and the CERCA Programme of the Generalitat de Catalunya. Many thanks to the International Sheep Genomics Consortium and especially to Dr. Hans Lenstra for kindly providing ovine 50K data. Taina F Cardoso was funded with a fellowship from the CAPES Foundation-Coordination of Improvement of Higher Education, Ministry of Education (MEC) of the Federal



Government of Brazil. The authors are grateful to the Canaria de Pelo, Gallega Ripollesa, Roja Mallorquina and Xisqueta breeding associations for their collaboration in sample collection.

## References

- Alexander D.H., & Lange K. (2011) Enhancements to the ADMIXTURE algorithm for individual ancestry estimation. *BMC Bioinformatics* **12**, 246.
- Alexander D. H., Novembre, J., & Lange K. (2009) Fast model-based estimation of ancestry in unrelated individuals. *Genome Research* **19**, 1655–4.
- Al-Mamun H.A., Kwan P., Clark S.A., Ferdosi M.H., Tellam R., & Gondro C. (2015) Genome-wide association study of body weight in Australian Merino sheep reveals an orthologous region on OAR6 to human and bovine genomic regions affecting height and weight. *Genetics Selection Evolution* **47**, 66.
- Archibald A.L., Cockett N.E., Dalrymple B.P., Faraut T., Kijas J.W., Maddox J.F., McEwan J.C., Hutton-Oddy V., Raadsma H.W., Wade C., Wang J., Wang W., Xun X. (2010) The sheep genome reference sequence: a work in progress. *Animal Genetics* **41**, 449–53.
- Barbato M., Orozco-terWengel P., Tapio M., & Bruford M.W. (2015) SNeP: a tool to estimate trends in recent effective population size trajectories using genome-wide SNP data. *Frontiers in Genetics* **6**, 109.
- Bosse M., Megens H.J., Madsen O., Paudel Y., Frantz L.A.F., Schook L.B., Crooijmans R.P.M.A., Groenen M.A.M. (2012) Regions of homozygosity in the porcine genome: consequence of demography and the recombination landscape. *PLoS Genetics* **8**, e1003100.

418 Bouwman A. C., Daetwyler H. D., Chamberlain A. J., Ponce C.H., Sargolzaei M.,  
 419 Schenkel F.S., Sahana G., Govignon-Gion A., Boitard S., Dolezal M., Pausch  
 420 H., Brøndum R.F., Bowman P.J., Thomsen B., Guldbrandtsen B., Lund M.S.,  
 421 Servin B., Garrick D.J., Reecy J., Vilkki J., Bagnato A., Wang M., Hoff J.L.,  
 422 Schnabel R.D., Taylor J.F., Vinkhuyzen A.A.E., Panitz F., Bendixen C., Holm  
 423 L., Gredler B., Hozé C., Boussaha M., Sanchez M.P., Rocha D., Capitan A.,  
 424 Tribout T., Barbat A., Croiseau P., Drögemüller C., Jagannathan V., Vander Jagt  
 425 C., Crowley J.J., Bieber A., Purfield D.C., Berry D.P., Emmerling R., Götz K.,  
 426 Frischknecht M., Russ I., Sölkner J., Van Tassell C.P., Fries R., Stothard P.,  
 427 Veerkamp R.F., Boichard D., Goddard M.E., & Hayes, B. J. (2018) Meta-  
 428 analysis of genome-wide association studies for cattle stature identifies common  
 429 genes that regulate body size in mammals. *Nature Genetics* **50**, 362-7.  
 430 Burgos-Paz W., Ramos-Onsins S. E., Pérez-Enciso M., & Ferretti L. (2014) Correcting  
 431 for unequal sampling in principal component analysis of genetic data.  
 432 Proceedings of the 10<sup>th</sup> World Congress of Genetics Applied to Livestock  
 433 Production (Vancouver, Canada).  
 434 Ceballos F.C., Joshi P.K., Clark D.W., Ramsay M., & Wilson J.F. (2018) Runs of  
 435 homozygosity: windows into population history and trait architecture. *Nature*  
 436 *Reviews Genetics* **19**, 220-34.  
 437 Chang C.C., Chow C.C., Tellier L.C., Vattikuti S., Purcell S.M., & Lee J.J. (2015)  
 438 Second-generation PLINK: rising to the challenge of larger and richer datasets.  
 439 *GigaScience* **4**, 7.  
 440 Chen B., Cole J.W., & Grond-Ginsbach C. (2017) Departure from Hardy Weinberg  
 441 equilibrium and genotyping error. *Frontiers in Genetics* **8**, 167.

442 Chen C., Huang H., & Wu C.H. (2017) Protein bioinformatics databases and resources.  
 443 *Methods Mol Biol* **1558**, 3–39.

444 Chitneedi P. K., Arranz J.J., Suarez-Vega A., García-Gámez E., & Gutiérrez-Gil B.  
 445 (2017) Estimations of linkage disequilibrium, effective population size and  
 446 ROH-based inbreeding coefficients in Spanish Churra sheep using imputed  
 447 high-density SNP genotypes. *Animal Genetics* **48**, 436–46.

448 Ciani E., Lasagna E., D’Andrea M., Alloggio I., Marroni F., Ceccobelli, S., Bermejo  
 449 J.V., Sarti F.M., Kijas J., Lenstra J.A., Pilla F., & the International Sheep  
 450 Genomics Consortium. (2015) Merino and Merino-derived sheep breeds: a  
 451 genome-wide intercontinental study. *Genetics Selection Evolution* **47**, 64.

452 Colli L., Milanesi, M. Talenti A., Bertolini F., Chen M., Crisà A., Daly K.G., Del Corvo  
 453 M., Guldbrandtsen B., Lenstra J.A., Rosen B.D., Vajana E., Catillo G., Joost S.,  
 454 Nicolazzi E.L., Rochat E., Rothschild M.F., Servin B., Sonstegard T.S., Steri R.,  
 455 Van Tassel C.P., Ajmone-Marsan P., Crepaldi P., Stella A., & the AdaptMap  
 456 Consortium. (2018) Genome-wide SNP profiling of worldwide goat populations  
 457 reveals strong partitioning of diversity and highlights post-domestication  
 458 migration routes. *Genetics Selection Evolution* **50**, 58.

459 Estévez J. (1990) El ganado ovino en la historia de España, Anales de la Real Academia  
 460 de Ciencias Veterinarias de Andalucía Oriental 2, Huéscar - Granada, pp. 21-46.

461 Excoffier L., Laval G., & Schneider S. (2007) Arlequin (version 3.0): An integrated  
 462 software package for population genetics data analysis. *Evolutionary*  
 463 *Bioinformatics* **1**, 47–50.

464 Gaouar S.B., Lafri M., Djaout A., El-Bouyahiaoui R., Bouri A., Bouchatal A., Maftah  
 465 A., Ciani E., & Da Silva A.B. (2017) Genome-wide analysis highlights genetic  
 466 dilution in Algerian sheep. *Heredity* **118**, 293–301.

467 Huang D.W., Sherman B.T., Tan Q., Collins J.R., Alvord W.G., Roayaei, J., Stephens  
468 R., Baseler M.W., Lane H.C., & Lempicki R.A. (2007) The DAVID Gene  
469 Functional Classification Tool: a novel biological module-centric algorithm to  
470 functionally analyze large gene lists. *Genome Biology* **8**, R183.

471 Huang D.W., Sherman B.T., & Lempicki R.A. (2009<sup>a</sup>) Bioinformatics enrichment tools:  
472 paths toward the comprehensive functional analysis of large gene lists. *Nucleic  
473 Acids Research* **37**, 1–13.

474 Huang D.W., Sherman B.T., & Lempicki R.A. (2009<sup>b</sup>) Systematic and integrative  
475 analysis of large gene lists using DAVID bioinformatics resources. *Nature  
476 Protocols* **4**, 44–57.

477 Kijas J. W., Lenstra J.A., Hayes B., Boitard S., Porto-Neto L.R., San Cristobal M.,  
478 Bertrand S., Russel J.M., Whan V., Gietzen K.J., Paiva S.R., Barendse W., Ciani  
479 E., Raadsma H.W., McEwan J.A., & Dalrymple B.E. (2012) Genome-wide  
480 analysis of the world's sheep breeds reveals high levels of historic mixture and  
481 strong recent selection. *PLoS Biology* **10**, e1001258.

482 Kimura K., Cuvier O., & Hirano T. (2001) Chromosome condensation by a human  
483 condensin complex in *Xenopus* egg extracts. *Journal of Biological Chemistry*  
484 **276**, 5417–20.

485 Kinsella R.J., Kähäri A., Haider S., Zamora J., Proctor G., Spudich G., Almeida-King  
486 J., Staines D., Derwent P., Kerhornou A., Kersey P., & Flicek P. (2011)  
487 Ensembl BioMart: a hub for data retrieval across taxonomic space. *Database*  
488 **2011**, bar030.

489 Kunieda T., Park J.M., Takeuchi H., & Kubo T. (2002) Identification and  
490 characterization of Mlr1,2: two mouse homologues of Mblk-1, a transcription  
491 factor from the honeybee brain. *FEBS Letters* **535**, 61–65.

492 Lencz T., Lambert C., DeRosse P., Burdick K. E., Morgan T.V., Kane J.M.,  
 493 Kucherlapati R., & Malhotra A.K. (2007) Runs of homozygosity reveal highly  
 494 penetrant recessive loci in schizophrenia. *Proceedings of the National Academy*  
 495 *of Sciences of the United States of America* **104**, 19942–7.  
 496 Lindholm-Perry A.K., Kuehn L.A., Oliver W.T., Sexten A.K., Miles J.R., Rempel L.  
 497 A., Cushman R.A., & Freetly H. C. (2013) Adipose and muscle tissue gene  
 498 expression of two genes (*NCAPG* and *LCORL*) located in a chromosomal region  
 499 associated with cattle feed intake and gain. *PloS One* **8**, e80882.  
 500 Maca-Meyer N., Arnay M., Rando J.C., Flores C., González A.M., Cabrera V.M., &  
 501 Larruga J.M. (2004) Ancient mtDNA analysis and the origin of the Guanches.  
 502 *European Journal of Human Genetics* **12**, 155–62.  
 503 Manunza A., Cardoso T.F., Noce A., Martínez A., Pons A., Bermejo L.A., Landi V.,  
 504 Sánchez A., Jordana J., Delgado J.V., Adán S., Capote J., Vidal O., Ugarte E.,  
 505 Arranz J.J., Calvo J.H., Casellas J., & Amills M. (2016) Population structure of  
 506 eleven Spanish ovine breeds and detection of selective sweeps with BayeScan  
 507 and hapFLK. *Scientific Reports* **6**, 27296.  
 508 Mastrangelo S., Ciani E., Sardina M. T., Sottile G., Pilla F., Portolano B., & Bi.Ov. Ita  
 509 Consortium. (2018) Runs of homozygosity reveal genome-wide autozygosity in  
 510 Italian sheep breeds. *Animal Genetics* **49**, 71–81.  
 511 McQuillan R., Leutenegger A.L., Abdel-Rahman R., Franklin C. S., Pericic M., Barac-  
 512 Lauc L., Smolej-Narancic N., Janicijevic B., Polasek O., Tenesa A., MacLeod  
 513 A.K., Farrington S.M., Rudan P., Hayward C., Vitart V., Rudan I., Wild S.H.,  
 514 Dunlop M.G., Wright A.F., Campbell H., & Wilson J. F. (2008) Runs of  
 515 homozygosity in European populations. *American Journal of Human Genetics*  
 516 **83**, 359–72.

- Muigai A. W. T., & Hanotte O. (2013) The origin of African sheep: archaeological and genetic perspectives. *The African Archaeological Review* **30**, 39–50.
- Nandolo W., Utsunomiya Y.T., Mészáros G., Wurzinger M., Khayadzadeh N., Torrecilha R.B.P., Mulindwa H.A., Gondwe T.N., Waldmann P., Ferenčaković M., Garcia J.F., Rosen BD., Bickhart D., van Tassell C.P., Curik I., & Sölkner J. (2018) Misidentification of runs of homozygosity islands in cattle caused by interference with copy number variation or large intermarker distances. *Genetics Selection Evolution* **50**, 43.
- Nazareno A.G., Bemmels J. B., Dick C.W. & Lohmann L.G. (2017) Minimum sample sizes for population genomics: an empirical study from an Amazonian plant species. *Molecular Ecology Resources* **17**, 1136–47.
- Pemberton T. J., Absher D., Feldman M.W., Myers R.M., Rosenberg N.A., & Li J.Z. (2012) Genomic patterns of homozygosity in worldwide human populations. *American Journal of Human Genetics* **91**, 275–92.
- Peripolli E., Munari D.P., Silva M.V.G.B., Lima A.L.F., Irgang R., & Baldi F. (2017) Runs of homozygosity: current knowledge and applications in livestock. *Animal Genetics* **48**, 255–71.
- Purfield D.C., Berry D.P., McParland S., & Bradley D.G. (2012) Runs of homozygosity and population history in cattle. *BMC Genetics* **13**, 70.
- Purfield D.C., McParland S., Wall E., & Berry D.P. (2017) The distribution of runs of homozygosity and selection signatures in six commercial meat sheep breeds. *PLoS ONE* **12**, e0176780.
- Ragab M., Sánchez J.P., & Baselga M. (2015) Effective population size and inbreeding depression on litter size in rabbits. A case study. *Journal of Animal Breeding and Genetics* **132**, 68–73.

- R Core Team (2018) R: A language and environment for statistical computing. R Foundation for Statistical Computing, Vienna, Austria.
- Smukowski C.S., & Noor M.A.F. (2011) Recombination rate variation in closely related species. *Heredity* **107**, 496–508.
- Szpiech Z.A., Xu J., Pemberton T. J., Peng W., Zöllner S., Rosenberg N.A., & Li J.Z. (2013) Long runs of homozygosity are enriched for deleterious variation. *American Journal of Human Genetics* **93**, 90–102.
- Takasuga A. (2015) PLAG1 and NCAPG-LCORL in livestock. *Animal Science Journal* **87**, 159–67.
- Wang G.D., Xie H.B., Peng M.S., Irwin D., & Zhang Y.P. (2014) Domestication genomics: evidence from animals. *Annual Review of Animal Biosciences* **2**, 65–84.
- Willing E.M., Dreyer C., & Van Oosterhout C. (2012) Estimates of genetic differentiation measured by  $F_{ST}$  do not necessarily require large sample sizes when using many SNP markers. *PLoS ONE* **7**, e42649.
- Zhang Q., Calus M.P., Guldbrandtsen B., Lund M.S., & Sahana G. (2015) Estimation of inbreeding using pedigree, 50k SNP chip genotypes and full sequence data in three cattle breeds. *BMC Genetics* **16**, 88.

**Table 1.** Descriptive statistics of ROH and inbreeding coefficients based on ROH ( $F_{ROH}$ ) identified in 11 Spanish sheep breeds<sup>1</sup>.

<b>FID</b>	<b>AL<sub>ROH</sub></b>	<b>NT<sub>ROH</sub></b>	<b>MN<sub>ROH</sub></b>	<b>F<sub>ROH</sub></b>
<b>Canaria</b>	6.426 ± 4.659	882	32.667	0.086 ± 0.052
<b>Castellana</b>	6.994 ± 4.584	170	7.391	0.023 ± 0.017
<b>Churra</b>	6.645 ± 4.963	2201	18.342	0.050 ± 0.041
<b>Gallega</b>	9.076 ± 6.776	421	16.84	0.075 ± 0.103
<b>Latxa</b>	5.941 ± 4.715	648	16.2	0.039 ± 0.031
<b>Ojalada</b>	7.491 ± 4.769	171	7.125	0.025 ± 0.021
<b>Rasa Aragonesa</b>	5.305 ± 2.607	54	2.455	0.044 ± 0.032
<b>Ripollesa</b>	7.360 ± 5.790	283	12.304	0.008 ± 0.012
<b>Roja Mallorquina</b>	5.970 ± 3.995	520	17.931	0.037 ± 0.033
<b>Segureña</b>	6.982 ± 6.282	71	5.917	0.017 ± 0.026
<b>Xisqueta</b>	7.323 ± 6.162	119	4.958	0.022 ± 0.029

<sup>1</sup>AL<sub>ROH</sub>, average length (in Mb) of ROH per individual and breed; NT<sub>ROH</sub>, average number of ROH found per breed; MN<sub>ROH</sub>, mean number of ROH per individual and breed; F<sub>ROH</sub>, inbreeding coefficient based on ROH.



## Legends to Figures

**Figure 1.** Population structure of 11 Spanish sheep breeds and reference populations from other countries of Europe (Italy, Switzerland, Greece, Cyprus, France and Germany), North Africa (Algeria and Egypt), Central Africa (Ethiopia and Kenya) and Near East (Iran and Turkey), **A.** Heatmap depicting the  $F_{ST}$  coefficients amongst pairs of ovine breeds. **B.** Ancestry contributions for each one of the breeds under analysis at  $K=33$ .

**Figure 2.** Weighted principal component analysis of 11 Spanish sheep breeds and reference populations from other countries of Europe (Italy, Switzerland, Greece, Cyprus, France and Germany), North Africa (Algeria and Egypt), Central Africa (Ethiopia and Kenya) and Near East (Iran and Turkey).

**Figure 3.** Prediction of the evolution, during the last 225 generations, of the effective population size ( $N_e$ ) of 11 Spanish sheep breeds.

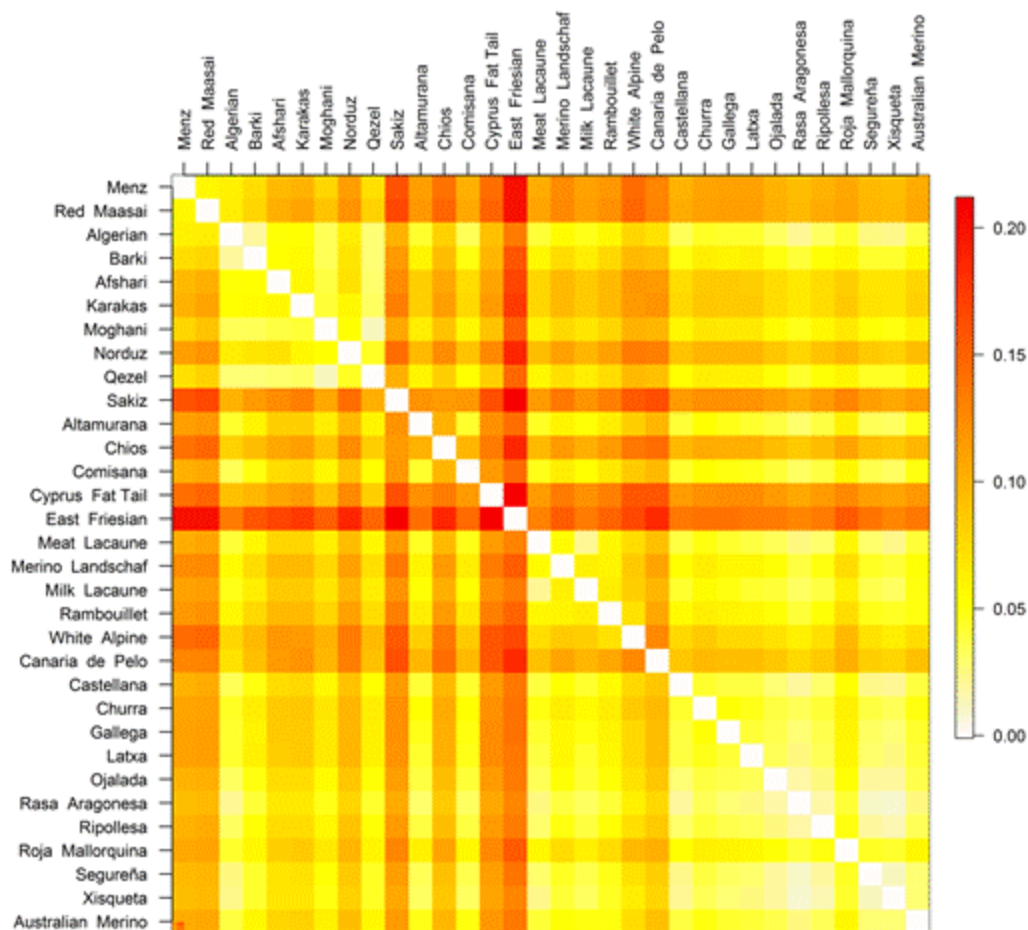
**Figure 4.** Number and total length of ROH found in sheep from 11 Spanish breeds. The number of ROH found per individual genome (*y-axis*) is plotted against ROH total size (*x-axis*).

**Figure 5.** Frequencies of ROH classified according to their size in 11 Spanish sheep breeds.

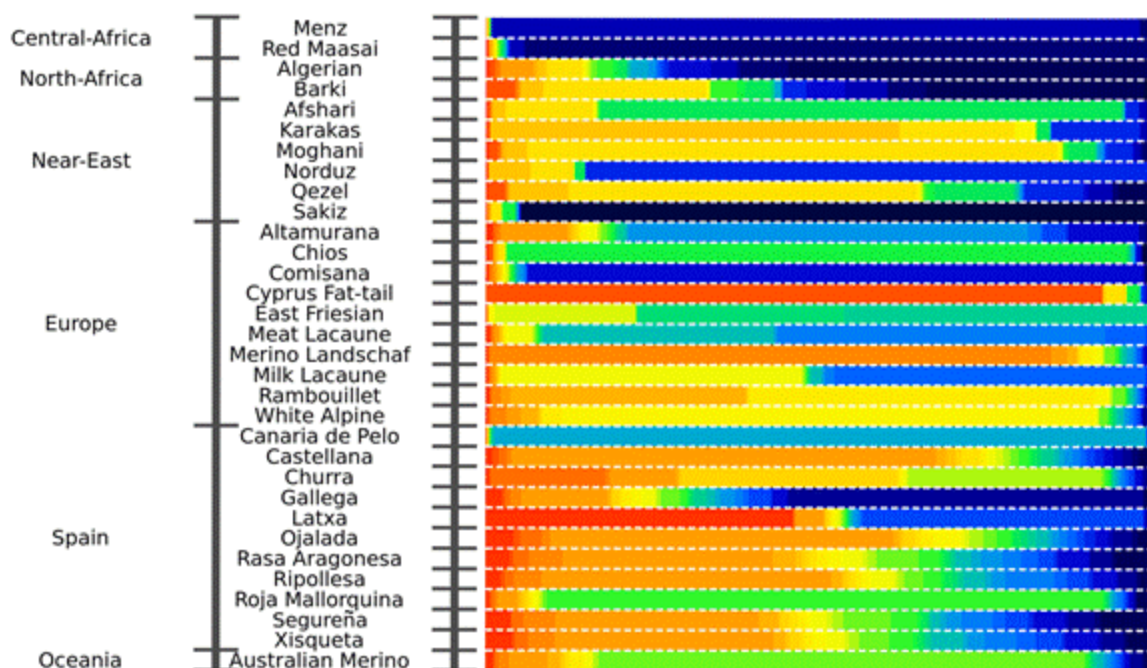
**Figure 6.** Boxplot depicting the magnitude and variation of inbreeding coefficients based on ROH coverage ( $F_{ROH}$ ) and corresponding to 11 Spanish sheep breeds.

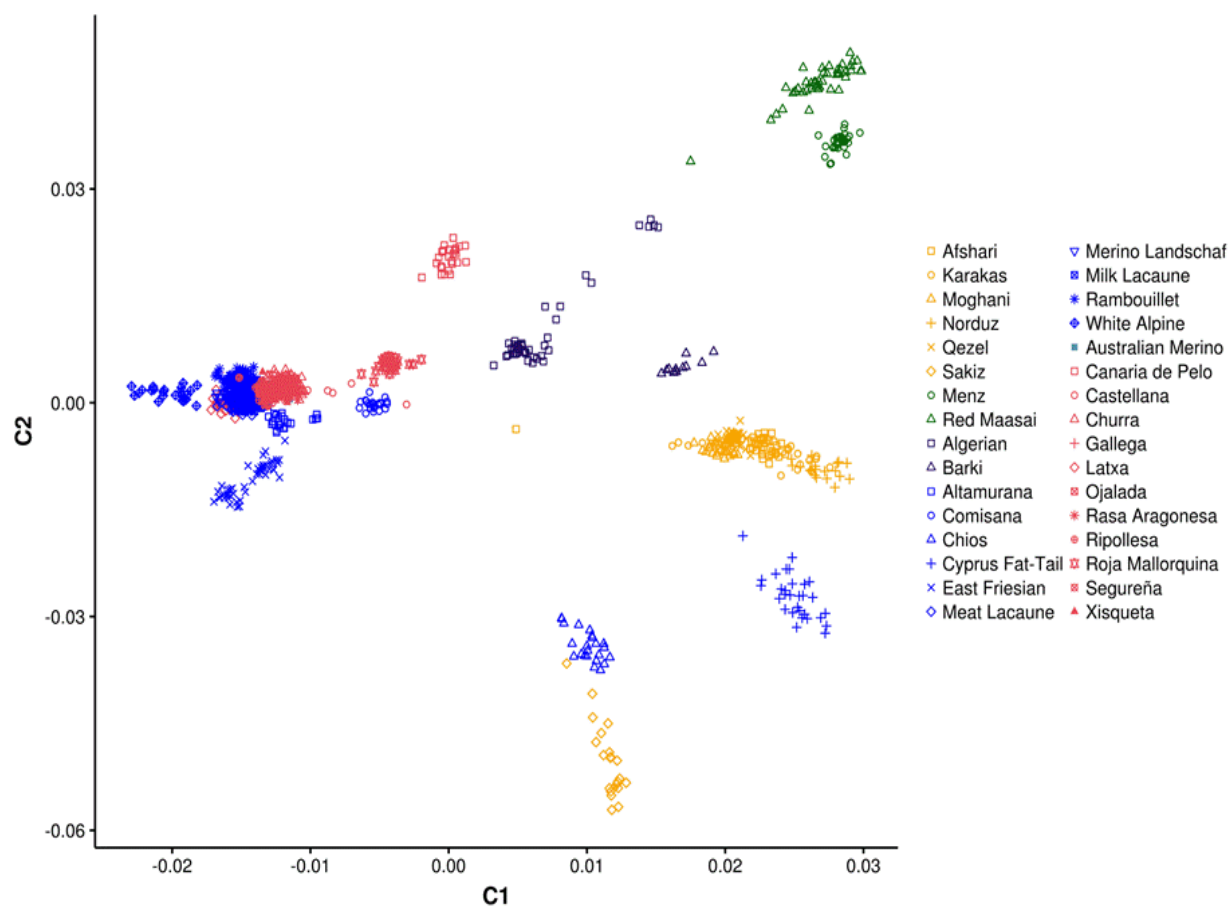
**Figure 7.** Identification of ROH hotspots in 11 Spanish sheep breeds. In the y-axis, we plot the frequency at which a given SNP can be found within a ROH, while in the x-axis we show the positional coordinates of the sheep genome distributed into 26 autosomal chromosomes.

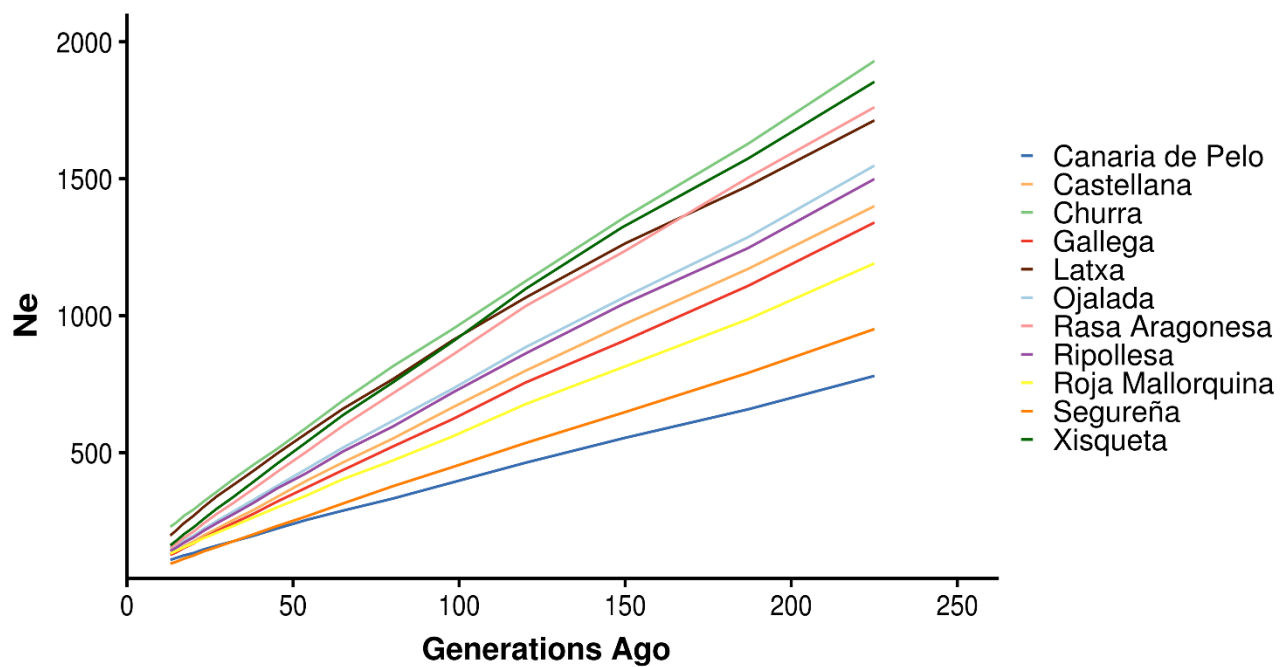
A

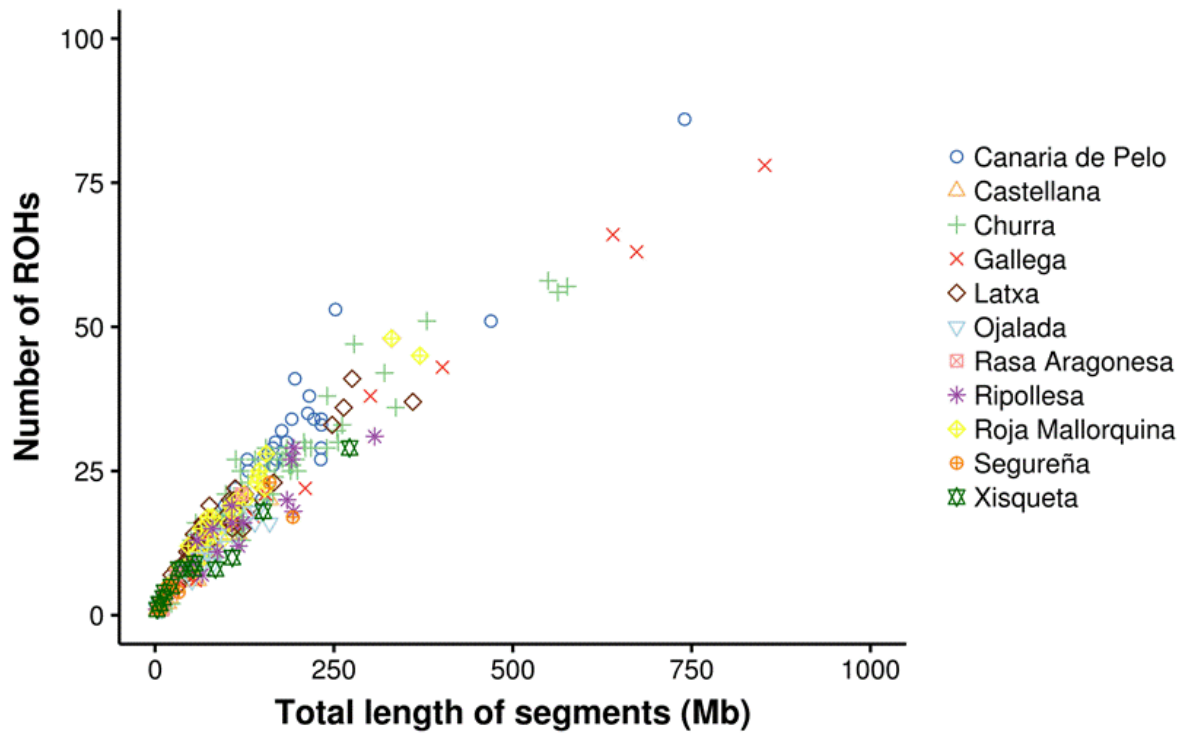


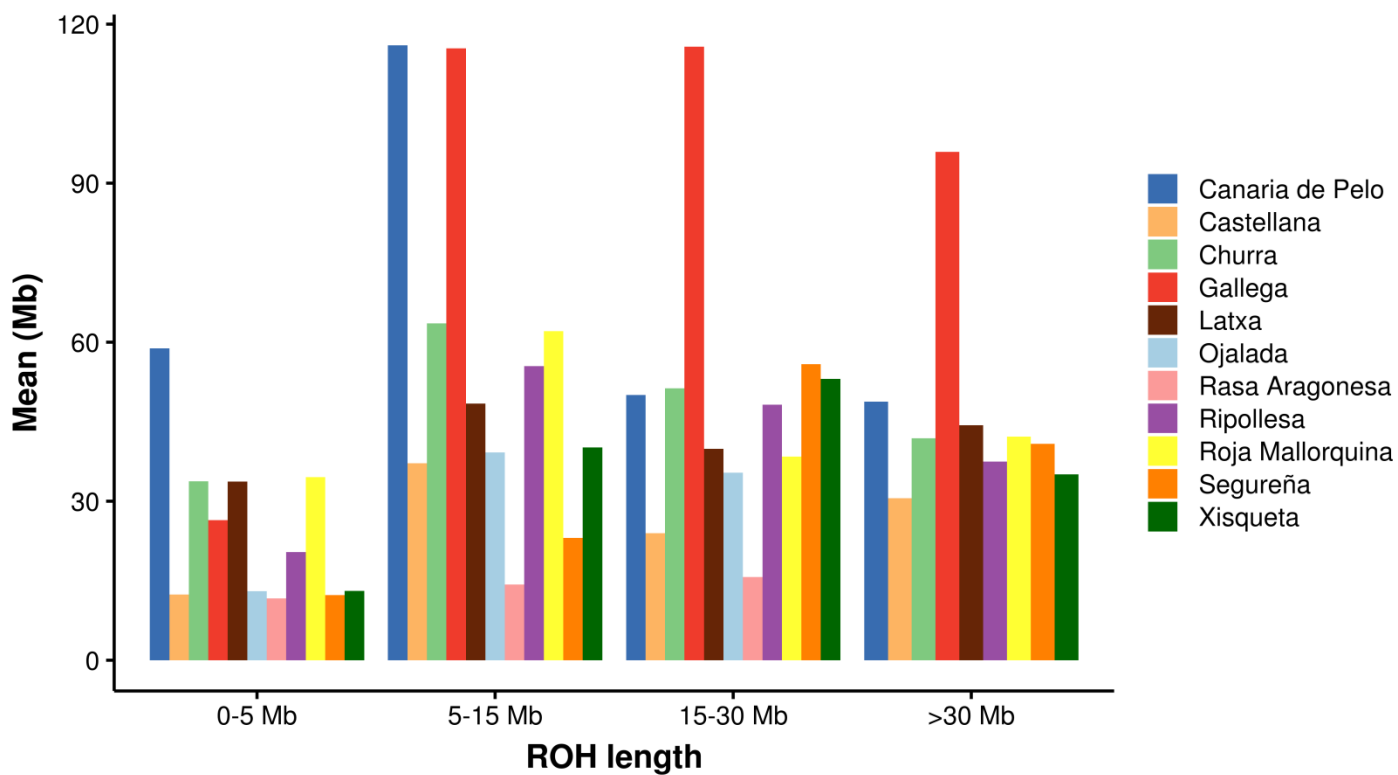
B

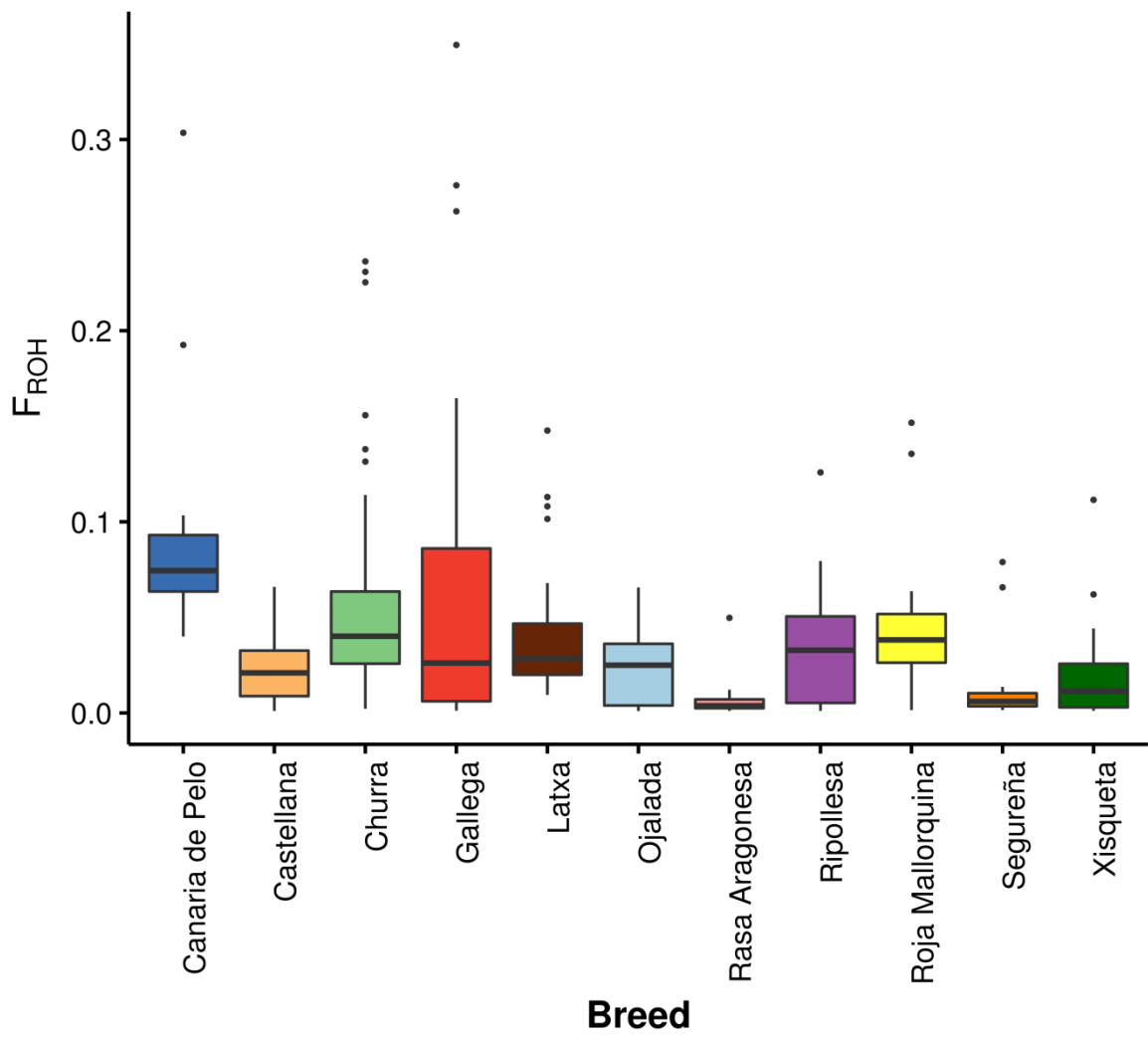




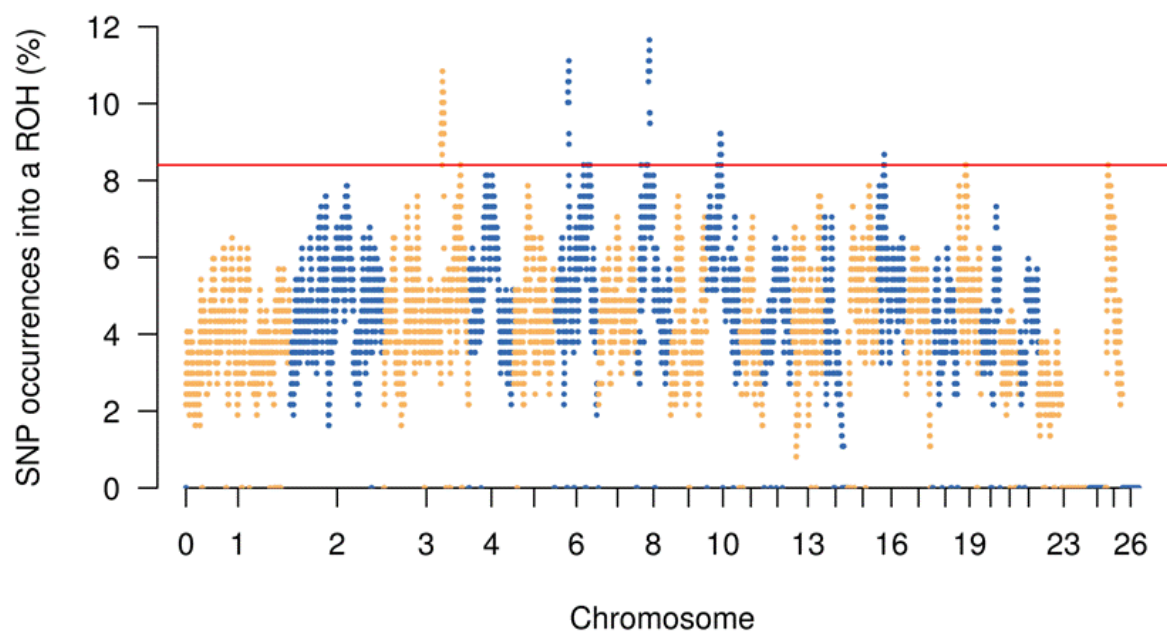












**Supplementary Table 1.** Breeding purpose of 11 Spanish sheep breeds.

<b>Breed</b>	<b>Breeding purpose</b>	<b>Census</b>	<b>Number of farms</b>
<b>Canaria de Pelo</b>	Meat	3,051	26
<b>Castellana</b>	Meat/Milk	54,006	79
<b>Churra</b>	Milk	147,435	124
<b>Gallega</b>	Meat	4,847	102
<b>Latxa</b>	Milk/Wool	86,431	213
<b>Ojalada</b>	Meat	11,325	15
<b>Rasa Aragonesa</b>	Meat	374,197	454
<b>Ripollesa</b>	Meat/Wool	36,467	48
<b>Roja Mallorquina</b>	Meat/Milk	3,912	55
<b>Segureña</b>	Meat	124,106	226
<b>Xisqueta</b>	Meat/Wool	61,277	84

**Supplementary Table 2.** Expected and observed heterozygosities, and pairwise  $F_{ST}$  values amongst 32 populations from Africa, Europe, Middle-East and Oceania.

	Ho*	He*	1	2	3	4	5	6	7	8	9	10	11	12	13	14	15	16	17	18	19	20	21	22	23	24	25	26	27	28	29	30	31	32
1. Menz	0.37	0.37	0																															
2. Red Maasai	0.33	0.32	0.06	0																														
3. Algerian	0.35	0.37	0.06	0.07	0																													
4. Barki	0.35	0.35	0.07	0.08	0.02	0																												
5. Afshari	0.36	0.35	0.1	0.1	0.05	0.05	0																											
6. Karakas	0.36	0.34	0.1	0.11	0.05	0.06	0.06	0																										
7. Moghani	0.37	0.36	0.08	0.09	0.04	0.03	0.04	0.04	0																									
8. Norduz	0.36	0.33	0.11	0.12	0.07	0.07	0.07	0.06	0.05	0																								
9. Qezel	0.37	0.36	0.07	0.08	0.03	0.03	0.03	0.03	0.01	0.05	0																							
10. Sakiz	0.34	0.31	0.16	0.17	0.1	0.11	0.12	0.13	0.11	0.14	0.1	0																						
11. Altamura	0.36	0.37	0.11	0.12	0.04	0.06	0.08	0.08	0.06	0.1	0.06	0.12	0																					
12. Chios	0.33	0.33	0.14	0.15	0.08	0.09	0.11	0.11	0.09	0.12	0.08	0.11	0.1	0																				
13. Comisana	0.38	0.36	0.1	0.11	0.04	0.05	0.08	0.08	0.06	0.09	0.05	0.12	0.04	0.1	0																			
14. Cyprus Fat-Tail	0.33	0.31	0.14	0.15	0.09	0.1	0.11	0.11	0.09	0.13	0.08	0.16	0.12	0.13	0.12	0																		
15. East Friesian	0.3	0.31	0.2	0.2	0.14	0.16	0.17	0.18	0.15	0.19	0.15	0.21	0.14	0.19	0.15	0.21	0																	
16. Meat Lacune	0.37	0.37	0.11	0.11	0.04	0.06	0.08	0.08	0.06	0.09	0.06	0.11	0.05	0.1	0.05	0.12	0.13	0																
17. Merino Landschaf	0.37	0.36	0.12	0.13	0.06	0.07	0.1	0.1	0.08	0.11	0.07	0.14	0.06	0.12	0.06	0.14	0.15	0.06	0															
18. Milk Lacune	0.37	0.37	0.11	0.11	0.05	0.06	0.09	0.09	0.07	0.1	0.06	0.12	0.05	0.1	0.05	0.12	0.14	0.02	0.06	0														
19. Rambouillet	0.35	0.36	0.12	0.12	0.06	0.08	0.1	0.1	0.08	0.11	0.08	0.13	0.06	0.12	0.07	0.13	0.15	0.06	0.06	0.07	0													
20. White Alpine	0.36	0.35	0.15	0.15	0.08	0.1	0.12	0.12	0.1	0.13	0.1	0.16	0.08	0.14	0.09	0.16	0.17	0.08	0.09	0.08	0.07	0												
21. Canaria de Pelo	0.34	0.33	0.13	0.13	0.07	0.09	0.12	0.12	0.1	0.13	0.09	0.16	0.1	0.14	0.1	0.16	0.19	0.09	0.11	0.1	0.11	0.13	0											
22. Castellana	0.38	0.37	0.1	0.1	0.03	0.05	0.08	0.08	0.06	0.09	0.05	0.12	0.04	0.1	0.04	0.12	0.14	0.04	0.05	0.04	0.06	0.08	0.09	0										
23. Churra	0.36	0.37	0.11	0.11	0.05	0.06	0.09	0.09	0.07	0.1	0.07	0.12	0.05	0.1	0.05	0.12	0.14	0.05	0.07	0.06	0.07	0.09	0.1	0.04	0									
24. Gallega	0.36	0.37	0.11	0.11	0.04	0.06	0.09	0.09	0.07	0.1	0.06	0.12	0.05	0.1	0.05	0.12	0.14	0.04	0.06	0.05	0.06	0.08	0.09	0.04	0.05	0								
25. Latxa	0.36	0.36	0.11	0.11	0.04	0.06	0.08	0.09	0.07	0.1	0.06	0.12	0.04	0.1	0.05	0.12	0.14	0.04	0.06	0.04	0.06	0.08	0.09	0.04	0.05	0.04	0							
26. Ojalada	0.38	0.37	0.1	0.1	0.03	0.05	0.07	0.08	0.06	0.09	0.05	0.11	0.04	0.09	0.04	0.11	0.13	0.04	0.05	0.04	0.05	0.07	0.09	0.03	0.04	0.04	0.03	0						
27. Rasa Aragonesa	0.39	0.38	0.09	0.1	0.02	0.04	0.07	0.07	0.05	0.08	0.04	0.11	0.03	0.09	0.03	0.11	0.13	0.03	0.04	0.03	0.04	0.06	0.08	0.02	0.03	0.03	0.03	0.03	0.02	0				
28. Ripollesa	0.37	0.37	0.1	0.1	0.03	0.05	0.07	0.08	0.06	0.09	0.05	0.11	0.04	0.09	0.04	0.12	0.14	0.03	0.05	0.04	0.05	0.07	0.09	0.03	0.04	0.04	0.03	0.03	0.02	0				
29. Roja Mallorquina	0.37	0.36	0.11	0.11	0.04	0.06	0.08	0.09	0.07	0.1	0.06	0.13	0.06	0.11	0.06	0.13	0.16	0.06	0.07	0.06	0.07	0.1	0.1	0.05	0.06	0.06	0.06	0.05	0.04	0.05	0			
30. Segureña	0.38	0.37	0.1	0.1	0.03	0.04	0.07	0.07	0.05	0.09	0.05	0.11	0.04	0.09	0.04	0.11	0.14	0.03	0.05	0.04	0.05	0.07	0.08	0.02	0.04	0.03	0.03	0.02	0.01	0.02	0.05	0		
31. Xisqueta	0.38	0.38	0.09	0.1	0.03	0.04	0.07	0.07	0.05	0.08	0.05	0.11	0.03	0.09	0.03	0.11	0.13	0.03	0.04	0.03	0.05	0.06	0.08	0.02	0.03	0.03	0.03	0.02	0.01	0.02	0.04	0.01	0	
32. Australian Merino	0.37	0.37	0.11	0.11	0.04	0.06	0.08	0.08	0.06	0.09	0.06	0.12	0.05	0.1	0.05	0.12	0.14	0.04	0.05	0.05	0.05	0.07	0.09	0.04	0.05	0.04	0.04	0.04	0.03	0.04	0.06	0.03	0.03	0

\* Ho, observed heterozygosity; He, expected heterozygosity

**Supplementary Table 3.** Most common runs of homozygosity identified in 11 Spanish sheep breeds.

<b>Chr*</b>	<b>SNP1 (start)</b>	<b>SNP2 (end)</b>	<b>Start (Bp)</b>	<b>End (Bp)</b>	<b>Number of SNPS</b>
3	OAR3_160600508.1	OAR3_169354544.1	150,506,932	158,263,553	142
	s08865.1	OAR3_217545698.1	201,717,119	202,149,552	11
6	OAR6_43010674.1	OAR6_43034224.1	38,617,412	38,639,963	2
	OAR6_84052409.1	OAR6_84589373.1	76,989,215	77,528,115	11
	OAR6_96699287.1	OAR6_97721391.1	88,255,946	89,185,503	14
	s11939.1	s45994.1	90,785,820	91,061,654	5
	OAR6_104107846.1	OAR6_104107846.1	94,852,406	94,852,407	1
8	OAR8_14229216.1	OAR8_14543945.1	12,681,411	13,002,444	8
	OAR8_28114086.1	OAR8_28114086.1	25,666,841	25,666,842	1
	s07003.1	OAR8_31142913.1	26,691,996	28,730,392	39
	OAR24_29566263.1	s09657.1	29,403,655	30,514,747	24
	OAR8_37778597.1	OAR8_38921990.1	35,134,129	36,257,232	25
10	OAR10_29511510.1	OAR10_29546872.1	29,476,678	29,512,572	3
	s16941.1	OAR10_33338187.1	32,968,431	33,053,891	3
	OAR10_36302356.1	OAR10_40708619.1	35,566,480	39,902,409	69
16	OAR16_16552788.1	OAR16_16984728.1	14,952,012	15,362,234	7
	s71017.1	OAR16_18729547.1	16,723,643	17,049,485	10
	OAR16_19016913.1	s65924.1	17,329,824	17,453,973	5
19	OAR19_19633578.1	OAR19_19633578.1	18,722,815	18,722,816	1
	OAR19_22440999.1	s08521.1	21,356,863	21,542,256	4
25	s30024.1	OAR25_8346669.1	7,356,301	8,519,942	2

\***Chr**, Chromosome; **bp**, SNP positions referred to Oar\_v3.1 assembly, expressed in base pair.

**Supplementary Table 4.** Genes mapping into ROH hotspots in 11 Spanish sheep breeds.

<b>Gene name</b>	<b>Chromosome</b>	<b>Gene start (bp)</b>	<b>Gene end (bp)</b>	<b>Strand</b>
<i>ADGRL3</i>	6	77,252,525	77,566,951	1
<i>AK9</i>	8	27,663,314	27,788,700	1
<i>AREG</i>	6	89,053,717	89,061,196	1
<i>ARID4B</i>	25	7,969,996	8,106,640	-1
<i>ARMC2</i>	8	28,288,684	28,408,704	-1
<i>ASCC3</i>	8	36,191,607	36,513,139	1
<i>ATP12A</i>	10	36,838,524	36,858,872	-1
<i>AVPR1A</i>	3	156,234,256	156,237,118	1
<i>B3GALNT2</i>	25	8,223,729	8,275,564	-1
<i>BEND3</i>	8	30,037,460	30,053,860	1
<i>C12orf56</i>	3	155,260,542	155,344,741	1
<i>C12orf66</i>	3	155,380,300	155,402,206	1
<i>C6orf203</i>	8	30,067,739	30,073,911	-1
<i>CAND1</i>	3	152,359,061	152,396,257	-1
<i>CCDC158</i>	6	90,874,665	90,952,433	-1
<i>CD164</i>	8	27,876,120	27,887,557	1
<i>CDC40</i>	8	27,087,524	27,132,267	-1
<i>CDK19</i>	8	26,592,432	26,760,228	1
<i>CDKN1B</i>	3	201,984,035	201,990,468	-1
<i>CENPJ</i>	10	36,669,829	36,713,175	1
<i>CEP57L1</i>	8	28,085,246	28,163,551	-1
<i>CPM</i>	3	150,801,360	150,873,795	1
<i>CREBL2</i>	3	202,059,701	202,061,497	-1
<i>CRYBG1</i>	8	30,465,808	30,521,543	-1
<i>CRYL1</i>	10	36,124,260	36,182,572	1
<i>CXCL1</i>	6	88,610,487	88,611,559	1
<i>CXCL6</i>	6	88,555,264	88,556,088	1
<i>CXCL8</i>	6	88,474,889	88,477,180	1
<i>DDO</i>	8	26,897,439	26,914,465	1
<i>DDX47</i>	3	201,898,376	201,912,018	-1
<i>DIMT1</i>	16	17,029,485	17,042,082	1
<i>DYRK2</i>	3	152,015,144	152,016,742	-1
<i>EEF1AKMT1</i>	10	36,005,923	36,011,902	1
<i>EPGN</i>	6	88,912,478	88,918,744	1
<i>EREG</i>	6	88,988,358	88,994,874	1
<i>FAM19A2</i>	3	157,614,169	157,749,302	1
<i>FGF9</i>	10	35,583,842	35,609,414	-1
<i>FIG4</i>	8	27,485,308	27,662,709	-1
<i>FOXO3</i>	8	28,595,346	28,713,940	-1
<i>GJA3</i>	10	36,304,573	36,305,769	1

<i>GJB2</i>	10	36,271,774	36,272,454	1
<i>GJB6</i>	10	36,253,000	36,253,785	1
<i>GNG4</i>	25	8,344,572	8,377,151	-1
<i>GNS</i>	3	154,929,508	154,975,699	1
<i>GPR19</i>	3	202,042,167	202,043,414	1
<i>GPRC5A</i>	3	201,836,871	201,842,949	-1
<i>GPRC5D</i>	3	201,807,778	201,813,703	1
<i>GRIK2</i>	8	34,947,839	35,493,542	-1
<i>GRIP1</i>	3	153,189,105	153,355,268	1
<i>GRM7</i>	19	18,544,027	19,149,524	-1
<i>HEBP1</i>	3	201,751,176	201,787,081	1
<i>HELB</i>	3	153,363,283	153,399,293	-1
<i>IFNG</i>	3	151,527,165	151,535,188	1
<i>IFT88</i>	10	36,045,326	36,103,818	-1
<i>IL22</i>	3	151,427,327	151,432,602	1
<i>IL26</i>	3	151,453,165	151,470,372	1
<i>IPO11</i>	16	16,829,254	16,993,920	-1
<i>IRAK3</i>	3	153,443,766	153,486,434	-1
<i>ITPR1</i>	19	21,424,244	21,769,620	-1
<i>KIF2A</i>	16	17,042,584	17,109,138	-1
<i>LATS2</i>	10	35,862,425	35,885,746	1
<i>LEMD3</i>	3	154,424,914	154,498,447	-1
<i>LLPH</i>	3	153,544,736	153,548,299	1
<i>LYST</i>	25	8,426,668	8,562,462	-1
<i>MDM1</i>	3	151,358,151	151,390,211	1
<i>METTL24</i>	8	26,996,941	27,076,802	1
<i>MICAL1</i>	8	27,816,425	27,825,784	1
<i>MICU2</i>	10	35,689,056	35,718,821	1
<i>MIRLET7I</i>	3	156,850,160	156,850,267	-1
<i>MON2</i>	3	156,866,668	156,976,887	-1
<i>MPHOSPH8</i>	10	36,540,304	36,586,948	-1
<i>MRPL57</i>	10	35,786,131	35,786,478	-1
<i>MSRB3</i>	3	154,219,234	154,397,986	-1
<i>MTHFD2L</i>	6	88,783,856	88,905,590	1
<i>NUP107</i>	3	150,809,405	151,035,873	-1
<i>PARP4</i>	10	36,588,963	36,660,928	-1
<i>PDSS2</i>	8	29,708,586	29,955,211	1
<i>PPBP</i>	6	88,576,093	88,576,890	1
<i>PPIL6</i>	8	27,828,274	27,867,331	1
<i>PPM1H</i>	3	156,511,682	156,807,677	1
<i>PSPC1</i>	10	36,464,910	36,513,716	1
<i>RAP1B</i>	3	151,070,755	151,077,096	-1
<i>RASSF3</i>	3	154,993,195	155,069,159	-1

<i>RASSF6</i>	6	88,284,202	88,337,481	-1
<i>RF00001</i>	3	153,593,732	153,593,849	-1
<i>RF00003</i>	3	153,252,419	153,252,583	1
<i>RF00007</i>	8	28,234,265	28,234,370	-1
<i>RF00026</i>	10	36,645,893	36,646,001	-1
<i>RF00100</i>	6	88,357,887	88,358,219	1
<i>RF00397</i>	25	7,937,897	7,938,031	-1
<i>RF00405</i>	3	150,633,576	150,633,685	1
<i>RF00420</i>	10	36,596,458	36,596,563	1
<i>RF00428</i>	3	151,000,897	151,001,028	-1
<i>RGS7BP</i>	16	14,852,860	14,957,323	-1
<i>RNF17</i>	10	36,713,315	36,828,899	-1
<i>RNF180</i>	16	15,082,900	15,388,087	-1
<i>RTN4IP1</i>	8	30,416,461	30,467,534	1
<i>RXFP2</i>	10	29,454,677	29,502,617	-1
<i>RXYLT1</i>	3	155,803,012	155,829,952	-1
<i>SAP18</i>	10	35,806,669	35,811,076	-1
<i>SCML4</i>	8	29,351,937	29,455,891	1
<i>SESN1</i>	8	28,163,840	28,274,720	1
<i>SKA3</i>	10	35,786,789	35,798,732	1
<i>SLC22A16</i>	8	26,856,958	26,890,048	1
<i>SLC35E3</i>	3	150,961,729	150,976,981	-1
<i>SMPD2</i>	8	27,826,059	27,828,595	-1
<i>SOBP</i>	8	29,529,698	29,677,712	-1
<i>SRGAP1</i>	3	155,478,249	155,772,717	-1
<i>TBC1D30</i>	3	154,824,770	154,914,055	-1
<i>TBK1</i>	3	155,157,065	155,199,629	-1
<i>TOMM20</i>	25	7,925,956	7,932,498	-1
<i>USP15</i>	3	157,020,163	157,148,008	-1
<i>WASF1</i>	8	27,180,834	27,200,014	1
<i>WIF1</i>	3	154,565,931	154,650,524	1
<i>XPO4</i>	10	35,915,236	35,985,140	1
<i>XPOT</i>	3	155,202,187	155,357,768	-1
<i>ZBTB24</i>	8	27,795,216	27,803,455	1
<i>ZDHHC20</i>	10	35,736,928	35,783,467	1
<i>ZMYM2</i>	10	36,322,774	36,386,924	-1
<i>ZMYM5</i>	10	36,423,167	36,450,667	1

**Supplementary Table 5.** Results of the functional classification with DAVID of genes mapping to putative ROH hotspots in 11 Spanish sheep breeds, using homo Sapiens as background.

Annotation Cluster 1	Enrichment Score*: 2.1685207324620484							
Category	Term	Count	%	P- value	Genes	List Total	Fold Enrichment	FDR
SP_PIR_KEYWORDS	growth factor	6	0.632	0.001	<i>CXCL1, PPBP, EREG, FGF9, EPGN, AREG</i>	99	8.90	0.69
GOTERM_MF_FAT	GO:0008083~growth factor activity	6	0.632	0.002	<i>CXCL1, PPBP, EREG, FGF9, EPGN, AREG</i>	74	6.54	2.68
SP_PIR_KEYWORDS	mitogen	3	0.316	0.017	<i>PPBP, EREG, FGF9</i>	99	14.95	19.00
GOTERM_BP_FAT	GO:0051781~positive regulation of cell division	3	0.316	0.023	<i>PPBP, EREG, FGF9</i>	82	12.69	30.73
GOTERM_BP_FAT	GO:0051302~regulation of cell division	3	0.316	0.032	<i>PPBP, EREG, FGF9</i>	82	10.53	40.67
Annotation Cluster 2	Enrichment Score*: 1.7418751941412498							
Category	Term	Count	%	P- value	Genes	List Total	Fold Enrichment	FDR
SP_PIR_KEYWORDS	cytokine	7	0.737	0.000	<i>CXCL1, PPBP, IFNG, IL26, CXCL6, AREG, IL22</i>	99	7.51	0.41
GOTERM_BP_FAT	GO:0007610~behavior	11	1.158	0.000	<i>CXCL1, PPBP, GRIK2, LYST, GRM7, IFNG, AVPR1A, SOBP, CXCL6, FIG4, DDO</i>	82	3.87	0.75
GOTERM_MF_FAT	GO:0005125~cytokine activity	7	0.737	0.001	<i>CXCL1, PPBP, IFNG, IL26, CXCL6, AREG, IL22</i>	74	6.30	1.01
INTERPRO	IPR001089:Small chemokine, C-X-C	3	0.316	0.002	<i>CXCL1, PPBP, CXCL6</i>	89	43.20	2.59
INTERPRO	IPR002473:Small chemokine, C-X-C/Interleukin 8	3	0.316	0.002	<i>CXCL1, PPBP, CXCL6</i>	89	40.11	3.00
INTERPRO	IPR018048:Small chemokine, C-X-C, conserved site	3	0.316	0.004	<i>CXCL1, PPBP, CXCL6</i>	89	33.03	4.41
KEGG_PATHWAY	hsa04062:Chemokine signaling pathway	6	0.632	0.006	<i>CXCL1, PPBP, RAPIB, CXCL6, FOXO3, GNG4</i>	33	4.94	5.55
GOTERM_BP_FAT	GO:0007626~locomotory behavior	7	0.737	0.006	<i>CXCL1, PPBP, LYST, IFNG, SOBP, CXCL6, FIG4</i>	82	4.21	9.11
GOTERM_BP_FAT	GO:0006952~defense response	10	1.053	0.011	<i>CXCL1, PPBP, GRIK2, TBK1, LYST, GRM7, IFNG, CXCL6, PARP4, IL22</i>	82	2.68	16.25
GOTERM_BP_FAT	GO:0042330~taxi	5	0.526	0.016	<i>CXCL1, PPBP, LYST, IFNG, CXCL6</i>	82	5.16	22.08
GOTERM_BP_FAT	GO:0006935~chemotaxis	5	0.526	0.016	<i>CXCL1, PPBP, LYST, IFNG, CXCL6</i>	82	5.16	22.08
INTERPRO	IPR001811:Small chemokine, interleukin-8-like	3	0.316	0.020	<i>CXCL1, PPBP, CXCL6</i>	89	13.70	22.32
SMART	SM00199:SCY	3	0.316	0.020	<i>CXCL1, PPBP, CXCL6</i>	50	13.29	18.47
KEGG_PATHWAY	hsa04060:Cytokine-cytokine receptor interaction	6	0.632	0.022	<i>CXCL1, PPBP, IFNG, IL26, CXCL6, IL22</i>	33	3.53	20.22
INTERPRO	IPR012351:Four-helical cytokine, core	3	0.316	0.025	<i>IFNG, IL26, IL22</i>	89	12.21	26.97
GOTERM_MF_FAT	GO:0008009~chemokine activity	3	0.316	0.028	<i>CXCL1, PPBP, CXCL6</i>	74	11.44	30.33



GOTERM_BP_FAT	GO:0009615~response to virus	4	0.421	0.028	<i>IRAK3, TBK1, LYST, IFNG</i>	82	6.05	36.02
GOTERM_CC_FAT	GO:0005615~extracellular space	9	0.947	0.031	<i>CXCL1, PPBP, EREG, FGF9, IFNG, IL26, CXCL6, AREG, IL22</i>	70	2.40	32.02
GOTERM_MF_FAT	GO:0042379~chemokine receptor binding	3	0.316	0.031	<i>CXCL1, PPBP, CXCL6</i>	74	10.74	33.43
GOTERM_BP_FAT	GO:0009617~response to bacterium	4	0.421	0.109	<i>IRAK3, PPBP, LYST, IFNG</i>	82	3.42	84.21
GOTERM_CC_FAT	GO:0044421~extracellular region part	9	0.947	0.144	<i>CXCL1, PPBP, EREG, FGF9, IFNG, IL26, CXCL6, AREG, IL22</i>	70	1.71	85.59
GOTERM_BP_FAT	GO:0042742~defense response to bacterium	3	0.316	0.145	<i>PPBP, LYST, IFNG</i>	82	4.42	91.77
GOTERM_BP_FAT	GO:0006955~immune response	7	0.737	0.232	<i>CXCL1, PPBP, TBK1, LYST, IFNG, CXCL6, CD164</i>	82	1.67	98.51
KEGG_PATHWAY	hsa04630:Jak-STAT signaling pathway	3	0.316	0.255	<i>IFNG, IL26, IL22</i>	33	2.98	94.65
GOTERM_BP_FAT	GO:0006954~inflammatory response	4	0.421	0.308	<i>CXCL1, CXCL6, PARP4, IL22</i>	82	2.03	99.72
GOTERM_BP_FAT	GO:0009611~response to wounding	5	0.526	0.392	<i>CXCL1, EREG, CXCL6, PARP4, IL22</i>	82	1.56	99.96
<b>Annotation Cluster 3</b>	<b>Enrichment Score*: 1.488797519723787</b>							
<b>Category</b>	<b>Term</b>	<b>Count</b>	<b>%</b>	<b>P-value</b>	<b>Genes</b>	<b>List Total</b>	<b>Fold Enrichment</b>	<b>FDR</b>
PIR_SUPERFAMILY	PIRSF002292:gap junction protein	3	0.316	0.002	<i>GJB6, GJA3, GJB2</i>	41	41.63	2.00
INTERPRO	IPR019570:Gap junction protein, cysteine-rich domain	3	0.316	0.005	<i>GJB6, GJA3, GJB2</i>	89	28.08	6.05
INTERPRO	IPR000500:Connexins	3	0.316	0.005	<i>GJB6, GJA3, GJB2</i>	89	28.08	6.05
INTERPRO	IPR017991:Connexin region	3	0.316	0.005	<i>GJB6, GJA3, GJB2</i>	89	26.74	6.64
INTERPRO	IPR017990:Connexin, conserved site	3	0.316	0.005	<i>GJB6, GJA3, GJB2</i>	89	26.74	6.64
INTERPRO	IPR013092:Connexin, N-terminal	3	0.316	0.005	<i>GJB6, GJA3, GJB2</i>	89	26.74	6.64
SMART	SM00037:CNX	3	0.316	0.006	<i>GJB6, GJA3, GJB2</i>	50	25.94	5.41
GOTERM_CC_FAT	GO:0005922~connexon complex	3	0.316	0.006	<i>GJB6, GJA3, GJB2</i>	70	24.90	7.42
SP_PIR_KEYWORDS	gap junction	3	0.316	0.007	<i>GJB6, GJA3, GJB2</i>	99	23.32	8.51
GOTERM_CC_FAT	GO:0005921~gap junction	3	0.316	0.011	<i>GJB6, GJA3, GJB2</i>	70	18.89	12.41
SP_PIR_KEYWORDS	cell junction	5	0.526	0.147	<i>GRIPI, GRIK2, GJB6, GJA3, GJB2</i>	99	2.43	85.99
GOTERM_CC_FAT	GO:0005911~cell-cell junction	3	0.316	0.274	<i>GJB6, GJA3, GJB2</i>	70	2.88	98.12
GOTERM_CC_FAT	GO:0030054~cell junction	5	0.526	0.306	<i>GRIPI, GRIK2, GJB6, GJA3, GJB2</i>	70	1.76	98.93
GOTERM_BP_FAT	GO:0007600~sensory perception	6	0.632	0.538	<i>CDKN1B, GRM7, SOBP, GJB6, GJA3, GJB2</i>	82	1.22	100.00
GOTERM_BP_FAT	GO:0050890~cognition	6	0.632	0.642	<i>CDKN1B, GRM7, SOBP, GJB6, GJA3, GJB2</i>	82	1.09	100.00
SP_PIR_KEYWORDS	disease mutation	8	0.842	0.711	<i>LYST, RXFP2, GJB6, FIG4, CENPJ, PDSS2, GJA3, GJB2</i>	99	0.98	100.00
GOTERM_BP_FAT	GO:0050877~neurological system process	7	0.737	0.743	<i>CDKN1B, GRIK2, GRM7, SOBP, GJB6, GJA3, GJB2</i>	82	0.95	100.00

<b>Annotation Cluster 4</b>	<b>Enrichment Score*: 1.4222170665945673</b>							
<b>Category</b>	<b>Term</b>	<b>Count</b>	<b>%</b>	<b>P-value</b>	<b>Genes</b>	<b>List Total</b>	<b>Fold Enrichment</b>	<b>FDR</b>
SP_PIR_KEYWORDS	growth factor	6	0.632	0.001	<i>CXCL1, PPBP, EREG, FGF9, EPGN, AREG</i>	99	8.90	0.69
GOTERM_MF_FAT	GO:0008083~growth factor activity	6	0.632	0.002	<i>CXCL1, PPBP, EREG, FGF9, EPGN, AREG</i>	74	6.54	2.68
UP_SEQ_FEATURE	domain:EGF-like	3	0.316	0.058	<i>EREG, EPGN, AREG</i>	99	7.62	55.98
INTERPRO	IPR000742:EGF-like, type 3	4	0.421	0.083	<i>EREG, EPGN, WIF1, AREG</i>	89	3.86	66.70
INTERPRO	IPR006210:EGF-like	4	0.421	0.090	<i>EREG, EPGN, WIF1, AREG</i>	89	3.72	69.79
SMART	SM00181:EGF	4	0.421	0.094	<i>EREG, EPGN, WIF1, AREG</i>	50	3.61	62.27
SP_PIR_KEYWORDS	egf-like domain	4	0.421	0.113	<i>EREG, EPGN, WIF1, AREG</i>	99	3.38	77.39
INTERPRO	IPR006209:EGF	3	0.316	0.145	<i>EREG, WIF1, AREG</i>	89	4.42	86.18
INTERPRO	IPR013032:EGF-like region, conserved site	4	0.421	0.202	<i>EREG, EPGN, WIF1, AREG</i>	89	2.56	94.21
<b>Annotation Cluster 5</b>	<b>Enrichment Score*: 1.3751598254347912</b>							
<b>Category</b>	<b>Term</b>	<b>Count</b>	<b>%</b>	<b>P-value</b>	<b>Genes</b>	<b>List Total</b>	<b>Fold Enrichment</b>	<b>FDR</b>
GOTERM_BP_FAT	GO:0001556~oocyte maturation	3	0.316	0.003	<i>EREG, RXFP2, FOXO3</i>	82	38.07	4.14
GOTERM_BP_FAT	GO:0048599~oocyte development	3	0.316	0.007	<i>EREG, RXFP2, FOXO3</i>	82	23.57	10.47
GOTERM_BP_FAT	GO:0045137~development of primary sexual characteristics	5	0.526	0.007	<i>EREG, FGF9, RXFP2, FOXO3, GJB2</i>	82	6.50	10.70
GOTERM_BP_FAT	GO:0009994~oocyte differentiation	3	0.316	0.008	<i>EREG, RXFP2, FOXO3</i>	82	22.50	11.42
GOTERM_BP_FAT	GO:0007548~sex differentiation	5	0.526	0.013	<i>EREG, FGF9, RXFP2, FOXO3, GJB2</i>	82	5.46	18.56
GOTERM_BP_FAT	GO:0003006~reproductive developmental process	6	0.632	0.020	<i>RNF17, EREG, FGF9, RXFP2, FOXO3, GJB2</i>	82	3.78	28.03
GOTERM_BP_FAT	GO:0048477~oogenesis	3	0.316	0.022	<i>EREG, RXFP2, FOXO3</i>	82	13.02	29.50
GOTERM_BP_FAT	GO:0007281~germ cell development	4	0.421	0.023	<i>RNF17, EREG, RXFP2, FOXO3</i>	82	6.53	30.63
GOTERM_BP_FAT	GO:0008406~gonad development	4	0.421	0.030	<i>EREG, FGF9, RXFP2, FOXO3</i>	82	5.89	38.07
GOTERM_BP_FAT	GO:0048608~reproductive structure development	4	0.421	0.040	<i>EREG, FGF9, RXFP2, FOXO3</i>	82	5.24	47.72
GOTERM_BP_FAT	GO:0007292~female gamete generation	3	0.316	0.058	<i>EREG, RXFP2, FOXO3</i>	82	7.61	61.34
GOTERM_BP_FAT	GO:0046546~development of primary male sexual characteristics	3	0.316	0.058	<i>FGF9, RXFP2, GJB2</i>	82	7.61	61.34
GOTERM_BP_FAT	GO:0046661~male sex differentiation	3	0.316	0.071	<i>FGF9, RXFP2, GJB2</i>	82	6.78	69.06
GOTERM_BP_FAT	GO:0048609~reproductive process in a multicellular organism	7	0.737	0.071	<i>SLC22A16, RNF17, EREG, RXFP2, AVPR1A, FOXO3, DDO</i>	82	2.37	69.38
GOTERM_BP_FAT	GO:0032504~multicellular organism reproduction	7	0.737	0.071	<i>SLC22A16, RNF17, EREG, RXFP2, AVPR1A, FOXO3, DDO</i>	82	2.37	69.38
GOTERM_BP_FAT	GO:0048610~reproductive cellular process	4	0.421	0.073	<i>RNF17, EREG, RXFP2, FOXO3</i>	82	4.07	70.28

GOTERM_BP_FAT	GO:0048469~cell maturation	3	0.316	0.074	<i>EREG, RXFP2, FOXO3</i>	82	6.60	70.82
GOTERM_BP_FAT	GO:0021700~developmental maturation	3	0.316	0.123	<i>EREG, RXFP2, FOXO3</i>	82	4.90	87.60
SP_PIR_KEYWORDS	differentiation	5	0.526	0.208	<i>SLC22A16, RNF17, EREG, FGF9, KIF2A</i>	99	2.11	94.42
GOTERM_BP_FAT	GO:0007276~gamete generation	5	0.526	0.212	<i>SLC22A16, RNF17, EREG, RXFP2,</i>	82	2.09	97.75
GOTERM_BP_FAT	GO:0019953~sexual reproduction	5	0.526	0.294	<i>SLC22A16, RNF17, EREG, RXFP2,</i>	82	1.80	99.61
SP_PIR_KEYWORDS	developmental protein	6	0.632	0.365	<i>SLC22A16, RNF17, EREG, FGF9, WIF1, KIF2A</i>	99	1.50	99.64
<b>Annotation Cluster 6</b>	<b>Enrichment Score*: 1.3483401161401698</b>							
<b>Category</b>	<b>Term</b>	<b>Count</b>	<b>%</b>	<b>P -value</b>	<b>Genes</b>	<b>List Total</b>	<b>Fold Enrichment</b>	<b>FDR</b>
GOTERM_BP_FAT	GO:0008285~negative regulation of cell proliferation	8	0.842	0.006	<i>CXCL1, CDKN1B, EREG, IFNG, RXFP2, GJB6, CD164, SESN1</i>	82	3.66	8.90
GOTERM_BP_FAT	GO:0022402~cell cycle process	7	0.737	0.122	<i>CDKN1B, EREG, IFNG, SKA3, CENPJ, SESN1, LATS2</i>	82	2.04	87.54
GOTERM_BP_FAT	GO:0007050~cell cycle arrest	3	0.316	0.127	<i>CDKN1B, IFNG, SESN1</i>	82	4.81	88.47
<b>Annotation Cluster 7</b>	<b>Enrichment Score*: 1.1288558188530375</b>							
<b>Category</b>	<b>Term</b>	<b>Count</b>	<b>%</b>	<b>P -value</b>	<b>Genes</b>	<b>List Total</b>	<b>Fold Enrichment</b>	<b>FDR</b>
SP_PIR_KEYWORDS	cytokine	7	0.737	0.000	<i>CXCL1, PPBP, IFNG, IL26, CXCL6, AREG, IL22</i>	99	7.51	0.41
SP_PIR_KEYWORDS	growth factor	6	0.632	0.001	<i>CXCL1, PPBP, EREG, FGF9, EPGN, AREG</i>	99	8.90	0.69
GOTERM_MF_FAT	GO:0005125~cytokine activity	7	0.737	0.001	<i>CXCL1, PPBP, IFNG, IL26, CXCL6, AREG, IL22</i>	74	6.30	1.01
GOTERM_MF_FAT	GO:0008083~growth factor activity	6	0.632	0.002	<i>CXCL1, PPBP, EREG, FGF9, EPGN, AREG</i>	74	6.54	2.68
GOTERM_BP_FAT	GO:0006952~defense response	10	1.053	0.011	<i>CXCL1, PPBP, GRIK2, TBK1, LYST, GRM7, IFNG, CXCL6, PARP4, IL22</i>	82	2.68	16.25
KEGG_PATHWAY	hsa04060:Cytokine-cytokine receptor interaction	6	0.632	0.022	<i>CXCL1, PPBP, IFNG, IL26, CXCL6, IL22</i>	33	3.53	20.22
GOTERM_CC_FAT	GO:0005615~extracellular space	9	0.947	0.031	<i>CXCL1, PPBP, EREG, FGF9, IFNG, IL26, CXCL6, AREG, IL22</i>	70	2.40	32.02
GOTERM_BP_FAT	GO:0007166~cell surface receptor linked signal transduction	18	1.895	0.046	<i>CXCL1, GPRC5D, GPR19, RGS7BP, FGF9, GRIK2, RXFP2, CXCL6, GPRC5A, PPBP, EREG, GRM7, IFNG, AVPR1A, WIF1, AREG, GNG4, IFT88</i>	82	1.60	53.03

GOTERM_BP_FAT	GO:0007186~G-protein coupled receptor protein signaling pathway	12	1.263	0.071	<i>CXCL1, GPRC5D, RGS7BP, PPBP, GPR19, GRM7, RXFP2, AVPR1A, CXCL6, AREG, GNG4, GPRC5A</i>	82	1.76	68.95
GOTERM_CC_FAT	GO:0044421~extracellular region part	9	0.947	0.144	<i>CXCL1, PPBP, EREG, FGF9, IFNG, IL26, CXCL6, AREG, IL22</i>	70	1.71	85.59
SP_PIR_KEYWORDS	transducer	7	0.737	0.287	<i>GPRC5D, GPR19, GRM7, RXFP2, AVPR1A, GNG4, GPRC5A</i>	99	1.56	98.48
GOTERM_BP_FAT	GO:0006954~inflammatory response	4	0.421	0.308	<i>CXCL1, CXCL6, PARP4, IL22</i>	82	2.03	99.72
SP_PIR_KEYWORDS	Secreted	11	1.158	0.358	<i>CXCL1, PPBP, EREG, FGF9, EPGN, IFNG, IL26, WIF1, CXCL6, CD164, IL22</i>	99	1.27	99.59
GOTERM_BP_FAT	GO:0009611~response to wounding	5	0.526	0.392	<i>CXCL1, EREG, CXCL6, PARP4, IL22</i>	82	1.56	99.96
GOTERM_CC_FAT	GO:0005576~extracellular region	12	1.263	0.531	<i>CXCL1, PPBP, EREG, FGF9, EPGN, IFNG, IL26, WIF1, CXCL6, AREG, CD164, IL22</i>	70	1.09	99.99
SP_PIR_KEYWORDS	signal	16	1.684	0.704	<i>CXCL1, CPM, GRIK2, IL26, FAM19A2, CXCL6, CD164, IL22, GNS, EREG, PPBP, EPGN, GRM7, IFNG, WIF1,</i>	99	0.96	100.00
UP_SEQ_FEATURE	signal peptide	16	1.684	0.713	<i>CXCL1, CPM, GRIK2, IL26, FAM19A2, CXCL6, CD164, IL22, GNS, EREG, PPBP, EPGN, GRM7, IFNG, WIF1,</i>	99	0.95	100.00
UP_SEQ_FEATURE	glycosylation site:N-linked (GlcNAc...)	19	2.000	0.816	<i>SLC22A16, CPM, GPR19, GRIK2, FGF9, RXFP2, CD164, IL22, GPRC5A, ITPR1, GNS, EREG, EPGN, GRM7, B3GALNT2, IFNG, AVPR1A, WIF1, AREG</i>	99	0.89	100.00
SP_PIR_KEYWORDS	glycoprotein	19	2.000	0.864	<i>SLC22A16, CPM, GPR19, GRIK2, FGF9, RXFP2, CD164, IL22, GPRC5A, ITPR1, GNS, EREG, EPGN, GRM7, B3GALNT2, IFNG, AVPR1A, WIF1, AREG</i>	99	0.85	100.00
UP_SEQ_FEATURE	disulfide bond	12	1.263	0.873	<i>CXCL1, CPM, PPBP, GPR19, EREG, EPGN, RXFP2, AVPR1A, WIF1, CXCL6, AREG, IL22</i>	99	0.82	100.00
SP_PIR_KEYWORDS	disulfide bond	12	1.263	0.897	<i>CXCL1, CPM, PPBP, GPR19, EREG, EPGN, RXFP2, AVPR1A, WIF1, CXCL6, AREG, IL22</i>	99	0.80	100.00
<b>Annotation Cluster 8</b>	<b>Enrichment Score*: 1.126616383466167</b>							
<b>Category</b>	<b>Term</b>	<b>Count</b>	<b>%</b>	<b>P -value</b>	<b>Genes</b>	<b>List Total</b>	<b>Fold Enrichment</b>	<b>FDR</b>

SP_PIR_KEYWORDS	growth factor	6	0.632	0.001	<i>CXCL1, PPBP, EREG, FGF9, EPGN, AREG</i>	99	8.90	0.69
GOTERM_MF_FAT	GO:0008083~growth factor activity	6	0.632	0.002	<i>CXCL1, PPBP, EREG, FGF9, EPGN, AREG</i>	74	6.54	2.68
GOTERM_BP_FAT	GO:0050678~regulation of epithelial cell proliferation	4	0.421	0.009	<i>CDKN1B, EREG, FGF9, EPGN</i>	82	9.29	13.19
GOTERM_BP_FAT	GO:0042127~regulation of cell proliferation	11	1.158	0.019	<i>CXCL1, CDKN1B, EREG, FGF9, EPGN, IFNG, RXFP2, AVPR1A, GJB6, CD164, SESN1</i>	82	2.31	26.03
GOTERM_BP_FAT	GO:0010647~positive regulation of cell	6	0.632	0.047	<i>EREG, GRIK2, FGF9, TBK1, EPGN,</i>	82	3.01	53.84
GOTERM_BP_FAT	GO:0051240~positive regulation of multicellular organismal process	5	0.526	0.059	<i>EREG, GRIK2, FGF9, IFNG, AVPR1A</i>	82	3.38	61.86
GOTERM_BP_FAT	GO:0010627~regulation of protein kinase cascade	5	0.526	0.062	<i>GRIK2, FGF9, TBK1, IFNG, IL22</i>	82	3.31	64.12
GOTERM_BP_FAT	GO:0009967~positive regulation of signal transduction	5	0.526	0.101	<i>EREG, FGF9, TBK1, EPGN, IFNG</i>	82	2.80	81.60
GOTERM_BP_FAT	GO:0008284~positive regulation of cell proliferation	6	0.632	0.102	<i>CDKN1B, EREG, FGF9, EPGN, IFNG, AVPR1A</i>	82	2.39	82.13
GOTERM_BP_FAT	GO:0001525~angiogenesis	3	0.316	0.222	<i>EREG, FGF9, EPGN</i>	82	3.34	98.19
GOTERM_BP_FAT	GO:0010740~positive regulation of protein kinase	3	0.316	0.264	<i>FGF9, TBK1, IFNG</i>	82	2.96	99.25
GOTERM_BP_FAT	GO:0044093~positive regulation of molecular function	6	0.632	0.274	<i>IRAK3, EREG, EPGN, IFNG, RXFP2, AVPR1A</i>	82	1.69	99.39
GOTERM_BP_FAT	GO:0048514~blood vessel morphogenesis	3	0.316	0.361	<i>EREG, FGF9, EPGN</i>	82	2.35	99.92
GOTERM_BP_FAT	GO:0043085~positive regulation of catalytic activity	5	0.526	0.379	<i>EREG, EPGN, IFNG, RXFP2, AVPR1A</i>	82	1.59	99.95
GOTERM_BP_FAT	GO:0001568~blood vessel development	3	0.316	0.433	<i>EREG, FGF9, EPGN</i>	82	2.02	99.99
GOTERM_BP_FAT	GO:0001944~vasculature development	3	0.316	0.445	<i>EREG, FGF9, EPGN</i>	82	1.97	99.99
GOTERM_BP_FAT	GO:0008283~cell proliferation	4	0.421	0.487	<i>CXCL1, EREG, RAP1B, AREG</i>	82	1.51	100.00
Annotation Cluster 9	Enrichment Score*: 1.0949122123422799							
Category	Term	Count	%	P-value	Genes	List Total	Fold Enrichment	FDR
GOTERM_BP_FAT	GO:0007605~sensory perception of sound	5	0.526	0.003	<i>CDKN1B, GRM7, SOBP, GJB6, GJB2</i>	82	8.50	4.24
GOTERM_BP_FAT	GO:0050954~sensory perception of mechanical	5	0.526	0.003	<i>CDKN1B, GRM7, SOBP, GJB6, GJB2</i>	82	8.01	5.24
GOTERM_BP_FAT	GO:0048839~inner ear development	4	0.421	0.012	<i>CDKN1B, FGF9, SOBP, GJB6</i>	82	8.35	17.26
GOTERM_BP_FAT	GO:0043583~ear development	4	0.421	0.019	<i>CDKN1B, FGF9, SOBP, GJB6</i>	82	6.95	26.73
GOTERM_BP_FAT	GO:0042471~ear morphogenesis	3	0.316	0.059	<i>FGF9, SOBP, GJB6</i>	82	7.50	62.37
GOTERM_BP_FAT	GO:0007423~sensory organ development	4	0.421	0.158	<i>CDKN1B, FGF9, SOBP, GJB6</i>	82	2.88	93.56
GOTERM_BP_FAT	GO:0048562~embryonic organ morphogenesis	3	0.316	0.189	<i>FGF9, SOBP, GJB6</i>	82	3.72	96.49
GOTERM_BP_FAT	GO:0048568~embryonic organ development	3	0.316	0.275	<i>FGF9, SOBP, GJB6</i>	82	2.88	99.41
GOTERM_BP_FAT	GO:0048598~embryonic morphogenesis	4	0.421	0.279	<i>FGF9, SOBP, GJB6, IFT88</i>	82	2.15	99.46
GOTERM_BP_FAT	GO:0007600~sensory perception	6	0.632	0.538	<i>CDKN1B, GRM7, SOBP, GJB6, GJA3, GJB2</i>	82	1.22	100.00

GOTERM_BP_FAT	GO:0050890~cognition	6	0.632	0.642	<i>CDKN1B, GRM7, SOBP, GJB6, GJA3, GJB2</i>	82	1.09	100.00
GOTERM_BP_FAT	GO:0050877~neurological system process	7	0.737	0.743	<i>CDKN1B, GRIK2, GRM7, SOBP, GJB6, GJA3, GJB2</i>	82	0.95	100.00
<b>Annotation Cluster 10</b>	<b>Enrichment Score*: 1.0591133954091583</b>							
<b>Category</b>	<b>Term</b>	<b>Count</b>	<b>%</b>	<b>P-value</b>	<b>Genes</b>	<b>List Total</b>	<b>Fold Enrichment</b>	<b>FDR</b>
GOTERM_BP_FAT	GO:0006913~nucleocytoplasmic transport	5	0.526	0.014	<i>XPOT, FGF9, IPO11, IFNG, NUP107</i>	82	5.29	20.48
GOTERM_BP_FAT	GO:0051169~nuclear transport	5	0.526	0.015	<i>XPOT, FGF9, IPO11, IFNG, NUP107</i>	82	5.22	21.27
GOTERM_CC_FAT	GO:0005635~nuclear envelope	5	0.526	0.025	<i>XPOT, IPO11, LEMD3, NUP107, ITPR1</i>	70	4.45	26.72
GOTERM_BP_FAT	GO:0046907~intracellular transport	9	0.947	0.043	<i>XPOT, GRIK2, FGF9, LYST, IPO11, IFNG, TOMM20, NUP107, MON2</i>	82	2.26	50.02
GOTERM_BP_FAT	GO:0017038~protein import	4	0.421	0.044	<i>FGF9, IPO11, IFNG, TOMM20</i>	82	5.04	51.13
GOTERM_BP_FAT	GO:0010647~positive regulation of cell	6	0.632	0.047	<i>EREG, GRIK2, FGF9, TBK1, EPGN,</i>	82	3.01	53.84
GOTERM_CC_FAT	GO:0031967~organelle envelope	8	0.842	0.049	<i>XPOT, WASF1, IPO11, TOMM20, LEMD3, NUP107, MON2, ITPR1</i>	70	2.36	46.51
GOTERM_CC_FAT	GO:0031975~envelope	8	0.842	0.050	<i>XPOT, WASF1, IPO11, TOMM20, LEMD3, NUP107, MON2, ITPR1</i>	70	2.35	47.01
GOTERM_BP_FAT	GO:0033365~protein localization in organelle	4	0.421	0.057	<i>FGF9, IPO11, IFNG, TOMM20</i>	82	4.52	60.92
GOTERM_BP_FAT	GO:0051240~positive regulation of multicellular organismal process	5	0.526	0.059	<i>EREG, GRIK2, FGF9, IFNG, AVPR1A</i>	82	3.38	61.86
GOTERM_BP_FAT	GO:0010627~regulation of protein kinase cascade	5	0.526	0.062	<i>GRIK2, FGF9, TBK1, IFNG, IL22</i>	82	3.31	64.12
GOTERM_CC_FAT	GO:0005643~nuclear pore	3	0.316	0.068	<i>XPOT, IPO11, NUP107</i>	70	6.93	58.21
GOTERM_BP_FAT	GO:0008104~protein localization	10	1.053	0.080	<i>GRIK2, FGF9, LYST, XPO4, IPO11, IFNG, TOMM20, NUP107, MON2</i>	82	1.87	73.75
GOTERM_BP_FAT	GO:0015031~protein transport	9	0.947	0.085	<i>GRIK2, FGF9, LYST, XPO4, IPO11, IFNG, TOMM20, NUP107, MON2</i>	82	1.95	75.85
GOTERM_BP_FAT	GO:0045184~establishment of protein localization	9	0.947	0.089	<i>GRIK2, FGF9, LYST, XPO4, IPO11, IFNG, TOMM20, NUP107, MON2</i>	82	1.93	77.29
GOTERM_CC_FAT	GO:0046930~pore complex	3	0.316	0.093	<i>XPOT, IPO11, NUP107</i>	70	5.77	70.30
GOTERM_BP_FAT	GO:0006606~protein import into nucleus	3	0.316	0.094	<i>FGF9, IPO11, IFNG</i>	82	5.75	79.26
GOTERM_BP_FAT	GO:0051170~nuclear import	3	0.316	0.098	<i>FGF9, IPO11, IFNG</i>	82	5.62	80.57
SP_PIR_KEYWORDS	protein transport	6	0.632	0.102	<i>LYST, XPO4, IPO11, TOMM20, NUP107, MON2</i>	99	2.40	73.64
GOTERM_BP_FAT	GO:0034504~protein localization in nucleus	3	0.316	0.109	<i>FGF9, IPO11, IFNG</i>	82	5.27	84.13
GOTERM_BP_FAT	GO:0006605~protein targeting	4	0.421	0.138	<i>FGF9, IPO11, IFNG, TOMM20</i>	82	3.07	90.69
GOTERM_BP_FAT	GO:0006886~intracellular protein transport	5	0.526	0.186	<i>GRIK2, FGF9, IPO11, IFNG, TOMM20</i>	82	2.21	96.24
GOTERM_BP_FAT	GO:0034613~cellular protein localization	5	0.526	0.232	<i>GRIK2, FGF9, IPO11, IFNG, TOMM20</i>	82	2.01	98.52

GOTERM_BP_FAT	GO:0070727~cellular macromolecule localization	5	0.526	0.236	<i>GRIK2, FGF9, IPO11, IFNG, TOMM20</i>	82	1.99	98.63
GOTERM_CC_FAT	GO:0012505~endomembrane system	7	0.737	0.246	<i>XPOT, RNF180, IPO11, LEMD3, NUP107, ITPR1, GJB2</i>	70	1.63	96.99
SP_PIR_KEYWORDS	transport	11	1.158	0.345	<i>XPOT, SLC22A16, GRIK2, LYST, XPO4, IPO11, TOMM20, NUP107, ATP12A, MON2, ITPR1</i>	99	1.28	99.47
GOTERM_CC_FAT	GO:0031090~organelle membrane	8	0.842	0.379	<i>RNF180, WASF1, TOMM20, LEMD3, FIG4, MON2, ITPR1, GJB2</i>	70	1.33	99.73
GOTERM_CC_FAT	GO:0019866~organelle inner membrane	3	0.316	0.534	<i>LEMD3, MON2, ITPR1</i>	70	1.67	99.99
<b>Annotation Cluster 11</b>	<b>Enrichment Score*: 0.9910640532547695</b>							
<b>Category</b>	<b>Term</b>	<b>Count</b>	<b>%</b>	<b>P-value</b>	<b>Genes</b>	<b>List Total</b>	<b>Fold Enrichment</b>	<b>FDR</b>
GOTERM_BP_FAT	GO:0031645~negative regulation of neurological system process	3	0.316	0.012	<i>GRIK2, IFNG, AVPR1A</i>	82	17.68	17.66
GOTERM_BP_FAT	GO:0010648~negative regulation of cell communication	6	0.632	0.016	<i>IRAK3, RGS7BP, GRIK2, FGF9, AVPR1A, LEMD3</i>	82	3.99	23.31
GOTERM_BP_FAT	GO:0051240~positive regulation of multicellular organismal process	5	0.526	0.059	<i>EREG, GRIK2, FGF9, IFNG, AVPR1A</i>	82	3.38	61.86
GOTERM_BP_FAT	GO:0051241~negative regulation of multicellular organismal process	4	0.421	0.075	<i>IRAK3, GRIK2, IFNG, AVPR1A</i>	82	4.02	71.36
GOTERM_BP_FAT	GO:0051969~regulation of transmission of nerve	3	0.316	0.220	<i>GRIK2, IFNG, AVPR1A</i>	82	3.37	98.10
GOTERM_BP_FAT	GO:0031644~regulation of neurological system	3	0.316	0.233	<i>GRIK2, IFNG, AVPR1A</i>	82	3.23	98.56
GOTERM_BP_FAT	GO:0042592~homeostatic process	6	0.632	0.470	<i>GRIK2, IFNG, AVPR1A, FOXO3, ATP12A, ITPR1</i>	82	1.32	100.00
GOTERM_BP_FAT	GO:0044057~regulation of system process	3	0.316	0.556	<i>GRIK2, IFNG, AVPR1A</i>	82	1.60	100.00
<b>Annotation Cluster 12</b>	<b>Enrichment Score*: 0.9287717630770937</b>							
<b>Category</b>	<b>Term</b>	<b>Count</b>	<b>%</b>	<b>P-value</b>	<b>Genes</b>	<b>List Total</b>	<b>Fold Enrichment</b>	<b>FDR</b>
GOTERM_BP_FAT	GO:0050678~regulation of epithelial cell proliferation	4	0.421	0.009	<i>CDKN1B, EREG, FGF9, EPGN</i>	82	9.29	13.19
GOTERM_BP_FAT	GO:0032675~regulation of interleukin-6 production	3	0.316	0.020	<i>IRAK3, EREG, IFNG</i>	82	13.75	27.04
GOTERM_BP_FAT	GO:0043086~negative regulation of catalytic activity	6	0.632	0.025	<i>IRAK3, CDKN1B, GRM7, RXFP2, CAND1, LATS2</i>	82	3.57	33.47
GOTERM_BP_FAT	GO:0044092~negative regulation of molecular function	6	0.632	0.050	<i>IRAK3, CDKN1B, GRM7, RXFP2, CAND1, LATS2</i>	82	2.96	55.79
GOTERM_BP_FAT	GO:0042325~regulation of phosphorylation	7	0.737	0.060	<i>IRAK3, CDKN1B, EREG, EPGN, IFNG, IL22, LATS2</i>	82	2.48	62.97

GOTERM_BP_FAT	GO:0019220~regulation of phosphate metabolic process	7	0.737	0.070	<i>IRAK3, CDKN1B, EREG, EPGN, IFNG, IL22, LATS2</i>	82	2.38	68.79
GOTERM_BP_FAT	GO:0051174~regulation of phosphorus metabolic process	7	0.737	0.070	<i>IRAK3, CDKN1B, EREG, EPGN, IFNG, IL22, LATS2</i>	82	2.38	68.79
GOTERM_BP_FAT	GO:0010638~positive regulation of organelle	3	0.316	0.088	<i>CDKN1B, EREG, EPGN</i>	82	5.96	77.16
GOTERM_BP_FAT	GO:0051130~positive regulation of cellular component organization	4	0.421	0.095	<i>CDKN1B, EREG, EPGN, CAND1</i>	82	3.65	79.52
GOTERM_BP_FAT	GO:0006469~negative regulation of protein kinase	3	0.316	0.096	<i>IRAK3, CDKN1B, LATS2</i>	82	5.69	79.92
GOTERM_BP_FAT	GO:0033673~negative regulation of kinase activity	3	0.316	0.101	<i>IRAK3, CDKN1B, LATS2</i>	82	5.50	81.82
GOTERM_BP_FAT	GO:0008284~positive regulation of cell proliferation	6	0.632	0.102	<i>CDKN1B, EREG, FGF9, EPGN, IFNG, AVPR1A</i>	82	2.39	82.13
GOTERM_BP_FAT	GO:0051348~negative regulation of transferase	3	0.316	0.113	<i>IRAK3, CDKN1B, LATS2</i>	82	5.16	85.19
GOTERM_BP_FAT	GO:0022402~cell cycle process	7	0.737	0.122	<i>CDKN1B, EREG, IFNG, SKA3, CENPJ, SESN1, LATS2</i>	82	2.04	87.54
GOTERM_BP_FAT	GO:0033043~regulation of organelle organization	4	0.421	0.141	<i>CDKN1B, EREG, EPGN, SKA3</i>	82	3.04	91.15
GOTERM_BP_FAT	GO:0045859~regulation of protein kinase activity	5	0.526	0.152	<i>IRAK3, CDKN1B, EREG, EPGN, LATS2</i>	82	2.39	92.82
GOTERM_BP_FAT	GO:0043549~regulation of kinase activity	5	0.526	0.166	<i>IRAK3, CDKN1B, EREG, EPGN, LATS2</i>	82	2.31	94.46
GOTERM_BP_FAT	GO:0051338~regulation of transferase activity	5	0.526	0.183	<i>IRAK3, CDKN1B, EREG, EPGN, LATS2</i>	82	2.22	96.06
SP_PIR_KEYWORDS	kinase	6	0.632	0.274	<i>CDK19, IRAK3, CDKN1B, TBK1, DYRK2, LATS2</i>	99	1.69	98.10
GOTERM_BP_FAT	GO:0044093~positive regulation of molecular function	6	0.632	0.274	<i>IRAK3, EREG, EPGN, IFNG, RXFP2, AVPR1A</i>	82	1.69	99.39
GOTERM_BP_FAT	GO:0001817~regulation of cytokine production	3	0.316	0.295	<i>IRAK3, EREG, IFNG</i>	82	2.73	99.63
GOTERM_BP_FAT	GO:0051726~regulation of cell cycle	4	0.421	0.318	<i>CDKN1B, EREG, EPGN, LATS2</i>	82	1.99	99.78
GOTERM_BP_FAT	GO:0002684~positive regulation of immune system	3	0.316	0.418	<i>IRAK3, EREG, IFNG</i>	82	2.08	99.98
GOTERM_BP_FAT	GO:0022403~cell cycle phase	4	0.421	0.453	<i>CDKN1B, EREG, SKA3, LATS2</i>	82	1.59	99.99
GOTERM_BP_FAT	GO:0010605~negative regulation of macromolecule metabolic process	3	0.316	0.939	<i>IRAK3, CDKN1B, EREG</i>	82	0.67	100.00
<b>Annotation Cluster 13</b>	<b>Enrichment Score*: 0.8999994266355725</b>							
<b>Category</b>	<b>Term</b>	<b>Count</b>	<b>%</b>	<b>P-value</b>	<b>Genes</b>	<b>List Total</b>	<b>Fold Enrichment</b>	<b>FDR</b>
GOTERM_BP_FAT	GO:0012502~induction of programmed cell death	6	0.632	0.043	<i>CDKN1B, GRIK2, LYST, DYRK2, FOXO3, SMPD2</i>	82	3.08	50.68
GOTERM_BP_FAT	GO:0043068~positive regulation of programmed cell death	7	0.737	0.045	<i>CDKN1B, GRIK2, LYST, IFNG, DYRK2, FOXO3, SMPD2</i>	82	2.67	52.16
GOTERM_BP_FAT	GO:0010942~positive regulation of cell death	7	0.737	0.046	<i>CDKN1B, GRIK2, LYST, IFNG, DYRK2, FOXO3, SMPD2</i>	82	2.65	52.83



GOTERM_BP_FAT	GO:0008219~cell death	9	0.947	0.065	<i>CDKN1B, GRIK2, IFNG, DYRK2, FOXO3, GJB6, PARP4, FIG4, ITPR1</i>	82	2.07	66.05
GOTERM_BP_FAT	GO:0016265~death	9	0.947	0.068	<i>CDKN1B, GRIK2, IFNG, DYRK2, FOXO3, GJB6, PARP4, FIG4, ITPR1</i>	82	2.05	67.26
GOTERM_BP_FAT	GO:0043065~positive regulation of apoptosis	6	0.632	0.115	<i>CDKN1B, LYST, IFNG, DYRK2, FOXO3, SMPD2</i>	82	2.30	85.82
GOTERM_BP_FAT	GO:0006917~induction of apoptosis	5	0.526	0.125	<i>CDKN1B, LYST, DYRK2, FOXO3,</i>	82	2.58	88.18
GOTERM_BP_FAT	GO:0042981~regulation of apoptosis	8	0.842	0.205	<i>CDKN1B, GRIK2, LYST, IFNG, RXFP2, DYRK2, FOXO3, SMPD2</i>	82	1.64	97.45
GOTERM_BP_FAT	GO:0043067~regulation of programmed cell death	8	0.842	0.212	<i>CDKN1B, GRIK2, LYST, IFNG, RXFP2, DYRK2, FOXO3, SMPD2</i>	82	1.63	97.78
GOTERM_BP_FAT	GO:0010941~regulation of cell death	8	0.842	0.215	<i>CDKN1B, GRIK2, LYST, IFNG, RXFP2, DYRK2, FOXO3, SMPD2</i>	82	1.62	97.90
GOTERM_BP_FAT	GO:0033554~cellular response to stress	6	0.632	0.251	<i>IFNG, AVPR1A, DYRK2, FOXO3, PARP4, SESN1</i>	82	1.75	99.01
GOTERM_BP_FAT	GO:0012501~programmed cell death	6	0.632	0.303	<i>CDKN1B, GRIK2, IFNG, DYRK2, FOXO3, GJB6</i>	82	1.62	99.69
GOTERM_BP_FAT	GO:0006915~apoptosis	5	0.526	0.489	<i>GRIK2, IFNG, DYRK2, FOXO3, GJB6</i>	82	1.37	100.00
<b>Annotation Cluster 14</b>	<b>Enrichment Score*: 0.8862431920157612</b>							
<b>Category</b>	<b>Term</b>	<b>Count</b>	<b>%</b>	<b>P-value</b>	<b>Genes</b>	<b>List Total</b>	<b>Fold Enrichment</b>	<b>FDR</b>
GOTERM_BP_FAT	GO:0045862~positive regulation of proteolysis	3	0.316	0.010	<i>RNF180, IFNG, IFT88</i>	82	19.80	14.43
GOTERM_BP_FAT	GO:0030162~regulation of proteolysis	3	0.316	0.040	<i>RNF180, IFNG, IFT88</i>	82	9.34	47.95
GOTERM_BP_FAT	GO:0032270~positive regulation of cellular protein metabolic process	3	0.316	0.408	<i>RNF180, IFNG, IFT88</i>	82	2.12	99.98
GOTERM_BP_FAT	GO:0051247~positive regulation of protein metabolic process	3	0.316	0.429	<i>RNF180, IFNG, IFT88</i>	82	2.04	99.99
GOTERM_BP_FAT	GO:0032268~regulation of cellular protein metabolic process	4	0.421	0.544	<i>RNF180, IFNG, IL22, IFT88</i>	82	1.39	100.00
<b>Annotation Cluster 15</b>	<b>Enrichment Score*: 0.821676537587384</b>							
<b>Category</b>	<b>Term</b>	<b>Count</b>	<b>%</b>	<b>P-value</b>	<b>Genes</b>	<b>List Total</b>	<b>Fold Enrichment</b>	<b>FDR</b>
GOTERM_CC_FAT	GO:0015630~microtubule cytoskeleton	8	0.842	0.028	<i>RASSF3, LYST, SKA3, PARP4, CENPJ, IFT88, LATS2, KIF2A</i>	70	2.66	29.85
SP_PIR_KEYWORDS	cytoskeleton	7	0.737	0.106	<i>WASF1, SKA3, MICAL1, PARP4, CENPJ, LATS2, KIF2A</i>	99	2.14	75.12
SP_PIR_KEYWORDS	microtubule	4	0.421	0.114	<i>RASSF3, SKA3, CENPJ, KIF2A</i>	99	3.36	77.73

GOTERM_CC_FAT	GO:0044430~cytoskeletal part	9	0.947	0.140	<i>RASSF3, SKA3, MICAL1, PARP4, CENPJ, IFT88, ITPR1, LATS2, KIF2A</i>	70	1.73	84.55
GOTERM_CC_FAT	GO:0005815~microtubule organizing center	4	0.421	0.156	<i>CENPJ, IFT88, LATS2, KIF2A</i>	70	2.89	87.89
GOTERM_CC_FAT	GO:0005874~microtubule	4	0.421	0.184	<i>RASSF3, SKA3, CENPJ, KIF2A</i>	70	2.67	92.01
GOTERM_CC_FAT	GO:0005819~spindle	3	0.316	0.188	<i>SKA3, PARP4, LATS2</i>	70	3.73	92.50
GOTERM_CC_FAT	GO:0005856~cytoskeleton	11	1.158	0.208	<i>RASSF3, LYST, WASF1, SKA3, MICAL1, PARP4, CENPJ, IFT88, ITPR1, LATS2, KIF2A</i>	70	1.45	94.44
GOTERM_CC_FAT	GO:0043228~non-membrane-bounded organelle	18	1.895	0.224	<i>GPR19, WASF1, ARID4B, CENPJ, ITPR1, LATS2, RASSF3, DDX47, HELB, LYST, PSPC1, SKA3, MICAL1, NUP107, PARP4, IFT88, MPHOSPH8, KIF2A</i>	70	1.27	95.70
GOTERM_CC_FAT	GO:0043232~intracellular non-membrane-bounded organelle	18	1.895	0.224	<i>GPR19, WASF1, ARID4B, CENPJ, ITPR1, LATS2, RASSF3, DDX47, HELB, LYST, PSPC1, SKA3, MICAL1, NUP107, PARP4, IFT88, MPHOSPH8, KIF2A</i>	70	1.27	95.70
GOTERM_CC_FAT	GO:0005813~centrosome	3	0.316	0.342	<i>CENPJ, LATS2, KIF2A</i>	70	2.45	99.44
<b>Annotation Cluster 16</b>	<b>Enrichment Score*: 0.7613977358948828</b>							
<b>Category</b>	<b>Term</b>	<b>Count</b>	<b>%</b>	<b>P-value</b>	<b>Genes</b>	<b>List Total</b>	<b>Fold Enrichment</b>	<b>FDR</b>
GOTERM_MF_FAT	GO:0008026~ATP-dependent helicase activity	3	0.316	0.105	<i>DDX47, HELB, ASCC3</i>	74	5.37	76.26
GOTERM_MF_FAT	GO:0070035~purine NTP-dependent helicase activity	3	0.316	0.105	<i>DDX47, HELB, ASCC3</i>	74	5.37	76.26
SP_PIR_KEYWORDS	helicase	3	0.316	0.149	<i>DDX47, HELB, ASCC3</i>	99	4.35	86.52
GOTERM_MF_FAT	GO:0004386~helicase activity	3	0.316	0.186	<i>DDX47, HELB, ASCC3</i>	74	3.76	93.04
GOTERM_MF_FAT	GO:0042623~ATPase activity, coupled	4	0.421	0.197	<i>DDX47, HELB, ASCC3, ATP12A</i>	74	2.58	94.16
SP_PIR_KEYWORDS	hydrolase	11	1.158	0.268	<i>GNS, CPM, DDX47, MTHFD2L, HELB, ASCC3, PPM1H, FIG4, ATP12A, USP15, SMPD2</i>	99	1.37	97.90
GOTERM_MF_FAT	GO:0016887~ATPase activity	4	0.421	0.290	<i>DDX47, HELB, ASCC3, ATP12A</i>	74	2.10	98.81
<b>Annotation Cluster 17</b>	<b>Enrichment Score*: 0.667349552508645</b>							
<b>Category</b>	<b>Term</b>	<b>Count</b>	<b>%</b>	<b>P-value</b>	<b>Genes</b>	<b>List Total</b>	<b>Fold Enrichment</b>	<b>FDR</b>
GOTERM_BP_FAT	GO:0031328~positive regulation of cellular biosynthetic process	10	1.053	0.021	<i>EREG, GRIP1, IFNG, RXFP2, AVPR1A, CAND1, DYRK2, FOXO3, AREG, IL22</i>	82	2.41	28.68
GOTERM_BP_FAT	GO:0009891~positive regulation of biosynthetic process	10	1.053	0.023	<i>EREG, GRIP1, IFNG, RXFP2, AVPR1A, CAND1, DYRK2, FOXO3, AREG, IL22</i>	82	2.37	30.77

GOTERM_BP_FAT	GO:0051054~positive regulation of DNA metabolic process	3	0.316	0.044	<i>EREG, IFNG, AREG</i>	82	8.84	51.47
GOTERM_BP_FAT	GO:0010604~positive regulation of macromolecule metabolic process	10	1.053	0.070	<i>RNF180, EREG, GRIPI1, IFNG, CAND1, DYRK2, FOXO3, AREG, IL22, IFT88</i>	82	1.93	68.50
GOTERM_BP_FAT	GO:0045935~positive regulation of nucleobase, nucleoside, nucleotide and nucleic acid metabolic	8	0.842	0.080	<i>EREG, GRIPI1, IFNG, RXFP2, CAND1, FOXO3, AREG, IL22</i>	82	2.12	73.40
GOTERM_BP_FAT	GO:0051173~positive regulation of nitrogen compound metabolic process	8	0.842	0.091	<i>EREG, GRIPI1, IFNG, RXFP2, CAND1, FOXO3, AREG, IL22</i>	82	2.05	78.01
GOTERM_BP_FAT	GO:0010557~positive regulation of macromolecule biosynthetic process	8	0.842	0.096	<i>EREG, GRIPI1, IFNG, CAND1, DYRK2, FOXO3, AREG, IL22</i>	82	2.02	80.13
GOTERM_BP_FAT	GO:0051052~regulation of DNA metabolic process	3	0.316	0.149	<i>EREG, IFNG, AREG</i>	82	4.34	92.39
GOTERM_BP_FAT	GO:0045893~positive regulation of transcription, DNA-dependent	5	0.526	0.320	<i>GRIPI1, IFNG, CAND1, FOXO3, IL22</i>	82	1.73	99.79
GOTERM_BP_FAT	GO:0051254~positive regulation of RNA metabolic process	5	0.526	0.325	<i>GRIPI1, IFNG, CAND1, FOXO3, IL22</i>	82	1.71	99.81
GOTERM_BP_FAT	GO:0045941~positive regulation of transcription	5	0.526	0.439	<i>GRIPI1, IFNG, CAND1, FOXO3, IL22</i>	82	1.46	99.99
GOTERM_BP_FAT	GO:0010628~positive regulation of gene expression	5	0.526	0.461	<i>GRIPI1, IFNG, CAND1, FOXO3, IL22</i>	82	1.42	99.99
GOTERM_BP_FAT	GO:0045944~positive regulation of transcription from RNA polymerase II promoter	3	0.316	0.656	<i>CAND1, FOXO3, IL22</i>	82	1.33	100.00
GOTERM_MF_FAT	GO:0016563~transcription activator activity	3	0.316	0.676	<i>GRIPI1, CAND1, FOXO3</i>	74	1.28	100.00
GOTERM_BP_FAT	GO:0006357~regulation of transcription from RNA polymerase II promoter	4	0.421	0.818	<i>SAP18, CAND1, FOXO3, IL22</i>	82	0.91	100.00
GOTERM_BP_FAT	GO:0006355~regulation of transcription, DNA-dependent	8	0.842	0.920	<i>CDKN1B, GRIPI1, IFNG, SAP18, CAND1, FOXO3, IL22, CREBL2</i>	82	0.74	100.00
GOTERM_BP_FAT	GO:0051252~regulation of RNA metabolic process	8	0.842	0.930	<i>CDKN1B, GRIPI1, IFNG, SAP18, CAND1, FOXO3, IL22, CREBL2</i>	82	0.73	100.00
GOTERM_MF_FAT	GO:0030528~transcription regulator activity	5	0.526	0.977	<i>GRIPI1, SAP18, CAND1, FOXO3,</i>	74	0.58	100.00
<b>Annotation Cluster 18</b>	<b>Enrichment Score*: 0.648823616670225</b>							
<b>Category</b>	<b>Term</b>	<b>Count</b>	<b>%</b>	<b>P-value</b>	<b>Genes</b>	<b>List Total</b>	<b>Fold Enrichment</b>	<b>FDR</b>
INTERPRO	IPR017979:GPCR, family 3, conserved site	3	0.316	0.006	<i>GPRC5D, GRM7, GPRC5A</i>	89	25.52	7.26
INTERPRO	IPR017978:GPCR, family 3, C-terminal	3	0.316	0.007	<i>GPRC5D, GRM7, GPRC5A</i>	89	23.40	8.56
KEGG_PATHWAY	hsa04080:Neuroactive ligand-receptor interaction	4	0.421	0.216	<i>GRIK2, GRM7, RXFP2, AVPR1A</i>	33	2.41	91.16
SP_PIR_KEYWORDS	transducer	7	0.737	0.287	<i>GPRC5D, GPR19, GRM7, RXFP2, AVPR1A, GNG4, GPRC5A</i>	99	1.56	98.48
SP_PIR_KEYWORDS	g-protein coupled receptor	6	0.632	0.403	<i>GPRC5D, GPR19, GRM7, RXFP2, AVPR1A, GPRC5A</i>	99	1.43	99.83

SP_PIR_KEYWORDS	receptor	9	0.947	0.563	<i>IRAK3, GPRC5D, GPR19, GRIK2, GRM7, RXFP2, AVPRIA, GPRC5A, ITPR1</i>	99	1.10	100.00
UP_SEQ_FEATURE	topological domain:Extracellular	13	1.368	0.755	<i>GPRC5D, GPR19, EREG, GRIK2, EPGN, GRM7, RXFP2, AVPRIA, GJB6, CD164, GPRC5A, GJA3, GJB2</i>	99	0.92	100.00
PIR_SUPERFAMILY	PIRSF800006:rhodopsin-like G protein-coupled	3	0.316	0.897	<i>GPR19, RXFP2, AVPRIA</i>	41	0.79	100.00
INTERPRO	IPR017452:GPCR, rhodopsin-like superfamily	3	0.316	0.901	<i>GPR19, RXFP2, AVPRIA</i>	89	0.77	100.00
INTERPRO	IPR000276:7TM GPCR, rhodopsin-like	3	0.316	0.902	<i>GPR19, RXFP2, AVPRIA</i>	89	0.77	100.00
<b>Annotation Cluster 19</b>	<b>Enrichment Score*: 0.5501672055565894</b>							
Category	Term	Count	%	P-value	Genes	List Total	Fold Enrichment	FDR
SP_PIR_KEYWORDS	magnesium	6	0.632	0.075	<i>IRAK3, MTHFD2L, DYRK2, ATP12A, LATS2, SMPD2</i>	99	2.64	62.21
GOTERM_MF_FAT	GO:0000287~magnesium ion binding	6	0.632	0.110	<i>IRAK3, MTHFD2L, DYRK2, ATP12A, LATS2, SMPD2</i>	74	2.33	77.98
INTERPRO	IPR008271:Serine/threonine protein kinase, active site	5	0.526	0.118	<i>CDK19, IRAK3, TBK1, DYRK2, LATS2</i>	89	2.64	79.43
INTERPRO	IPR017442:Serine/threonine protein kinase-related	5	0.526	0.122	<i>CDK19, IRAK3, TBK1, DYRK2, LATS2</i>	89	2.61	80.70
GOTERM_MF_FAT	GO:0004672~protein kinase activity	7	0.737	0.125	<i>CDK19, IRAK3, TBK1, EPGN, WIF1, DYRK2, LATS2</i>	74	2.03	82.24
SP_PIR_KEYWORDS	serine/threonine-protein kinase	5	0.526	0.130	<i>CDK19, IRAK3, TBK1, DYRK2, LATS2</i>	99	2.55	82.25
GOTERM_BP_FAT	GO:0007243~protein kinase cascade	5	0.526	0.181	<i>TBK1, EPGN, IFNG, LATS2, SMPD2</i>	82	2.23	95.87
GOTERM_MF_FAT	GO:0042623~ATPase activity, coupled	4	0.421	0.197	<i>DDX47, HELB, ASCC3, ATP12A</i>	74	2.58	94.16
GOTERM_BP_FAT	GO:0016310~phosphorylation	8	0.842	0.202	<i>CDK19, IRAK3, TBK1, EPGN, IFNG, DYRK2, MON2, LATS2</i>	82	1.65	97.27
GOTERM_BP_FAT	GO:0006468~protein amino acid phosphorylation	7	0.737	0.209	<i>CDK19, IRAK3, TBK1, EPGN, IFNG, DYRK2, LATS2</i>	82	1.73	97.65
INTERPRO	IPR017441:Protein kinase, ATP binding site	5	0.526	0.220	<i>CDK19, IRAK3, TBK1, DYRK2, LATS2</i>	89	2.06	95.66
UP_SEQ_FEATURE	domain:Protein kinase	5	0.526	0.220	<i>CDK19, IRAK3, TBK1, DYRK2, LATS2</i>	99	2.06	96.71
GOTERM_MF_FAT	GO:0004674~protein serine/threonine kinase activity	5	0.526	0.223	<i>CDK19, IRAK3, TBK1, DYRK2, LATS2</i>	74	2.04	96.16
UP_SEQ_FEATURE	nucleotide phosphate-binding region:ATP	8	0.842	0.224	<i>CDK19, IRAK3, DDX47, ASCC3, TBK1, DYRK2, LATS2, KIF2A</i>	99	1.61	96.89
SP_PIR_KEYWORDS	atp-binding	10	1.053	0.234	<i>CDK19, IRAK3, DDX47, HELB, ASCC3, TBK1, DYRK2, ATP12A, LATS2, KIF2A</i>	99	1.47	96.31
INTERPRO	IPR000719:Protein kinase, core	5	0.526	0.244	<i>CDK19, IRAK3, TBK1, DYRK2, LATS2</i>	89	1.97	97.07
SP_PIR_KEYWORDS	kinase	6	0.632	0.274	<i>CDK19, IRAK3, CDKN1B, TBK1, DYRK2, LATS2</i>	99	1.69	98.10
GOTERM_MF_FAT	GO:0016887~ATPase activity	4	0.421	0.290	<i>DDX47, HELB, ASCC3, ATP12A</i>	74	2.10	98.81
UP_SEQ_FEATURE	binding site:ATP	5	0.526	0.303	<i>CDK19, IRAK3, TBK1, DYRK2, LATS2</i>	99	1.78	99.29

SP_PIR_KEYWORDS	nucleotide-binding	11	1.158	0.356	<i>CDK19, IRAK3, DDX47, HELB, ASCC3, TBK1, RAP1B, DYRK2, ATP12A, LATS2, KIF2A</i>	99	1.27	99.57
GOTERM_BP_FAT	GO:0006793~phosphorus metabolic process	8	0.842	0.364	<i>CDK19, IRAK3, TBK1, EPGN, IFNG, DYRK2, MON2, LATS2</i>	82	1.36	99.93
GOTERM_BP_FAT	GO:0006796~phosphate metabolic process	8	0.842	0.364	<i>CDK19, IRAK3, TBK1, EPGN, IFNG, DYRK2, MON2, LATS2</i>	82	1.36	99.93
INTERPRO	IPR002290:Serine/threonine protein kinase	3	0.316	0.398	<i>CDK19, DYRK2, LATS2</i>	89	2.17	99.84
SMART	SM00220:S_TKc	3	0.316	0.410	<i>CDK19, DYRK2, LATS2</i>	50	2.10	99.45
SP_PIR_KEYWORDS	transferase	9	0.947	0.417	<i>CDK19, IRAK3, TBK1, B3GALNT2, DYRK2, PARP4, ZDHHC20, PDSS2,</i>	99	1.25	99.88
UP_SEQ_FEATURE	active site:Proton acceptor	5	0.526	0.438	<i>CDK19, TBK1, DYRK2, LATS2, SMPD2</i>	99	1.47	99.96
GOTERM_MF_FAT	GO:0005524~ATP binding	10	1.053	0.452	<i>CDK19, IRAK3, DDX47, HELB, ASCC3, TBK1, DYRK2, ATP12A, LATS2, KIF2A</i>	74	1.19	99.96
GOTERM_MF_FAT	GO:0032559~adenyl ribonucleotide binding	10	1.053	0.469	<i>CDK19, IRAK3, DDX47, HELB, ASCC3, TBK1, DYRK2, ATP12A, LATS2, KIF2A</i>	74	1.17	99.97
GOTERM_MF_FAT	GO:0000166~nucleotide binding	14	1.474	0.502	<i>CDK19, TBK1, LEMD3, ATP12A, LATS2, IRAK3, CRYL1, DDX47, ASCC3, HELB, PSPC1, RAP1B, DYRK2, KIF2A</i>	74	1.09	99.99
GOTERM_MF_FAT	GO:0030554~adenyl nucleotide binding	10	1.053	0.535	<i>CDK19, IRAK3, DDX47, HELB, ASCC3, TBK1, DYRK2, ATP12A, LATS2, KIF2A</i>	74	1.11	99.99
GOTERM_MF_FAT	GO:0001883~purine nucleoside binding	10	1.053	0.554	<i>CDK19, IRAK3, DDX47, HELB, ASCC3, TBK1, DYRK2, ATP12A, LATS2, KIF2A</i>	74	1.10	100.00
GOTERM_MF_FAT	GO:0001882~nucleoside binding	10	1.053	0.562	<i>CDK19, IRAK3, DDX47, HELB, ASCC3, TBK1, DYRK2, ATP12A, LATS2, KIF2A</i>	74	1.09	100.00
GOTERM_MF_FAT	GO:0032555~purine ribonucleotide binding	11	1.158	0.595	<i>CDK19, IRAK3, DDX47, HELB, ASCC3, TBK1, RAP1B, DYRK2, ATP12A, LATS2, KIF2A</i>	74	1.05	100.00
GOTERM_MF_FAT	GO:0032553~ribonucleotide binding	11	1.158	0.595	<i>CDK19, IRAK3, DDX47, HELB, ASCC3, TBK1, RAP1B, DYRK2, ATP12A, LATS2, KIF2A</i>	74	1.05	100.00
GOTERM_MF_FAT	GO:0017076~purine nucleotide binding	11	1.158	0.652	<i>CDK19, IRAK3, DDX47, HELB, ASCC3, TBK1, RAP1B, DYRK2, ATP12A, LATS2, KIF2A</i>	74	1.01	100.00
<b>Annotation Cluster 20</b>	<b>Enrichment Score*: 0.5245166212806537</b>							
<b>Category</b>	<b>Term</b>	<b>Count</b>	<b>%</b>	<b>P-value</b>	<b>Genes</b>	<b>List Total</b>	<b>Fold Enrichment</b>	<b>FDR</b>

GOTERM_MF_FAT	GO:0046983~protein dimerization activity	6	0.632	0.189	<i>IRAK3, CRYL1, RNF17, GRIK2, PDSS2, CREBL2</i>	74	1.94	93.34
GOTERM_MF_FAT	GO:0042803~protein homodimerization activity	4	0.421	0.290	<i>IRAK3, CRYL1, RNF17, GRIK2</i>	74	2.10	98.81
GOTERM_MF_FAT	GO:0042802~identical protein binding	5	0.526	0.488	<i>IRAK3, CRYL1, RNF17, GRIK2, GJA3</i>	74	1.37	99.98
<b>Annotation Cluster 21</b>	<b>Enrichment Score*: 0.5224967758348501</b>							
<b>Category</b>	<b>Term</b>	<b>Count</b>	<b>%</b>	<b>P-value</b>	<b>Genes</b>	<b>List Total</b>	<b>Fold Enrichment</b>	<b>FDR</b>
GOTERM_BP_FAT	GO:0040008~regulation of growth	5	0.526	0.148	<i>CDKN1B, FGF9, IFNG, AVPR1A, GNG4</i>	82	2.42	92.20
GOTERM_BP_FAT	GO:0001558~regulation of cell growth	3	0.316	0.324	<i>CDKN1B, AVPR1A, GNG4</i>	82	2.55	99.81
GOTERM_BP_FAT	GO:0008361~regulation of cell size	3	0.316	0.350	<i>CDKN1B, AVPR1A, GNG4</i>	82	2.40	99.90
GOTERM_BP_FAT	GO:0032535~regulation of cellular component size	3	0.316	0.485	<i>CDKN1B, AVPR1A, GNG4</i>	82	1.83	100.00
<b>Annotation Cluster 22</b>	<b>Enrichment Score*: 0.5224068415021378</b>							
<b>Category</b>	<b>Term</b>	<b>Count</b>	<b>%</b>	<b>P-value</b>	<b>Genes</b>	<b>List Total</b>	<b>Fold Enrichment</b>	<b>FDR</b>
GOTERM_CC_FAT	GO:0044456~synapse part	4	0.421	0.147	<i>GRIP1, GRIK2, GRM7, ITPR1</i>	70	2.97	86.19
GOTERM_CC_FAT	GO:0045211~postsynaptic membrane	3	0.316	0.165	<i>GRIP1, GRIK2, GRM7</i>	70	4.06	89.36
GOTERM_MF_FAT	GO:0015267~channel activity	5	0.526	0.201	<i>GRIK2, GRM7, ITPR1, GJA3, GJB2</i>	74	2.13	94.56
GOTERM_MF_FAT	GO:0022803~passive transmembrane transporter	5	0.526	0.202	<i>GRIK2, GRM7, ITPR1, GJA3, GJB2</i>	74	2.12	94.66
GOTERM_CC_FAT	GO:0045202~synapse	4	0.421	0.300	<i>GRIP1, GRIK2, GRM7, ITPR1</i>	70	2.06	98.81
GOTERM_MF_FAT	GO:0022836~gated channel activity	3	0.316	0.523	<i>GRIK2, GRM7, ITPR1</i>	74	1.70	99.99
GOTERM_MF_FAT	GO:0005216~ion channel activity	3	0.316	0.643	<i>GRIK2, GRM7, ITPR1</i>	74	1.36	100.00
GOTERM_MF_FAT	GO:0022838~substrate specific channel activity	3	0.316	0.660	<i>GRIK2, GRM7, ITPR1</i>	74	1.32	100.00
<b>Annotation Cluster 23</b>	<b>Enrichment Score*: 0.5190338548468313</b>							
<b>Category</b>	<b>Term</b>	<b>Count</b>	<b>%</b>	<b>P-value</b>	<b>Genes</b>	<b>List Total</b>	<b>Fold Enrichment</b>	<b>FDR</b>
GOTERM_CC_FAT	GO:0031967~organelle envelope	8	0.842	0.049	<i>XPOT, WASF1, IPO11, TOMM20, LEMD3, NUP107, MON2, ITPR1</i>	70	2.36	46.51
GOTERM_CC_FAT	GO:0031975~envelope	8	0.842	0.050	<i>XPOT, WASF1, IPO11, TOMM20, LEMD3, NUP107, MON2, ITPR1</i>	70	2.35	47.01
GOTERM_CC_FAT	GO:0031090~organelle membrane	8	0.842	0.379	<i>RNF180, WASF1, TOMM20, LEMD3, FIG4, MON2, ITPR1, GJB2</i>	70	1.33	99.73
GOTERM_CC_FAT	GO:0031966~mitochondrial membrane	3	0.316	0.632	<i>WASF1, TOMM20, MON2</i>	70	1.39	100.00
GOTERM_CC_FAT	GO:0005740~mitochondrial envelope	3	0.316	0.666	<i>WASF1, TOMM20, MON2</i>	70	1.31	100.00
GOTERM_CC_FAT	GO:0005739~mitochondrion	6	0.632	0.709	<i>WASF1, HEBP1, TOMM20, RTN4IP1, MON2, MSRB3</i>	70	1.01	100.00
GOTERM_CC_FAT	GO:0044429~mitochondrial part	3	0.316	0.838	<i>WASF1, TOMM20, MON2</i>	70	0.92	100.00

<b>Annotation Cluster 24</b>	<b>Enrichment Score*: 0.5139189604884302</b>							
<b>Category</b>	<b>Term</b>	<b>Count</b>	<b>%</b>	<b>P-value</b>	<b>Genes</b>	<b>List Total</b>	<b>Fold Enrichment</b>	<b>FDR</b>
GOTERM_BP_FAT	GO:0007049~cell cycle	9	0.947	0.092	<i>CDKN1B, EREG, IFNG, SKA3, CENPJ, SESN1, MPHOSPH8, LATS2, CREBL2</i>	82	1.91	78.68
GOTERM_BP_FAT	GO:0022402~cell cycle process	7	0.737	0.122	<i>CDKN1B, EREG, IFNG, SKA3, CENPJ, SESN1, LATS2</i>	82	2.04	87.54
SP_PIR_KEYWORDS	cell cycle	4	0.421	0.418	<i>CDKN1B, SKA3, LATS2, CREBL2</i>	99	1.69	99.88
GOTERM_BP_FAT	GO:0022403~cell cycle phase	4	0.421	0.453	<i>CDKN1B, EREG, SKA3, LATS2</i>	82	1.59	99.99
GOTERM_BP_FAT	GO:0000279~M phase	3	0.316	0.590	<i>EREG, SKA3, LATS2</i>	82	1.50	100.00
GOTERM_BP_FAT	GO:0000278~mitotic cell cycle	3	0.316	0.654	<i>CDKN1B, SKA3, LATS2</i>	82	1.34	100.00
<b>Annotation Cluster 25</b>	<b>Enrichment Score*: 0.49278078561395233</b>							
<b>Category</b>	<b>Term</b>	<b>Count</b>	<b>%</b>	<b>P-value</b>	<b>Genes</b>	<b>List Total</b>	<b>Fold Enrichment</b>	<b>FDR</b>
GOTERM_BP_FAT	GO:0043623~cellular protein complex assembly	4	0.421	0.073	<i>GRIK2, WASF1, IPO11, CENPJ</i>	82	4.07	70.28
GOTERM_BP_FAT	GO:0034622~cellular macromolecular complex	4	0.421	0.297	<i>GRIK2, WASF1, IPO11, CENPJ</i>	82	2.08	99.64
GOTERM_BP_FAT	GO:0070271~protein complex biogenesis	5	0.526	0.358	<i>GRIK2, WASF1, IPO11, CENPJ, PDSS2</i>	82	1.63	99.92
GOTERM_BP_FAT	GO:0006461~protein complex assembly	5	0.526	0.358	<i>GRIK2, WASF1, IPO11, CENPJ, PDSS2</i>	82	1.63	99.92
GOTERM_BP_FAT	GO:0034621~cellular macromolecular complex subunit organization	4	0.421	0.361	<i>GRIK2, WASF1, IPO11, CENPJ</i>	82	1.85	99.92
GOTERM_BP_FAT	GO:0065003~macromolecular complex assembly	5	0.526	0.568	<i>GRIK2, WASF1, IPO11, CENPJ, PDSS2</i>	82	1.24	100.00
GOTERM_BP_FAT	GO:0043933~macromolecular complex subunit organization	5	0.526	0.621	<i>GRIK2, WASF1, IPO11, CENPJ, PDSS2</i>	82	1.16	100.00
<b>Annotation Cluster 26</b>	<b>Enrichment Score*: 0.4833250623420468</b>							
<b>Category</b>	<b>Term</b>	<b>Count</b>	<b>%</b>	<b>P-value</b>	<b>Genes</b>	<b>List Total</b>	<b>Fold Enrichment</b>	<b>FDR</b>
GOTERM_BP_FAT	GO:0006164~purine nucleotide biosynthetic process	3	0.316	0.222	<i>MTHFD2L, ATP12A, MON2</i>	82	3.34	98.19
GOTERM_BP_FAT	GO:0009165~nucleotide biosynthetic process	3	0.316	0.306	<i>MTHFD2L, ATP12A, MON2</i>	82	2.66	99.71
GOTERM_BP_FAT	GO:0006163~purine nucleotide metabolic process	3	0.316	0.306	<i>MTHFD2L, ATP12A, MON2</i>	82	2.66	99.71
GOTERM_BP_FAT	GO:0034654~nucleobase, nucleoside, nucleotide and nucleic acid biosynthetic process	3	0.316	0.322	<i>MTHFD2L, ATP12A, MON2</i>	82	2.56	99.80
GOTERM_BP_FAT	GO:0034404~nucleobase, nucleoside and nucleotide biosynthetic process	3	0.316	0.322	<i>MTHFD2L, ATP12A, MON2</i>	82	2.56	99.80
GOTERM_BP_FAT	GO:0044271~nitrogen compound biosynthetic process	3	0.316	0.583	<i>MTHFD2L, ATP12A, MON2</i>	82	1.52	100.00
<b>Annotation Cluster 27</b>	<b>Enrichment Score*: 0.4272423121442745</b>							

Category	Term	Count	%	P-value	Genes	List Total	Fold Enrichment	FDR
GOTERM_MF_FAT	GO:0022890~inorganic cation transmembrane transporter activity	4	0.421	0.053	<i>SLC22A16, ATP12A, MON2, ITPR1</i>	74	4.65	50.72
SP_PIR_KEYWORDS	ion transport	5	0.526	0.340	<i>SLC22A16, GRIK2, ATP12A, MON2,</i>	99	1.68	99.42
SP_PIR_KEYWORDS	transport	11	1.158	0.345	<i>XPOT, SLC22A16, GRIK2, LYST, XPO4, IPO11, TOMM20, NUP107, ATP12A, MON2, ITPR1</i>	99	1.28	99.47
GOTERM_BP_FAT	GO:0006812~cation transport	5	0.526	0.424	<i>SLC22A16, CDKN1B, ATP12A, MON2, ITPR1</i>	82	1.49	99.98
GOTERM_BP_FAT	GO:0006811~ion transport	6	0.632	0.490	<i>SLC22A16, CDKN1B, GRIK2, ATP12A, MON2, ITPR1</i>	82	1.29	100.00
GOTERM_BP_FAT	GO:0015672~monovalent inorganic cation transport	3	0.316	0.571	<i>CDKN1B, ATP12A, MON2</i>	82	1.56	100.00
GOTERM_BP_FAT	GO:0055085~transmembrane transport	4	0.421	0.668	<i>SLC22A16, NUP107, MON2, ITPR1</i>	82	1.16	100.00
GOTERM_BP_FAT	GO:0030001~metal ion transport	3	0.316	0.772	<i>CDKN1B, ATP12A, ITPR1</i>	82	1.06	100.00
<b>Annotation Cluster 28</b>	<b>Enrichment Score*: 0.4070438317198611</b>							
Category	Term	Count	%	P-value	Genes	List Total	Fold Enrichment	FDR
GOTERM_BP_FAT	GO:0055065~metal ion homeostasis	4	0.421	0.125	<i>GRIK2, AVPR1A, ATP12A, ITPR1</i>	82	3.22	88.07
GOTERM_BP_FAT	GO:0055080~cation homeostasis	4	0.421	0.245	<i>GRIK2, AVPR1A, ATP12A, ITPR1</i>	82	2.31	98.87
GOTERM_BP_FAT	GO:0006874~cellular calcium ion homeostasis	3	0.316	0.300	<i>GRIK2, AVPR1A, ITPR1</i>	82	2.70	99.66
GOTERM_BP_FAT	GO:0055074~calcium ion homeostasis	3	0.316	0.311	<i>GRIK2, AVPR1A, ITPR1</i>	82	2.63	99.74
GOTERM_BP_FAT	GO:0006875~cellular metal ion homeostasis	3	0.316	0.328	<i>GRIK2, AVPR1A, ITPR1</i>	82	2.53	99.83
SP_PIR_KEYWORDS	ion transport	5	0.526	0.340	<i>SLC22A16, GRIK2, ATP12A, MON2,</i>	99	1.68	99.42
GOTERM_BP_FAT	GO:0048878~chemical homeostasis	5	0.526	0.368	<i>GRIK2, AVPR1A, FOXO3, ATP12A,</i>	82	1.61	99.93
GOTERM_BP_FAT	GO:0030005~cellular di-, tri-valent inorganic cation homeostasis	3	0.316	0.395	<i>GRIK2, AVPR1A, ITPR1</i>	82	2.18	99.97
GOTERM_BP_FAT	GO:0055066~di-, tri-valent inorganic cation	3	0.316	0.421	<i>GRIK2, AVPR1A, ITPR1</i>	82	2.07	99.98
GOTERM_BP_FAT	GO:0050801~ion homeostasis	4	0.421	0.445	<i>GRIK2, AVPR1A, ATP12A, ITPR1</i>	82	1.61	99.99
GOTERM_BP_FAT	GO:0030003~cellular cation homeostasis	3	0.316	0.451	<i>GRIK2, AVPR1A, ITPR1</i>	82	1.95	99.99
GOTERM_BP_FAT	GO:0042592~homeostatic process	6	0.632	0.470	<i>GRIK2, IFNG, AVPR1A, FOXO3, ATP12A, ITPR1</i>	82	1.32	100.00
GOTERM_BP_FAT	GO:0006811~ion transport	6	0.632	0.490	<i>SLC22A16, CDKN1B, GRIK2, ATP12A, MON2, ITPR1</i>	82	1.29	100.00
GOTERM_BP_FAT	GO:0006873~cellular ion homeostasis	3	0.316	0.660	<i>GRIK2, AVPR1A, ITPR1</i>	82	1.32	100.00
GOTERM_BP_FAT	GO:0055082~cellular chemical homeostasis	3	0.316	0.669	<i>GRIK2, AVPR1A, ITPR1</i>	82	1.30	100.00
GOTERM_BP_FAT	GO:0019725~cellular homeostasis	3	0.316	0.774	<i>GRIK2, AVPR1A, ITPR1</i>	82	1.06	100.00



Annotation Cluster 29	Enrichment Score*: 0.38445124362570404							
Category	Term	Count	%	P-value	Genes	List Total	Fold Enrichment	FDR
SP_PIR_KEYWORDS	cell membrane	18	1.895	0.051	<i>SLC22A16, CPM, GPRC5D, GPR19, RGS7BP, GRIP1, GRIK2, RXFP2, GJB6, CD164, GPRC5A, GJA3, GJB2, EREG, GRM7, AVPR1A, RAP1B, GNG4</i>	99	1.59	47.75
GOTERM_CC_FAT	GO:0005887~integral to plasma membrane	10	1.053	0.188	<i>GPR19, EREG, GRIK2, EPGN, GRM7, AVPR1A, CD164, ATP12A, GPRC5A, SMPD2</i>	70	1.54	92.51
GOTERM_CC_FAT	GO:0031226~intrinsic to plasma membrane	10	1.053	0.206	<i>GPR19, EREG, GRIK2, EPGN, GRM7, AVPR1A, CD164, ATP12A, GPRC5A, SMPD2</i>	70	1.50	94.30
GOTERM_CC_FAT	GO:0044459~plasma membrane part	15	1.579	0.295	<i>GPR19, GRIP1, GRIK2, GJB6, CD164, ATP12A, GPRC5A, GJA3, GJB2, EREG, EPGN, GRM7, AVPR1A, GNG4, SMPD2</i>	70	1.24	98.70
GOTERM_CC_FAT	GO:0005886~plasma membrane	21	2.211	0.586	<i>SLC22A16, CPM, GPRC5D, GPR19, RGS7BP, GRIP1, GRIK2, RXFP2, GJB6, ATP12A, CD164, GPRC5A, GJA3, GJB2, EREG, EPGN, GRM7, AVPR1A, RAP1B, GNG4, SMPD2</i>	70	1.02	100.00
GOTERM_CC_FAT	GO:0031224~intrinsic to membrane	30	3.158	0.604	<i>SLC22A16, GPRC5D, CPM, RGS7BP, GRIK2, LEMD3, ATP12A, GPRC5A, GJA3, B3GALNT2, ZDHHC20, XPOT, GPR19, IPO11, RXFP2, GJB6, CD164, ITPR1, MON2, GJB2, RNF180, EREG, SLC35E3, EPGN, GRM7, TOMM20, AVPR1A, NUP107, AREG, SMPD2</i>	70	1.00	100.00
SP_PIR_KEYWORDS	transmembrane	25	2.632	0.659	<i>SLC22A16, GPRC5D, GRIK2, LEMD3, ATP12A, GPRC5A, GJA3, B3GALNT2, ZDHHC20, GPR19, RXFP2, GJB6, CD164, ITPR1, MON2, GJB2, RNF180, EREG, SLC35E3, EPGN, GRM7, TOMM20, AVPR1A, AREG, SMPD2</i>	99	0.98	100.00
UP_SEQ_FEATURE	topological domain:Cytoplasmic	17	1.789	0.676	<i>GPRC5D, GPR19, GRIK2, RXFP2, GJB6, CD164, ATP12A, GPRC5A, ITPR1, GJA3, GJB2, EREG, EPGN, GRM7, B3GALNT2, TOMM20, AVPR1A</i>	99	0.97	100.00

SP_PIR_KEYWORDS	membrane	31	3.263	0.693	SLC22A16, GPRC5D, CPM, RGS7BP, GRIK2, GRIPI1, LEMD3, ATP12A, GPRC5A, GJA3, B3GALNT2, ZDHHC20, GNG4, GPR19, RXFP2, GJB6, FIG4, CD164, ITPR1, MON2, GJB2, RNF180, EREG, SLC35E3, EPGN, GRM7, TOMM20, AVPR1A, RAP1B, AREG,	99	0.96	100.00
GOTERM_CC_FAT	GO:0016021~integral to membrane	28	2.947	0.694	SLC22A16, GPRC5D, GRIK2, LEMD3, ATP12A, GPRC5A, GJA3, B3GALNT2, ZDHHC20, XPOT, GPR19, IPO11, RXFP2, GJB6, CD164, ITPR1, MON2, GJB2, RNF180, EREG, SLC35E3, EPGN, GRM7, TOMM20, AVPR1A, NUP107, AREG, SMPD2	70	0.97	100.00
UP_SEQ_FEATURE	transmembrane region	24	2.526	0.729	SLC22A16, GPRC5D, GPR19, GRIK2, RXFP2, LEMD3, GJB6, ATP12A, CD164, GPRC5A, ITPR1, GJA3, GJB2, RNF180, EREG, EPGN, SLC35E3, GRM7, B3GALNT2, AVPR1A, TOMM20, AREG, ZDHHC20, SMPD2	99	0.94	100.00
UP_SEQ_FEATURE	topological domain:Extracellular	13	1.368	0.755	GPRC5D, GPR19, EREG, GRIK2, EPGN, GRM7, RXFP2, AVPR1A, GJB6, CD164, GPRC5A, GJA3, GJB2	99	0.92	100.00
<b>Annotation Cluster 30</b>	<b>Enrichment Score*: 0.25989130151612383</b>							
<b>Category</b>	<b>Term</b>	<b>Count</b>	<b>%</b>	<b>P-value</b>	<b>Genes</b>	<b>List Total</b>	<b>Fold Enrichment</b>	<b>FDR</b>
GOTERM_BP_FAT	GO:0006928~cell motion	4	0.421	0.545	SLC22A16, LYST, WASF1, IFNG	82	1.39	100.00
GOTERM_BP_FAT	GO:0051674~localization of cell	3	0.316	0.552	SLC22A16, LYST, IFNG	82	1.61	100.00
GOTERM_BP_FAT	GO:0048870~cell motility	3	0.316	0.552	SLC22A16, LYST, IFNG	82	1.61	100.00
<b>Annotation Cluster 31</b>	<b>Enrichment Score*: 0.2555111568636755</b>							
<b>Category</b>	<b>Term</b>	<b>Count</b>	<b>%</b>	<b>P-value</b>	<b>Genes</b>	<b>List Total</b>	<b>Fold Enrichment</b>	<b>FDR</b>
GOTERM_BP_FAT	GO:0048878~chemical homeostasis	5	0.526	0.368	GRIK2, AVPR1A, FOXO3, ATP12A,	82	1.61	99.93
GOTERM_BP_FAT	GO:0042592~homeostatic process	6	0.632	0.470	GRIK2, IFNG, AVPR1A, FOXO3, ATP12A, ITPR1	82	1.32	100.00
GOTERM_CC_FAT	GO:0005624~membrane fraction	5	0.526	0.643	GRIK2, LEMD3, FOXO3, ITPR1, SMPD2	70	1.13	100.00
GOTERM_CC_FAT	GO:0005626~insoluble fraction	5	0.526	0.672	GRIK2, LEMD3, FOXO3, ITPR1, SMPD2	70	1.09	100.00

GOTERM_CC_FAT	GO:0000267~cell fraction	6	0.632	0.706	<i>GRIK2, IL26, LEMD3, FOXO3, ITPR1, SMPD2</i>	70	1.01	100.00
<b>Annotation Cluster 32</b>	<b>Enrichment Score*: 0.17973247318705154</b>							
<b>Category</b>	<b>Term</b>	<b>Count</b>	<b>%</b>	<b>P -value</b>	<b>Genes</b>	<b>List Total</b>	<b>Fold Enrichment</b>	<b>FDR</b>
GOTERM_BP_FAT	GO:0010033~response to organic substance	5	0.526	0.633	<i>IRAK3, IFNG, AVPR1A, GNG4, LATS2</i>	82	1.14	100.00
GOTERM_BP_FAT	GO:0009725~response to hormone stimulus	3	0.316	0.650	<i>AVPR1A, GNG4, LATS2</i>	82	1.35	100.00
GOTERM_BP_FAT	GO:0009719~response to endogenous stimulus	3	0.316	0.703	<i>AVPR1A, GNG4, LATS2</i>	82	1.22	100.00
<b>Annotation Cluster 33</b>	<b>Enrichment Score*: 0.12233613185272882</b>							
<b>Category</b>	<b>Term</b>	<b>Count</b>	<b>%</b>	<b>P -value</b>	<b>Genes</b>	<b>List Total</b>	<b>Fold Enrichment</b>	<b>FDR</b>
GOTERM_CC_FAT	GO:0031410~cytoplasmic vesicle	4	0.421	0.681	<i>PPBP, GRIP1, GPRC5A, ITPR1</i>	70	1.14	100.00
GOTERM_CC_FAT	GO:0031982~vesicle	4	0.421	0.709	<i>PPBP, GRIP1, GPRC5A, ITPR1</i>	70	1.09	100.00
GOTERM_CC_FAT	GO:0005783~endoplasmic reticulum	5	0.526	0.771	<i>RNF180, GRIP1, GPRC5A, ITPR1,</i>	70	0.95	100.00
GOTERM_CC_FAT	GO:0016023~cytoplasmic membrane-bounded vesicle	3	0.316	0.804	<i>PPBP, GRIP1, ITPR1</i>	70	1.00	100.00
GOTERM_CC_FAT	GO:0031988~membrane-bounded vesicle	3	0.316	0.818	<i>PPBP, GRIP1, ITPR1</i>	70	0.96	100.00
<b>Annotation Cluster 34</b>	<b>Enrichment Score*: 0.09664426030652046</b>							
<b>Category</b>	<b>Term</b>	<b>Count</b>	<b>%</b>	<b>P -value</b>	<b>Genes</b>	<b>List Total</b>	<b>Fold Enrichment</b>	<b>FDR</b>
GOTERM_BP_FAT	GO:0045449~regulation of transcription	16	1.684	0.609	<i>SCML4, ZMYM2, GRIP1, ARID4B, SAP18, FOXO3, IL22, ZBTB24, IRAK3, CDKN1B, EREG, ASCC3, IFNG, PSPC1, CAND1, CREBL2</i>	82	1.01	100.00
SP_PIR_KEYWORDS	transcription regulation	10	1.053	0.717	<i>SCML4, ZMYM2, ASCC3, ARID4B, PSPC1, SAP18, CAND1, FOXO3,</i>	99	0.96	100.00
SP_PIR_KEYWORDS	Transcription	10	1.053	0.741	<i>SCML4, ZMYM2, ASCC3, ARID4B, PSPC1, SAP18, CAND1, FOXO3,</i>	99	0.94	100.00
GOTERM_BP_FAT	GO:0006350~transcription	11	1.158	0.828	<i>SCML4, ZMYM2, EREG, ASCC3, ARID4B, PSPC1, SAP18, CAND1, FOXO3, ZBTB24, CREBL2</i>	82	0.86	100.00
SP_PIR_KEYWORDS	dna-binding	5	0.526	0.989	<i>ARID4B, LEMD3, FOXO3, ZBTB24, CREBL2</i>	99	0.52	100.00
GOTERM_MF_FAT	GO:0003677~DNA binding	7	0.737	0.994	<i>SCML4, ARID4B, LEMD3, FOXO3, PARP4, ZBTB24, CREBL2</i>	74	0.53	100.00
<b>Annotation Cluster 35</b>	<b>Enrichment Score*: 0.0760891030134105</b>							

Category	Term	Count	%	P-value	Genes	List Total	Fold Enrichment	FDR
GOTERM_BP_FAT	GO:0045934~negative regulation of nucleobase, nucleoside, nucleotide and nucleic acid metabolic	3	0.316	0.817	<i>CDKN1B, EREG, GRM7</i>	82	0.97	100.00
GOTERM_BP_FAT	GO:0051172~negative regulation of nitrogen compound metabolic process	3	0.316	0.823	<i>CDKN1B, EREG, GRM7</i>	82	0.95	100.00
GOTERM_BP_FAT	GO:0031327~negative regulation of cellular biosynthetic process	3	0.316	0.855	<i>CDKN1B, EREG, GRM7</i>	82	0.88	100.00
GOTERM_BP_FAT	GO:0009890~negative regulation of biosynthetic	3	0.316	0.863	<i>CDKN1B, EREG, GRM7</i>	82	0.86	100.00
<b>Annotation Cluster 36</b>	<b>Enrichment Score*: 0.07593946676781624</b>							
Category	Term	Count	%	P-value	Genes	List Total	Fold Enrichment	FDR
SP_PIR_KEYWORDS	metal-binding	14	1.474	0.766	<i>CPM, RNF17, ZMYM2, ZMYM5, SOBP, ATP12A, LATS2, ZBTB24, MSRB3, RNF180, GNS, MICAL1, ZDHHC20, SMPD2</i>	99	0.92	100.00
SP_PIR_KEYWORDS	zinc	10	1.053	0.798	<i>RNF180, CPM, ZMYM2, RNF17, ZMYM5, SOBP, MICAL1, ZDHHC20, ZBTB24, MSRB3</i>	99	0.89	100.00
GOTERM_MF_FAT	GO:0046872~metal ion binding	21	2.211	0.829	<i>CPM, RNF17, MTHFD2L, ZMYM2, ZMYM5, SOBP, ATP12A, ITPR1, LATS2, ZBTB24, MSRB3, GNS, RNF180, IRAK3, GRM7, HEBP1, MICAL1, DYRK2, ZDHHC20, RTN4IP1, SMPD2</i>	74	0.89	100.00
GOTERM_MF_FAT	GO:0043169~cation binding	21	2.211	0.842	<i>CPM, RNF17, MTHFD2L, ZMYM2, ZMYM5, SOBP, ATP12A, ITPR1, LATS2, ZBTB24, MSRB3, GNS, RNF180, IRAK3, GRM7, HEBP1, MICAL1, DYRK2, ZDHHC20, RTN4IP1, SMPD2</i>	74	0.88	100.00
GOTERM_MF_FAT	GO:0008270~zinc ion binding	11	1.158	0.860	<i>RNF180, CPM, ZMYM2, RNF17, ZMYM5, SOBP, MICAL1, ZDHHC20, RTN4IP1, ZBTB24, MSRB3</i>	74	0.84	100.00
GOTERM_MF_FAT	GO:0043167~ion binding	21	2.211	0.862	<i>CPM, RNF17, MTHFD2L, ZMYM2, ZMYM5, SOBP, ATP12A, ITPR1, LATS2, ZBTB24, MSRB3, GNS, RNF180, IRAK3, GRM7, HEBP1, MICAL1, DYRK2, ZDHHC20, RTN4IP1, SMPD2</i>	74	0.87	100.00

SP_PIR_KEYWORDS	zinc-finger	7	0.737	0.881	<i>RNF180, ZMYM2, RNF17, ZMYM5, SOBP, ZDHHC20, ZBTB24</i>	99	0.79	100.00
GOTERM_MF_FAT	GO:0046914~transition metal ion binding	13	1.368	0.886	<i>RNF17, ZMYM2, CPM, ZMYM5, SOBP, ZBTB24, MSRB3, RNF180, HEBP1, MICAL1, DYRK2, ZDHHC20, RTN4IP1</i>	74	0.82	100.00
<b>Annotation Cluster 37</b>	<b>Enrichment Score*: 0.07471262524024755</b>							
<b>Category</b>	<b>Term</b>	<b>Count</b>	<b>%</b>	<b>P-value</b>	<b>Genes</b>	<b>List Total</b>	<b>Fold Enrichment</b>	<b>FDR</b>
GOTERM_CC_FAT	GO:0005730~nucleolus	4	0.421	0.735	<i>DDX47, GPR19, PSPC1, ITPR1</i>	70	1.05	100.00
SP_PIR_KEYWORDS	rna-binding	3	0.316	0.766	<i>XPOT, DDX47, PSPC1</i>	99	1.08	100.00
GOTERM_CC_FAT	GO:0044451~nucleoplasm part	3	0.316	0.808	<i>ZMYM2, PSPC1, SAP18</i>	70	0.99	100.00
GOTERM_CC_FAT	GO:0031981~nuclear lumen	7	0.737	0.810	<i>XPOT, DDX47, ZMYM2, GPR19, PSPC1, SAP18, ITPR1</i>	70	0.88	100.00
GOTERM_CC_FAT	GO:0005654~nucleoplasm	4	0.421	0.864	<i>XPOT, ZMYM2, PSPC1, SAP18</i>	70	0.83	100.00
GOTERM_CC_FAT	GO:0043233~organelle lumen	8	0.842	0.878	<i>XPOT, DDX47, ZMYM2, PPBP, GPR19, PSPC1, SAP18, ITPR1</i>	70	0.80	100.00
GOTERM_CC_FAT	GO:0031974~membrane-enclosed lumen	8	0.842	0.891	<i>XPOT, DDX47, ZMYM2, PPBP, GPR19, PSPC1, SAP18, ITPR1</i>	70	0.79	100.00
GOTERM_MF_FAT	GO:0003723~RNA binding	3	0.316	0.918	<i>XPOT, DDX47, PSPC1</i>	74	0.73	100.00
GOTERM_CC_FAT	GO:0070013~intracellular organelle lumen	7	0.737	0.932	<i>XPOT, DDX47, ZMYM2, GPR19, PSPC1, SAP18, ITPR1</i>	70	0.72	100.00

\***Enrichment Score**, -10x the geometric mean of the collective p-values, score >1.3 is equivalent to 0.05 in -log scale.

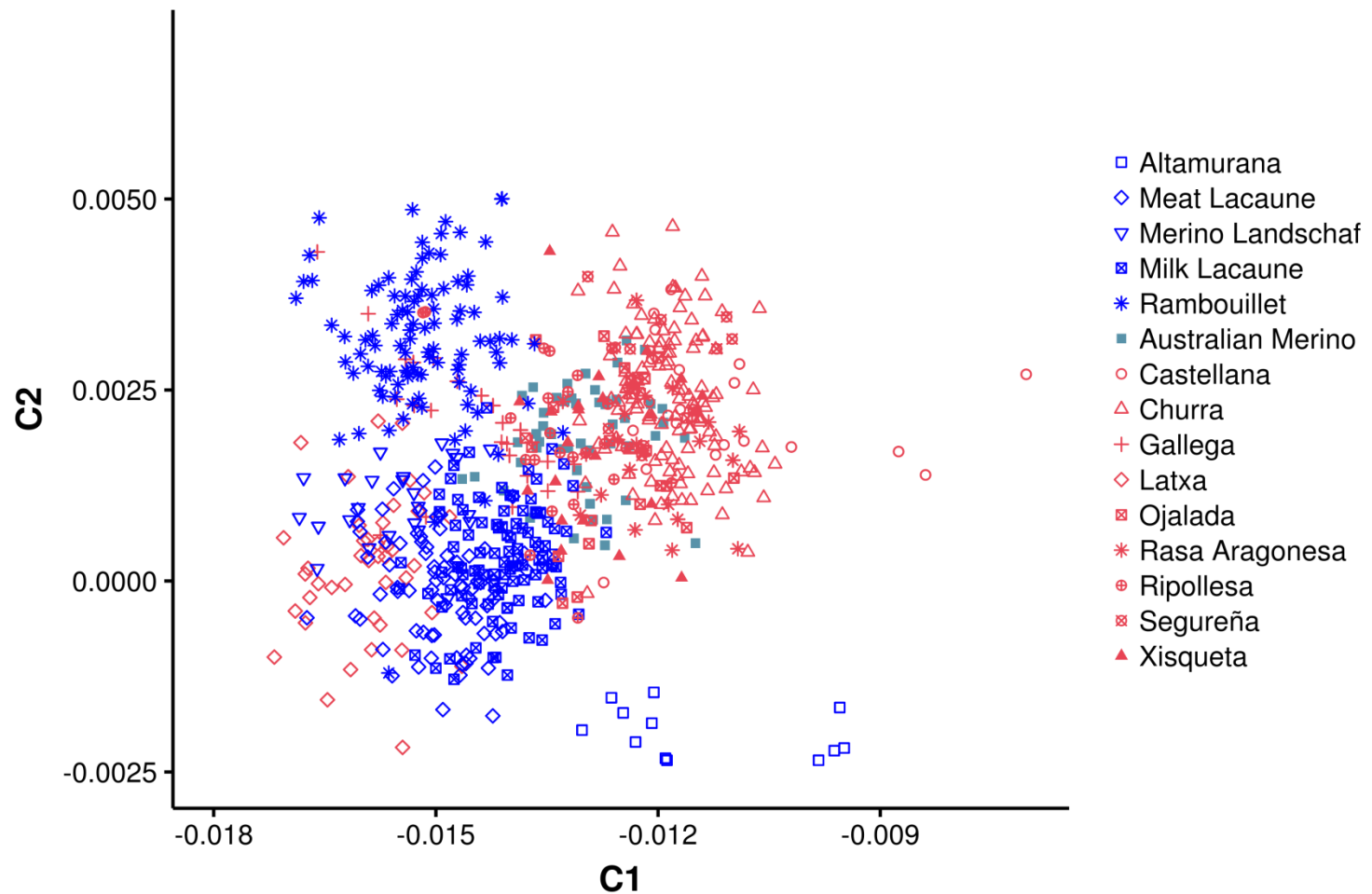
**Supplementary Table 6.** Comparison of ROH hotspots found in sheep populations in different studies based on the ovine genome assembly 3.1 (positions are indicated in Mb).

Chr*	Current Research	Mastrangelo et al. (2018) Meat breeds	Mastrangelo et al. (2018) Milk breeds	Mastrangelo et al. (2018) Wool breeds	Mastrangelo et al. (2018) Milk-Meat breeds	Purfield et al. (2017) Meat breeds
<b>1</b>		-	131.62-131.99	-	-	-
	-	-	-	-	178.04-188.4	-
	-	195.23-207.26	-	-	-	-
	-	-	-	-	214.73-228.13	-
<b>2</b>	-	-	-	-	-	35.78-35.93
	-	-	-	-	-	36.08-39.59
	-	-	76.24-90.43	-	-	-
	-	-	101.07-103.4	-	-	-
	-	-	-	-	-	107.77-111.34
	-	-	-	-	-	115.48-122.52
	-	-	-	-	-	123.36-126.34
	-	130.02-132.36	-	-	-	
<b>3</b>	-	<b>15.82-16.42</b>	<b>15-16.4</b>	-	-	-
	-	27.34-29.33	-	-	-	-
	-	-	30.29-32.73	-	-	-
	-	-	-	-	-	44.48-47.29
	-	-	110.78-112.42	-	-	-
	150.5-158.26	-	-	-	-	-
	201.71-202.14	-	-	-	-	-
<b>4</b>	-	53.4-55.2	-	-	-	-
<b>5</b>	-	-	-	38.74-44.27	-	
	-	-	-	-	-	47.02-48.82
	-	-	-	-	-	49.38-49.9
	-	-	-	-	-	59.73-60
	-	-	-	73.71-75.9	-	-
	-	-	-	79.65-89.49	-	-
	-	-	99.76-100.41	-	-	-
<b>6</b>	<b>38.61-38.63</b>	-	-	-	<b>37.08-39.16</b>	-
	-	-	-	-	41.38-43.29	-
	76.98-77.52	-	-	-	-	-
	88.25-89.18	-	-	-	-	-
	90.78-91.06	-	-	-	-	-

	94.85	-	-	-	-	-
<b>7</b>	-	-	47.76-49.6	-	-	-
<b>8</b>	12.6-13.00	-	-	-	-	-
	25.66	-	-	-	-	-
	26.69-28.73	-	-	-	-	-
	29.40-30.51	-	-	-	-	-
	35.13-36.25	-	-	-	-	-
<b>9</b>	-	49.15-49.28	-	-	-	-
<b>10</b>	-	-	-	<b>18.63-23.13</b>	<b>18.63-25.62</b>	-
	29.47-29.51	-	-	-	-	-
	32.96-33.05	-	-	-	-	-
	35.56-39.90	-	-	-	-	-
	-	-	-	48.1-48.28	-	-
<b>12</b>	-	32.02-32.17	-	-	-	-
<b>15</b>	-	-	-	19.84-23.88	-	-
	-	31.53-33.69	-	-	-	-
<b>16</b>	14.95-15.36	-	-	-	-	-
	16.72-17.04	-	-	-	-	-
	17.32-17.45	-	-	-	-	-
<b>19</b>	18.72	-	-	-	-	-
	21.35-21.54	-	-	-	-	-
<b>22</b>	-	-	-	-	-	19.39-19.5
	-	-	-	21.45-30.81	-	-
	-	-	-	32.95-35.08	-	-
<b>23</b>	-	-	36.63-39.06	-	-	-
<b>25</b>	7.35-8.51	-	-	-	-	-
<b>26</b>	-	-	-	42.57-43.33	-	-

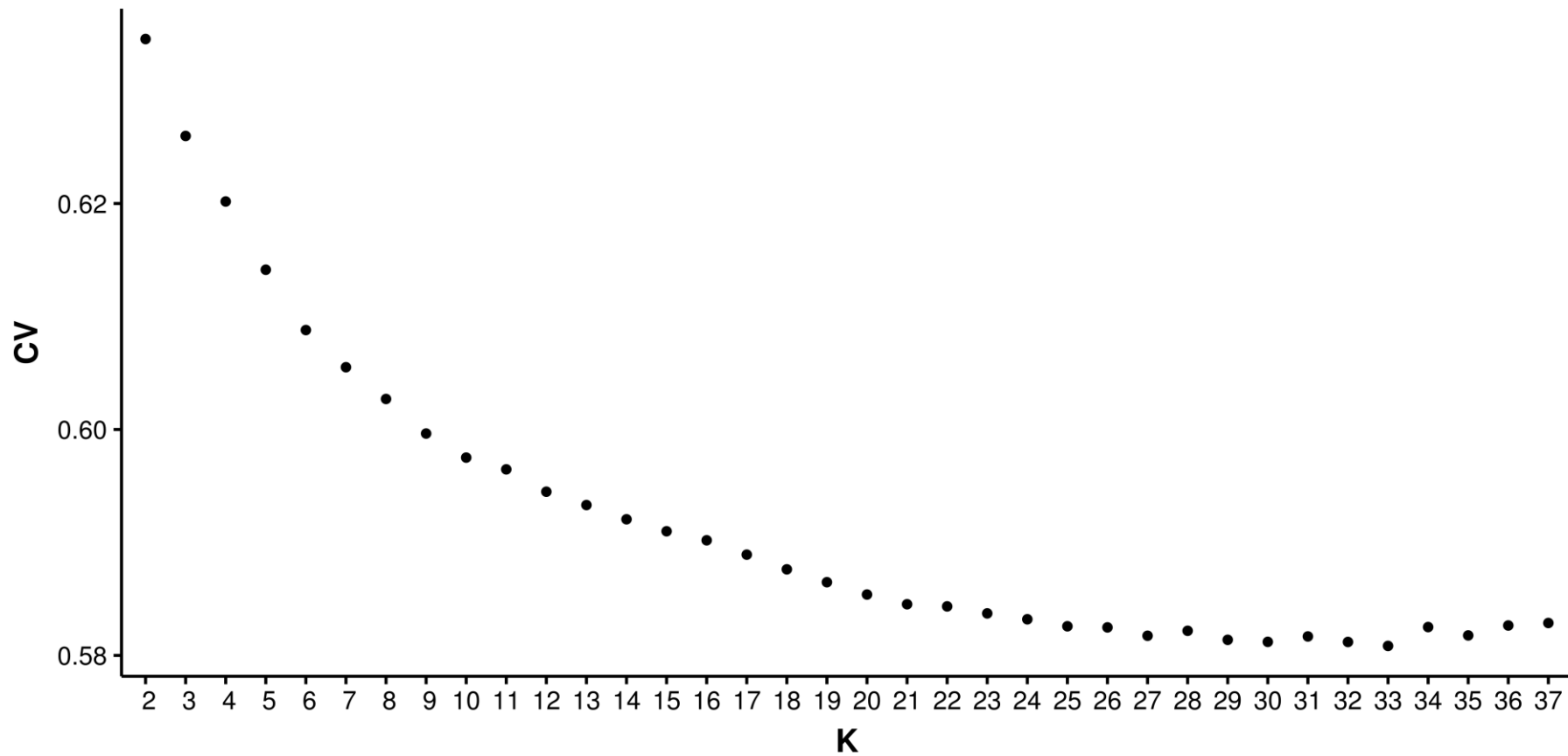
\*Chr, Chromosome.

**Supplementary Figure 1.** Weighted principal component analysis of 11 Spanish sheep breeds and reference populations from Europe.

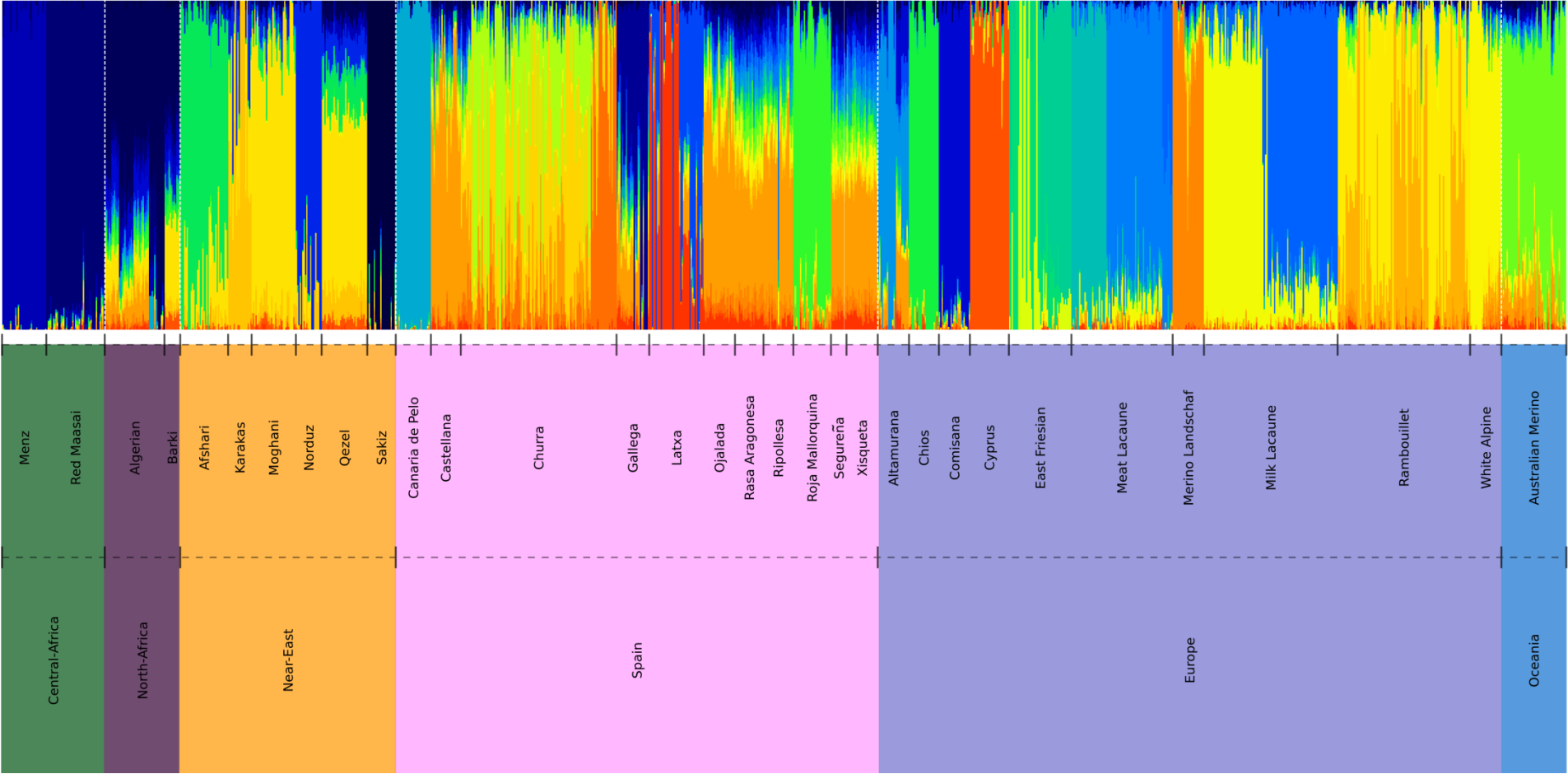




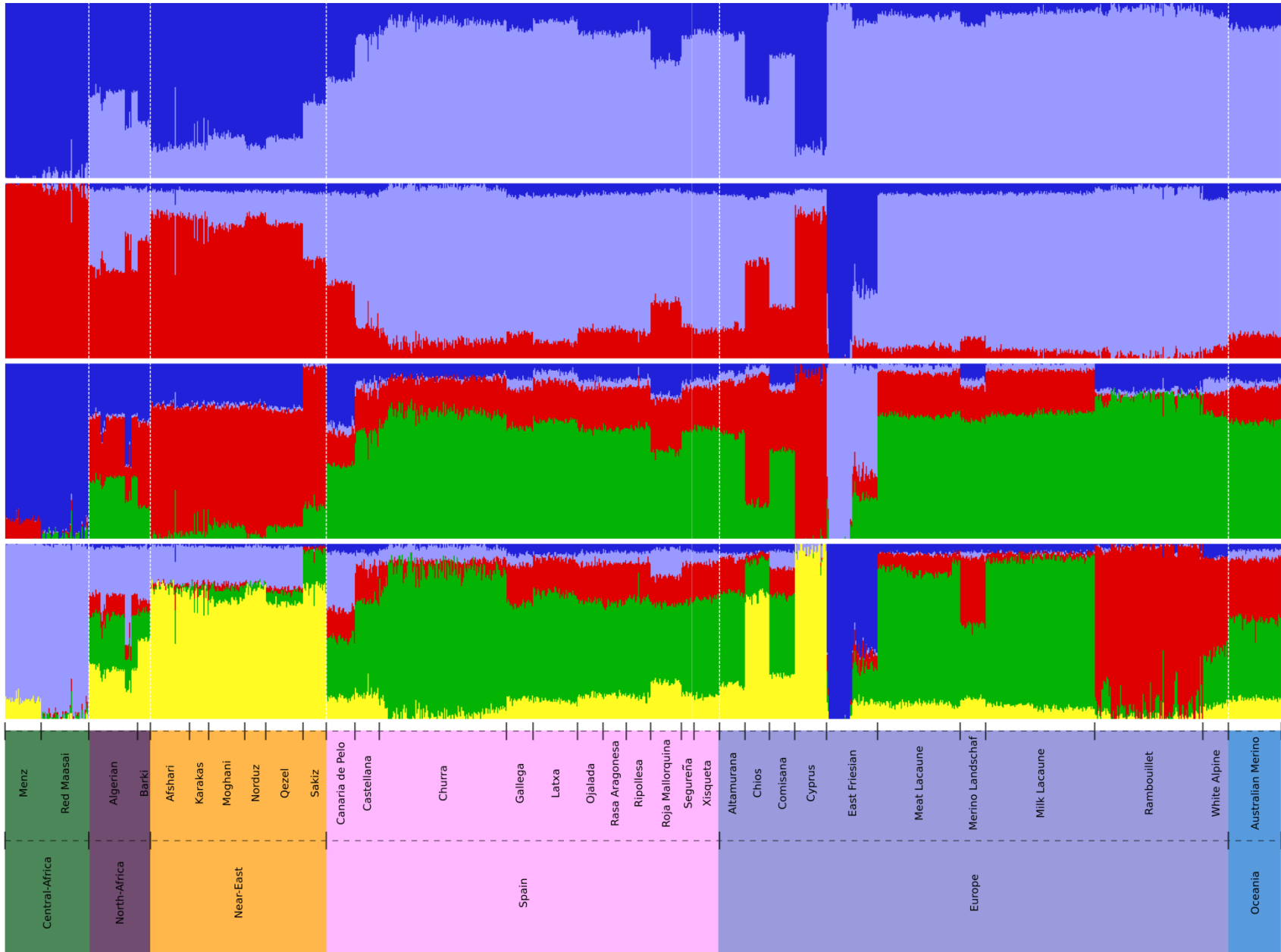
**Supplementary Figure 2.** Plot of ADMIXTURE cross-validation error from  $K = 2$  through  $K = 37$ . It can be seen that at  $K=33$  the cross-validation error is minimized.

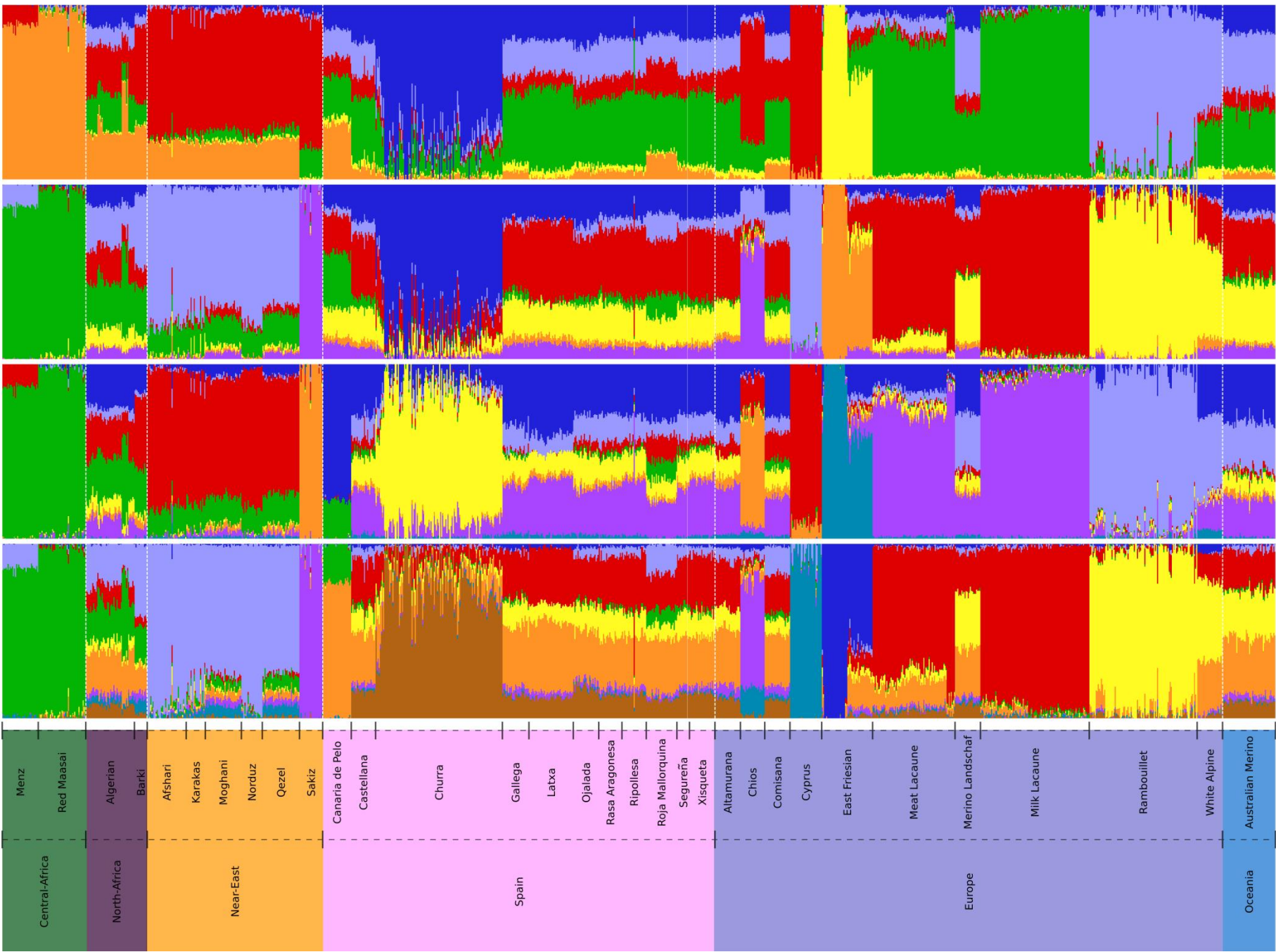


**Supplementary Figure 3.** Admixture analysis (K= 33) of 11 Spanish sheep breeds and reference populations from Europe, North Africa, Central Africa and Near East.

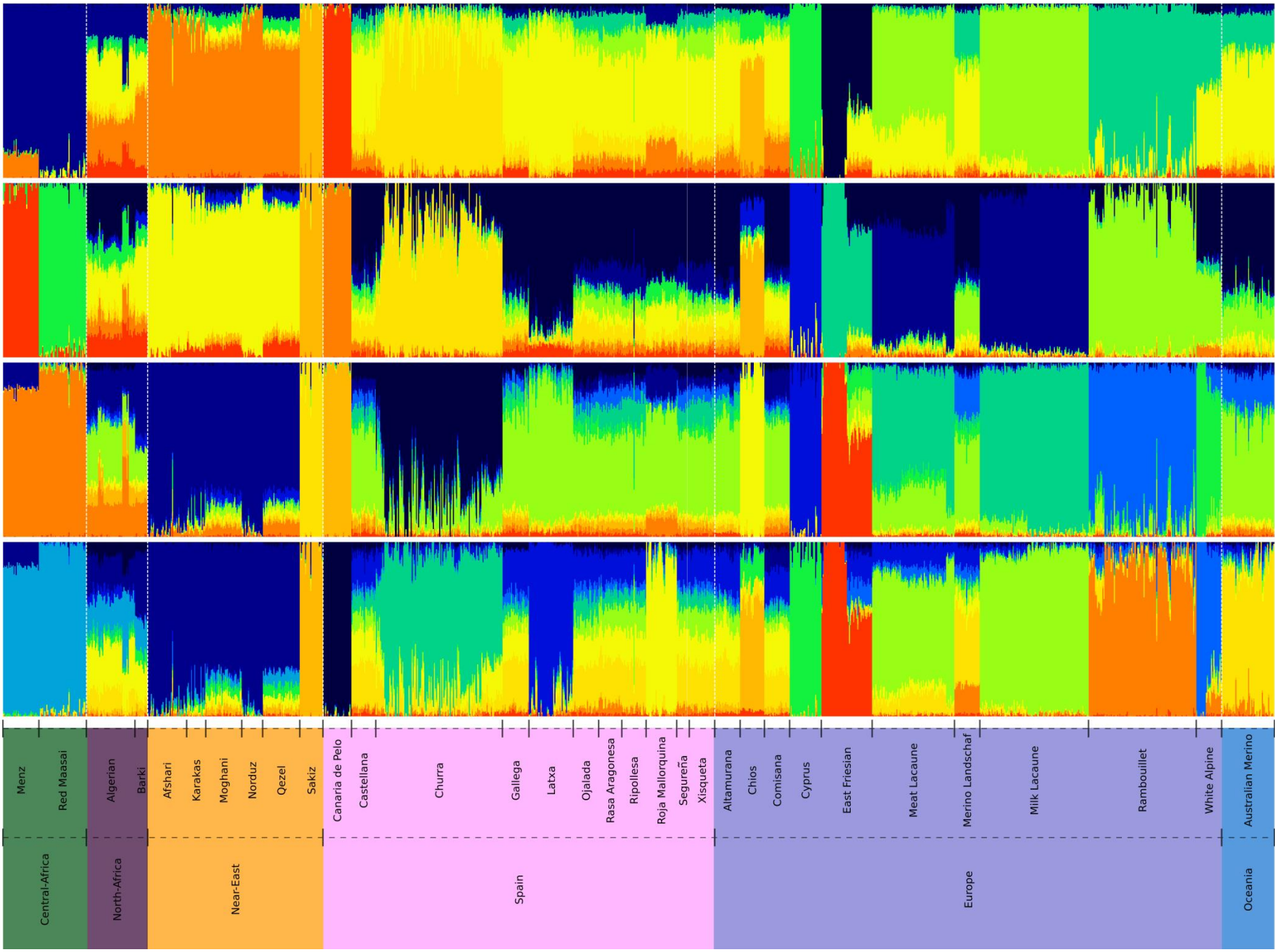


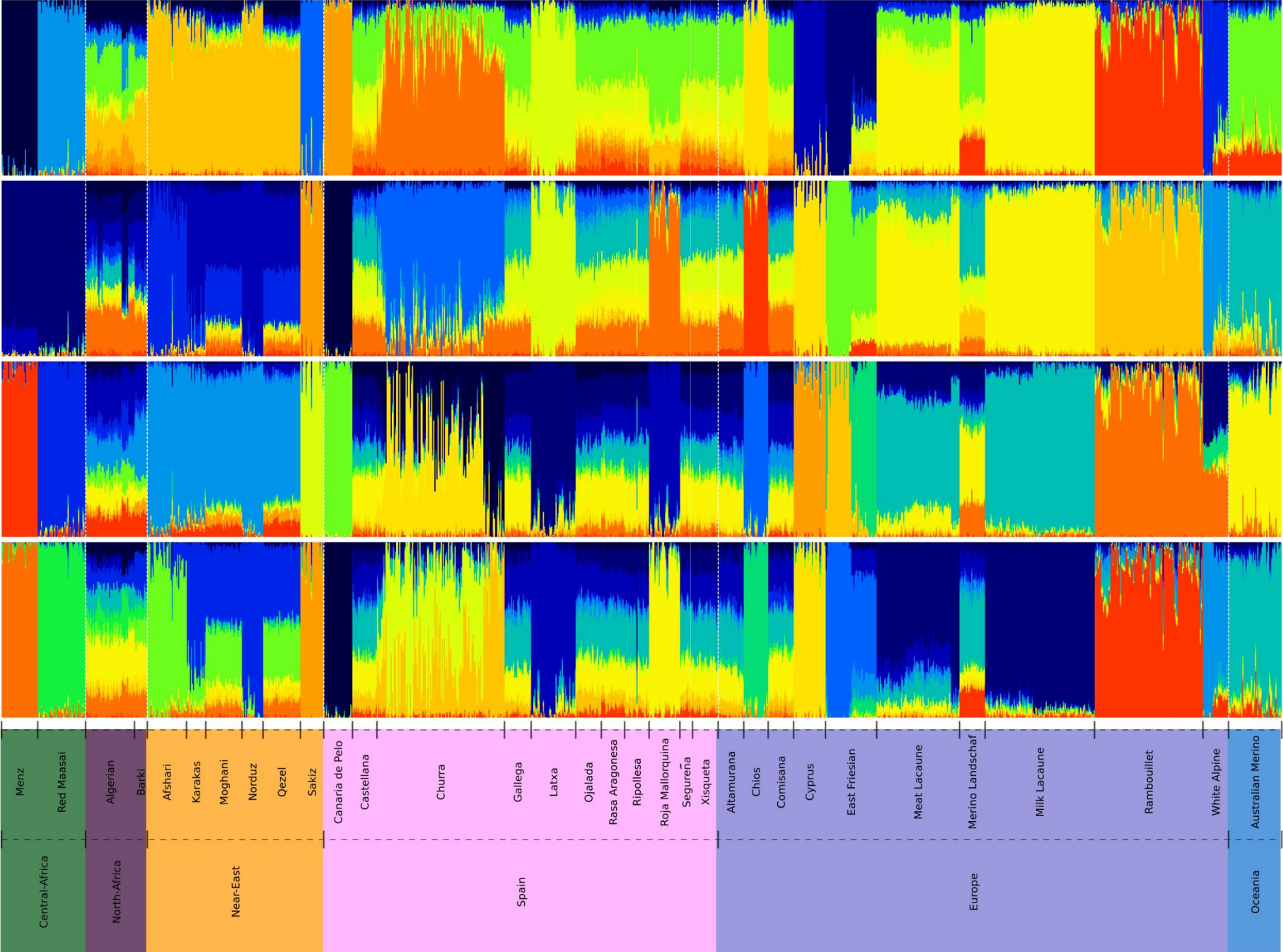
**Supplementary Figure 4.** Admixture analysis (K= 2-37) of 11 Spanish sheep breeds and reference populations from Europe, North Africa, Central Africa and Near East.

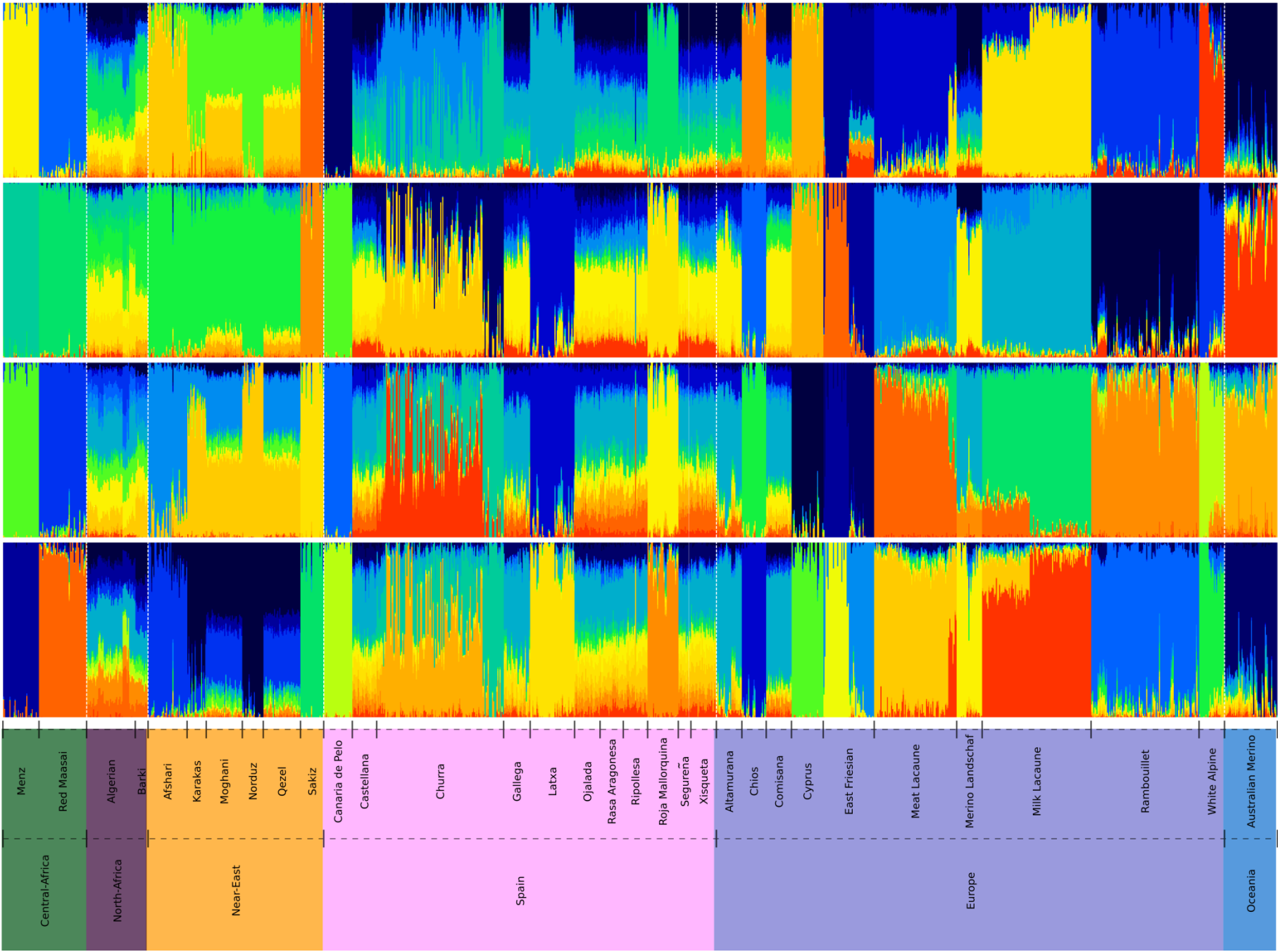




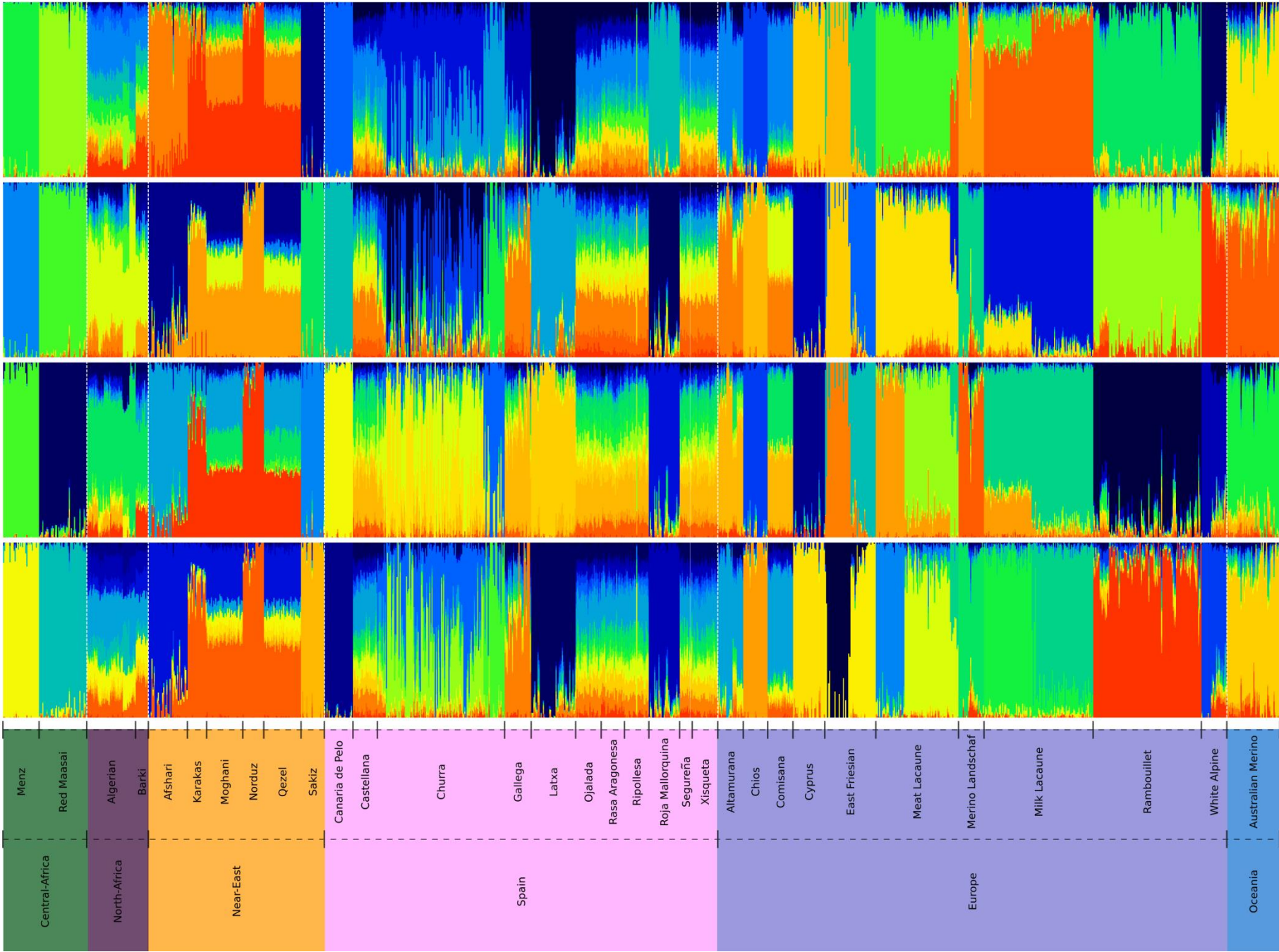




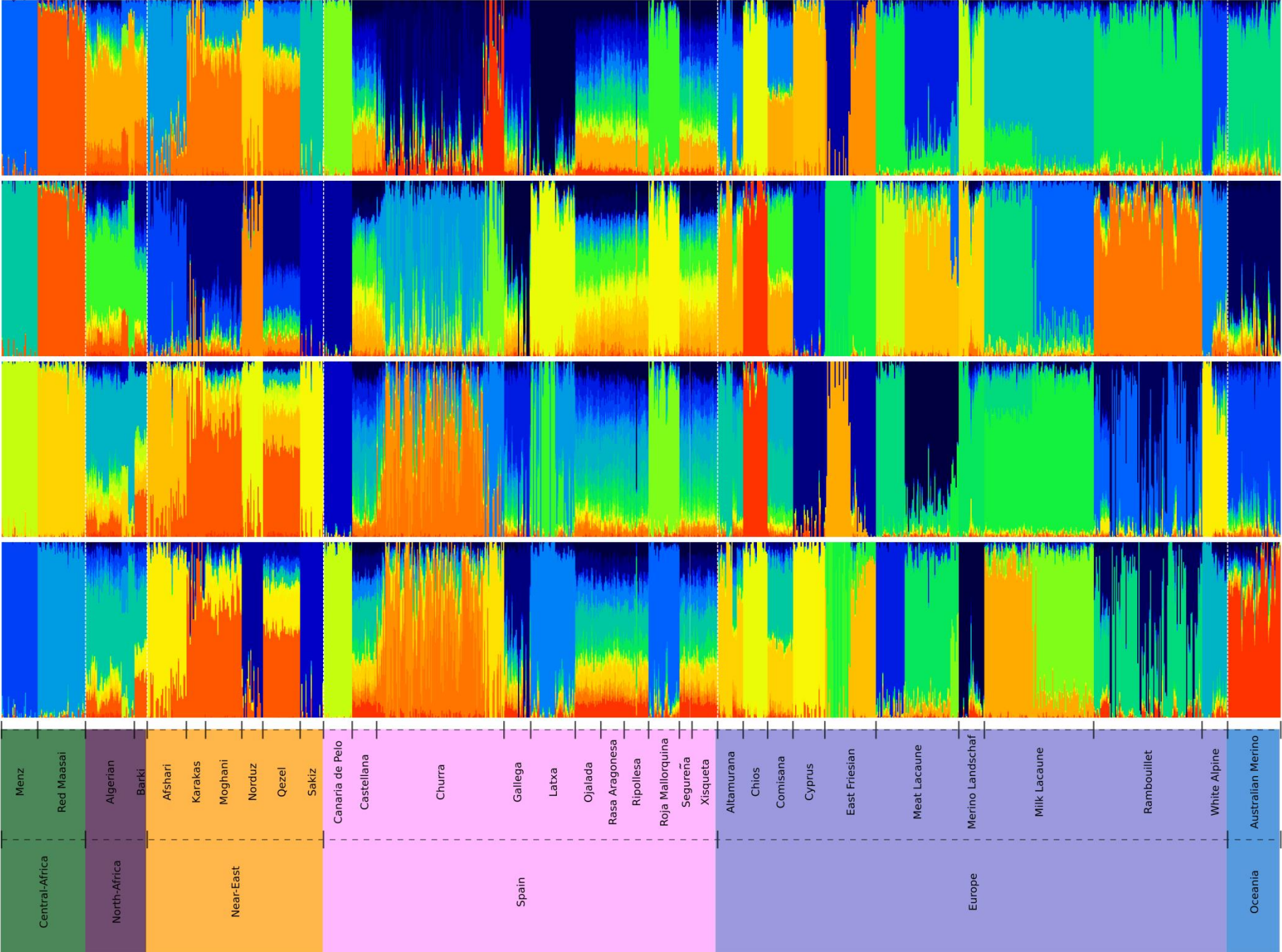


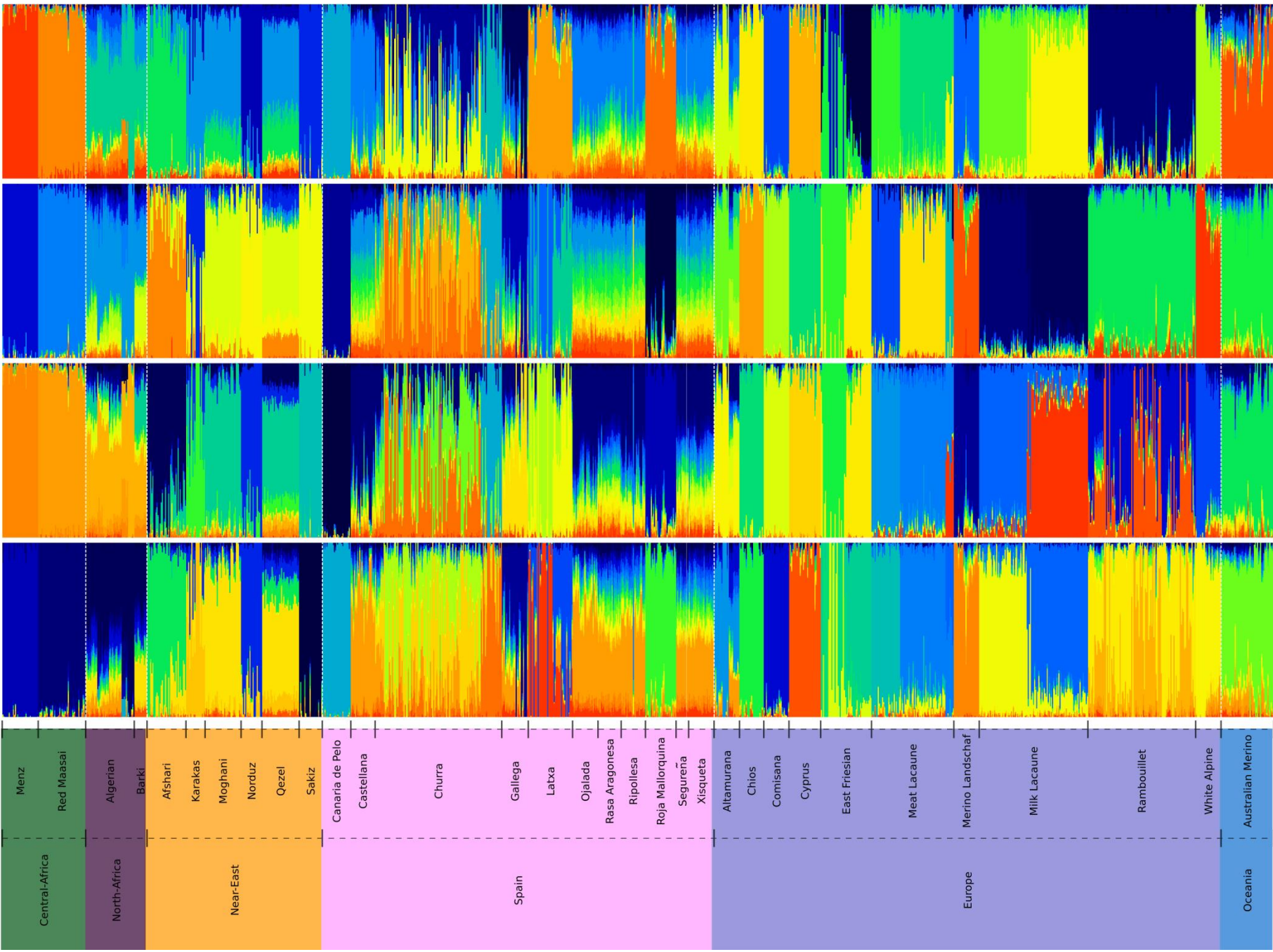




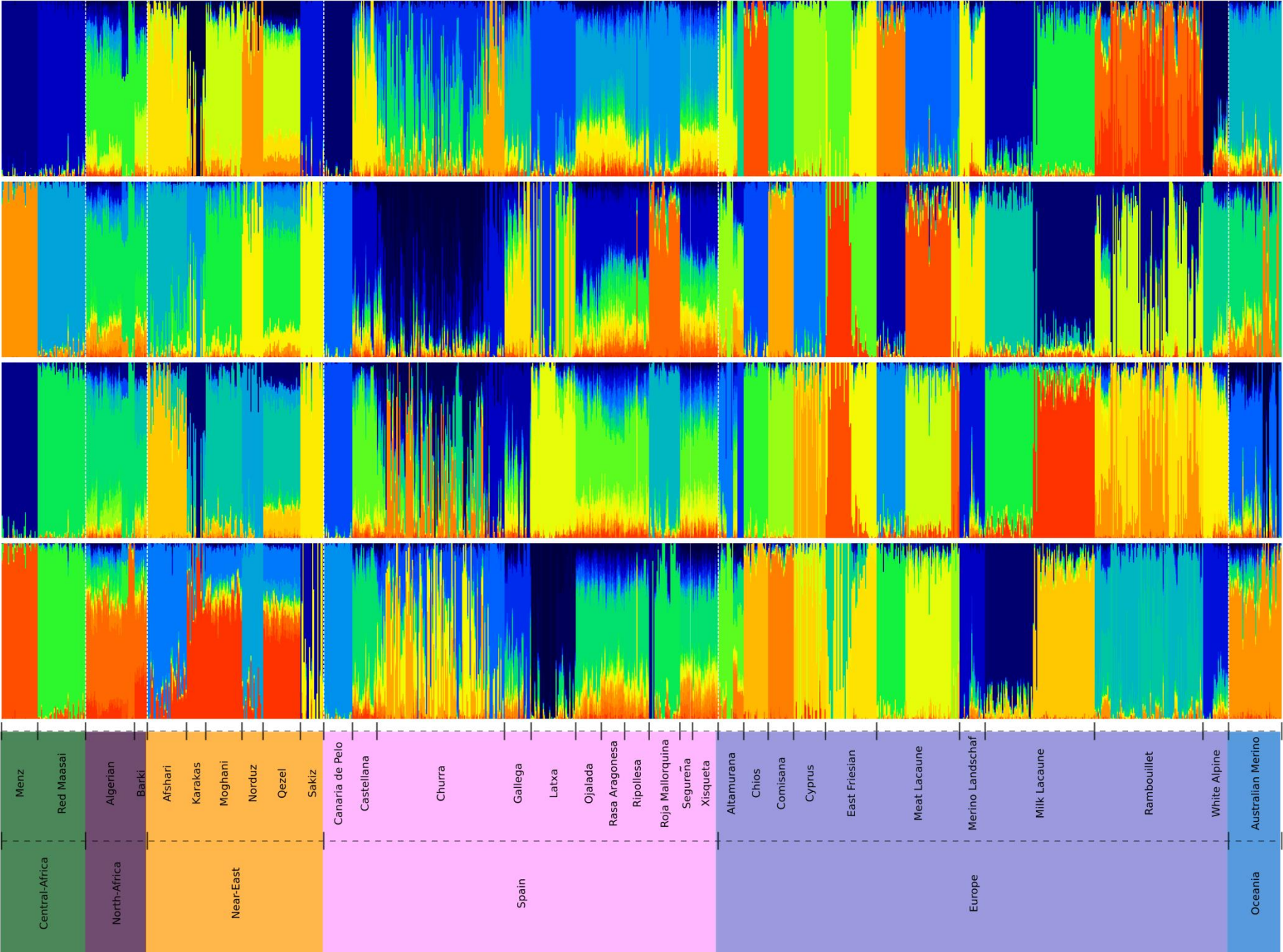












**Supplementary Figure 5.** A reduced view of **Figure 2** focused on sheep with less than 50 ROH and less than 300 Mb of total ROH coverage. This analysis includes 11 Spanish sheep breeds.

